NUCLEAR STRUCTURE STUDIED WITH SPECTROSCOPY AND REACTIONS

A. Obertelli

CEA Saclay

TU Darmstadt, IKP, February 2017

Energy scales of Nuclear Structure

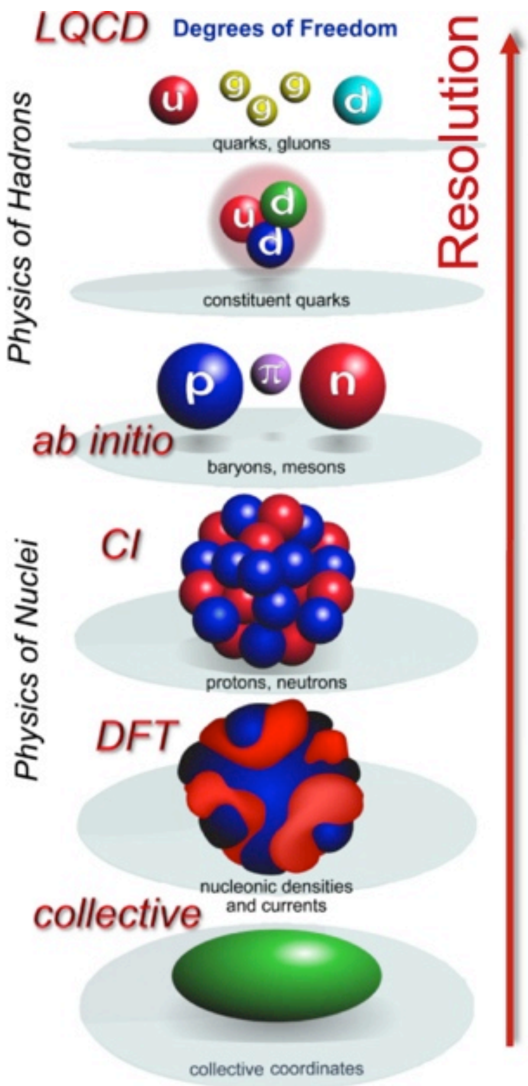

- Nucleons and nuclei are composite systems ruled by **QCD**
- The first nucleonic excited state is the Δ resonance at 300 MeV above ground state. it is therefore common to assume a **separation of scales** between nuclear and hadronic physics
- Nuclear physics can be considered as driven by an effective field theory with **nucleons as low-energy degrees of freedom**
- Many phenomena or collective behaviour can be described by few order parameters. *Ex.* Rotation spectrum
- **Spectroscopy** is the fingerprint of nuclear structure

Neutron-rich nuclei: new dimensions to explore

- **Exotic nuclei open new dimensions to explore: isospin, binding energy**

Stable = Specific **Radioactive = General**

Lecture 1: radii, halos and neutron skins

- Iterative process of « understanding »:
  - general law / new model from existing observations
  - New behavior or limitations of models from a more complete observation
  - derive more complete theory or model

γ spectrum of the decay of superdeformed band of ^{152}Dy

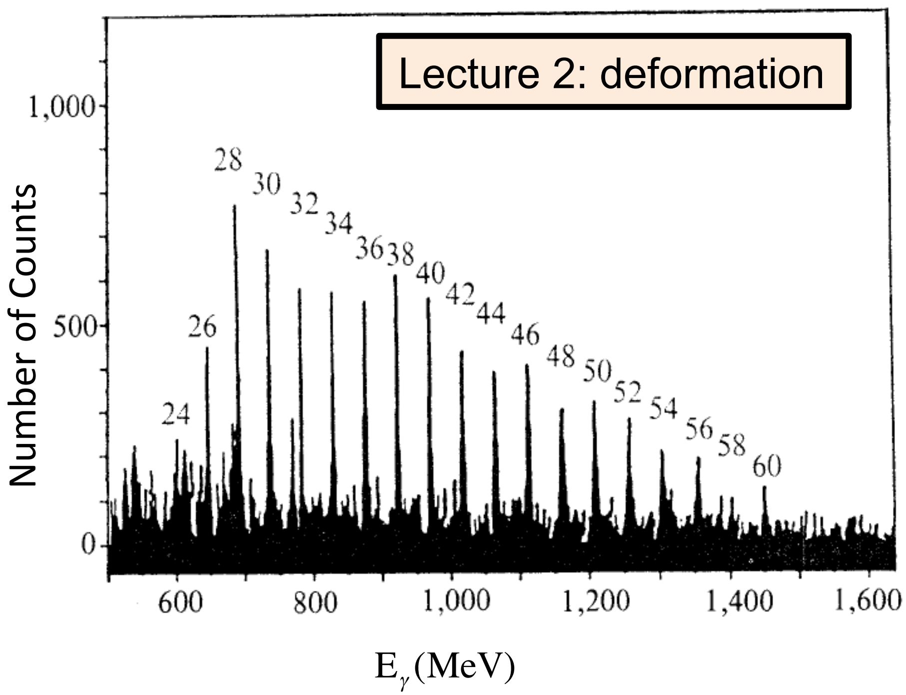

First 2$^+$ excitation energies (even-even nuclei)

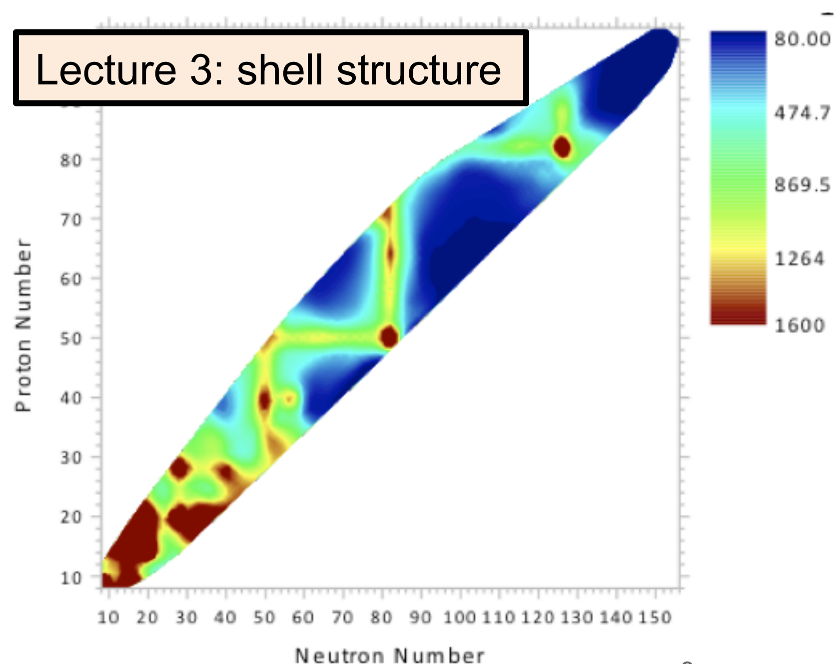

Reactions: tools to excite and probe nuclear states

B. Jonson, Physics Report **389** (2004)

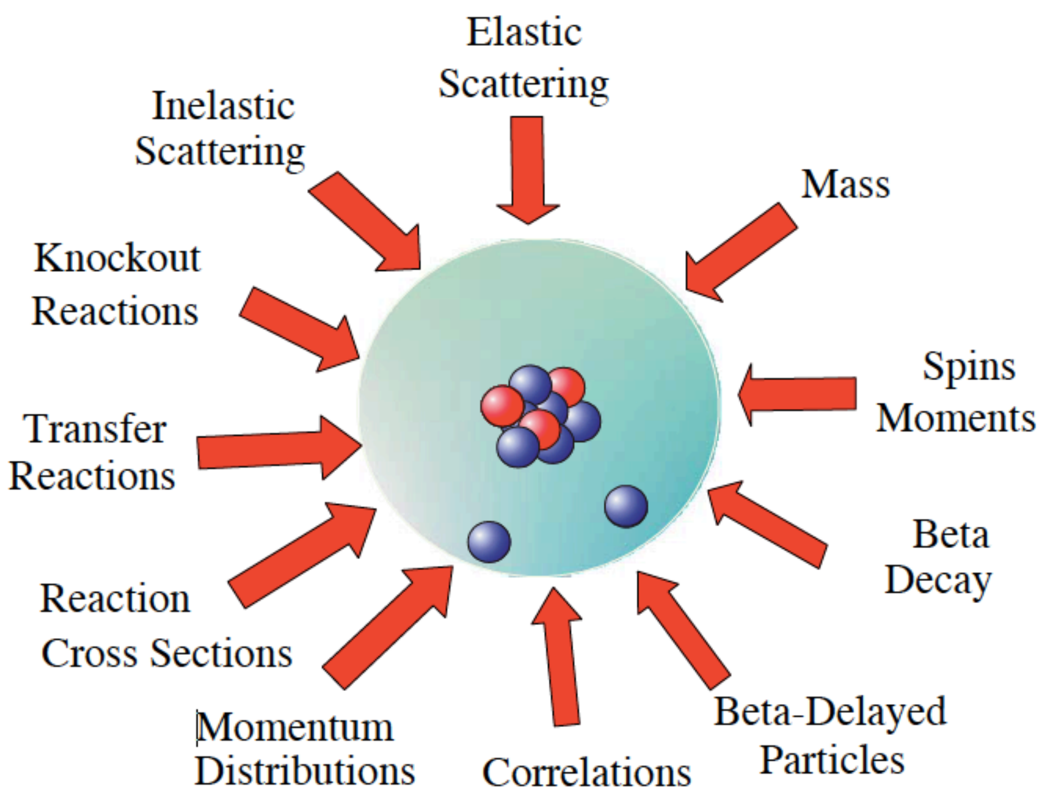

Lecture 4: direct reactions

Outline

- Today, lecture 1: **Radii, Neutron skins and Halos** (4 hours)
  + lecture by Christian Drischler, TU Darmstadt
  The nuclear EoS from an ab-initio point of view (1 hour)

- Wednesday, lecture 2 : **Nuclear deformation** (3 hours)
  + lecture by Damian Ralet, CSNSM (Orsay, France)
  Gamma-ray techniques and AGATA (2 hours)

- Thursday, lecture 3 : **The nuclear shell structure** (3 hours)
  + lecture by Francesca Giacoppo, GSI
  Superheavy elements (2 hours)

- Friday, lecture 4: **Direct transfer and knockout reactions** (3 hours)
  + lecture by Kai Hebeler, TU Darmstadt
  Non-observability and reaction-structure interplay (1 hour)

LECTURE 1: RADII, NEUTRON SKINS AND HALOS

NUCLEAR STRUCTURE
STUDIED WITH
SPECTROSCOPY AND REACTIONS

Special thanks to: A. Corsi, M. Vandebrouck (CEA), T. Cocolios (KU Leuven), R. Garcia Riuz (CERN) for slides

Lecture 1: Radii, neutron skins and halos

- **Matter radii, skins and halos: history and definitions**
- **Hyperfine structure and isotopic shifts**
- **Electron elastic scattering**
  - The charge form factor
  - Physics case: the historical ^{208}Pb example
  - RIB: The SCRIT facility and the LISE project at FAIR

Charge radius & density

- **Weak interaction experiments**
  - The weak charge form factor
  - Physics case: the PREX experiment and neutron skin of ^{208}Pb
- **Strong interaction experiments**
  - Proton elastic scattering
  - Coherent $\pi 0$ photoproduction
  - Antiprotonic atoms
- **Indirect methods (examples)**
  - Inelastic scattering
  - Dipole polarizability
  - Giant Resonances

Matter radius

The size of a nucleus

- 1911, discovery of the atomic nucleus by E. Rutherford, UK
  E. Rutherford, Philos. Mag., vol. 6, p. 21 (1911).
- 10^{-4} the size of the atom from sub-barrier alpha (back)scattering
- The nucleus: « a fly in a cathedral » (E. Rutherford)

- Assuming a constant saturation density ($\rho=\rho_0$), the nuclear radius R should follow:

$$A \propto \frac{4}{3}\pi R^3 \Rightarrow R \propto A^{1/3}$$

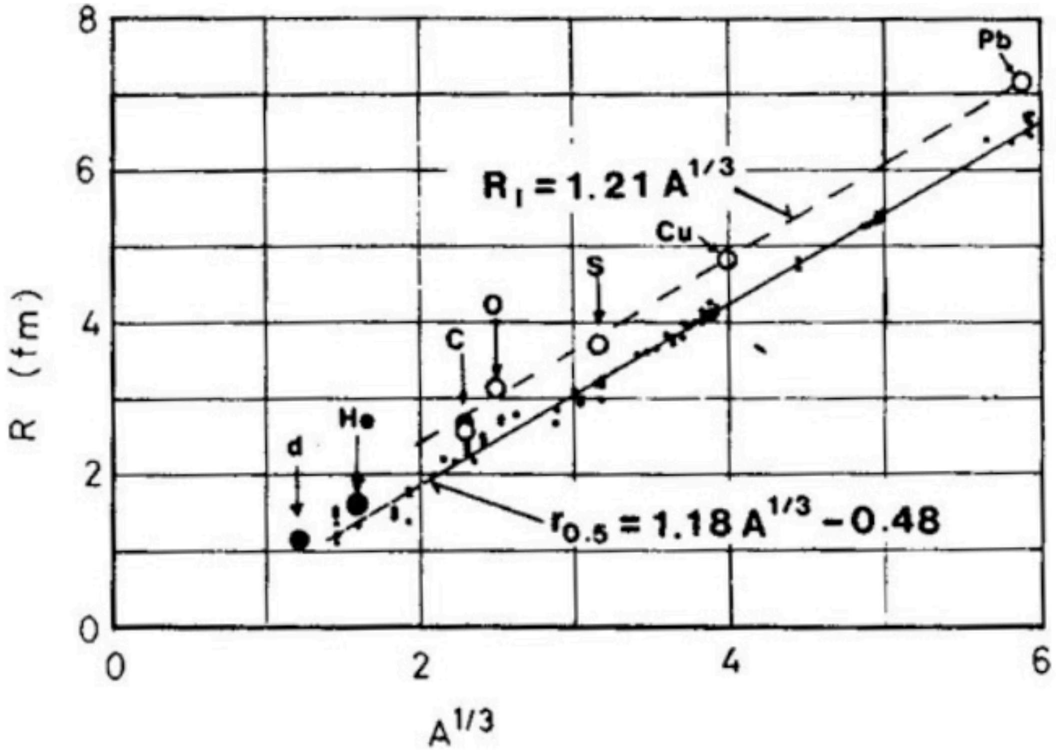

Simplest method: the interaction cross section

- Nuclear interaction is **short range and strong**: nuclear potential follows the matter density profile
- Interaction cross section: change in Z or N from the incident nucleus

$$\sigma_R = \sigma_I + \sigma_{inelastic}$$

If σ_{inel} small enough, $\sigma_R \cong \sigma_I$ (true at relativistic energies)

- One can define an « interaction radius » of a nucleus (« black disc » approximation):

$$\sigma_I(A,B) = \pi\left[R_I(A) + R_I(B)\right]^2$$

- The target « interaction radius » can be extracted from a symmetric reaction:

$$\sigma_I(A,A) = 4\pi\left[R_I(A)\right]^2$$

- Leading to the interaction radius of the projectile:

$$R_I(B) = \sqrt{\frac{\sigma_I(A,B)}{\pi}} - \sqrt{\frac{\sigma_I(A,A)}{4\pi}}$$

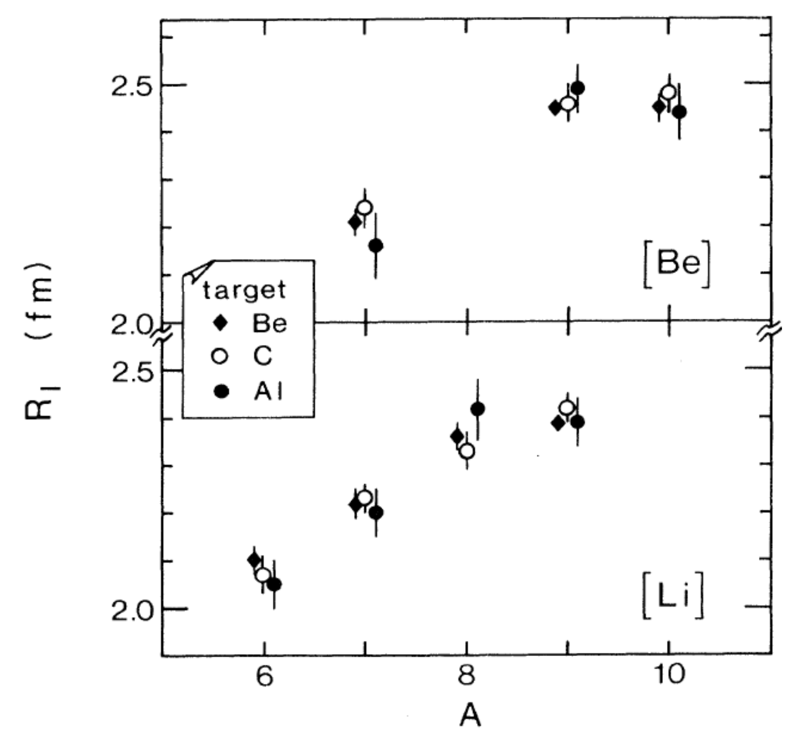

Glauber model: optical limit approximation

$$\sigma_R = 2\pi \int_0^{\infty} [1 - T(r)]\, r\, dr$$

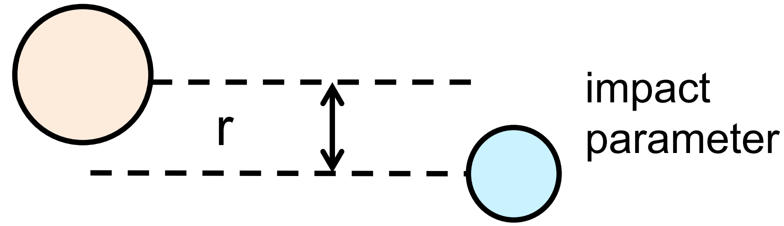

T(*r*):Transmission function

$$T(r) = \exp\left[-\bar{\sigma} \int_{-\infty}^{\infty} q(r,z)\, dz \right]$$

$\bar{\sigma}$ **:effective *NN* cross-sections**

$$q(z) = \int_{-\infty}^{\infty} d\eta\, 2\pi \int_0^{\infty} \rho_T(r,z,b,\eta)\, \rho_P(r,z,b,\eta)\, b\, db$$

ρ of target

ρ of projectile

$$\langle r^2 \rangle = \int_0^{\infty} r^2 \rho_P(r) \bullet 4\pi r^2 dr$$

Mean square radii

The transmission method

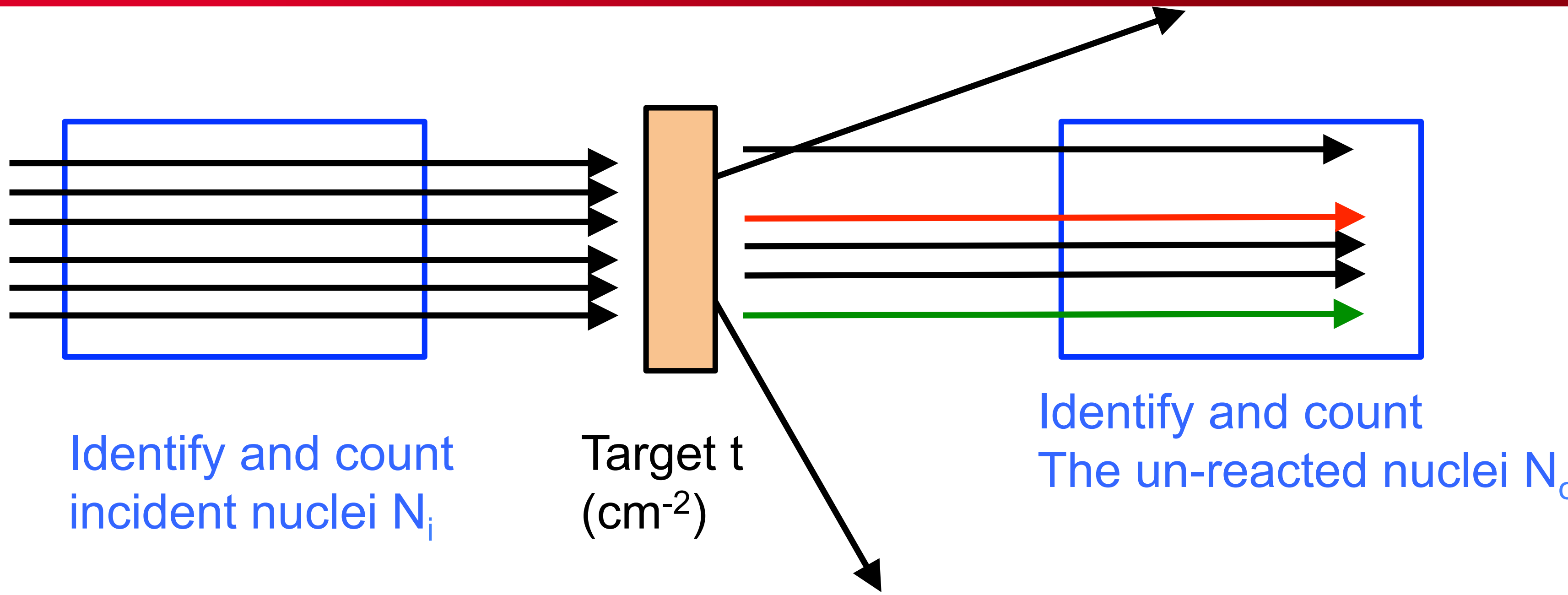

- In a slice δz of the target at a position z inside the target (0<z<t):

$$\delta N(z) = -N(z) \times \sigma_I \times \delta z$$

- Integrating along the target length, one gets:

$$N_o = N_i e^{-\sigma_I t} \quad \Rightarrow \quad \sigma_I = \frac{\ln\left(N_o / N_i \right)}{t}$$

$$\sigma_R = \sigma_I + \sigma_{inelastic}$$

Estimate of σ_{inel} may be important

Production of rare isotopes: history

- Fragmentation experiment at Bevalac, berkeley
- ^{48}Ca at 212 MeV/amu onto a Be target
- Yield of RIs after fragmentation found quite high
  W. D. Westfall et al., Phys. Rev. Lett. 43, 1859 (**1979**).

In conclusion, fragmentation of relativistic heavy ions seems firmly established as a practical means for the production of nuclei far from stability. The observation of these neutron-rich nuclei can be used to make quantitative tests of mass formulas. Beyond these global comparisons with mass formulas, the production cross sections appear to be sensitive to the microscopic level structure of the observed nucleus. In addition, the variations of the production cross sections indicate that, given increased beam intensities, which will be available in the near future, it is practical to determine the limit of stability up to $Z \cong 20$.

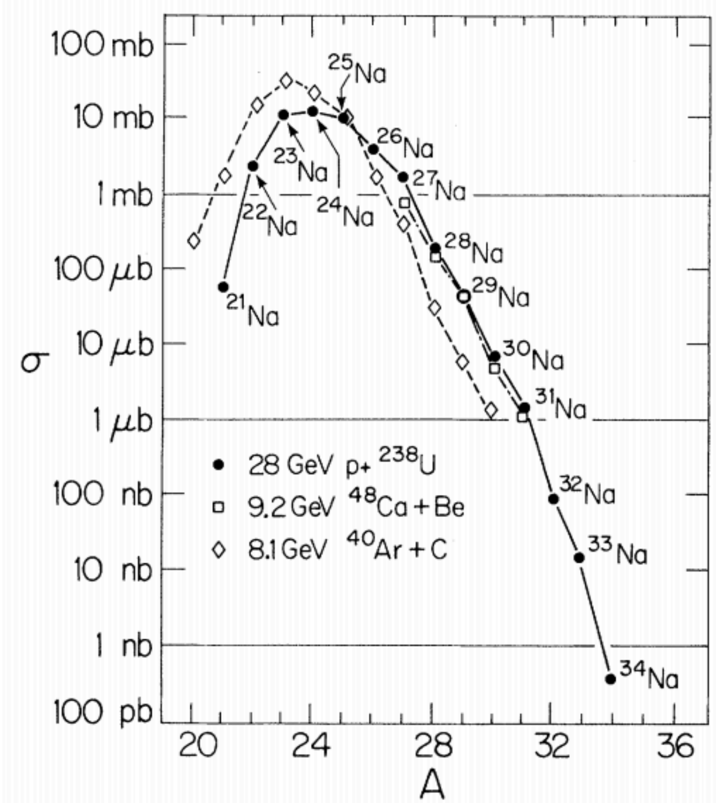

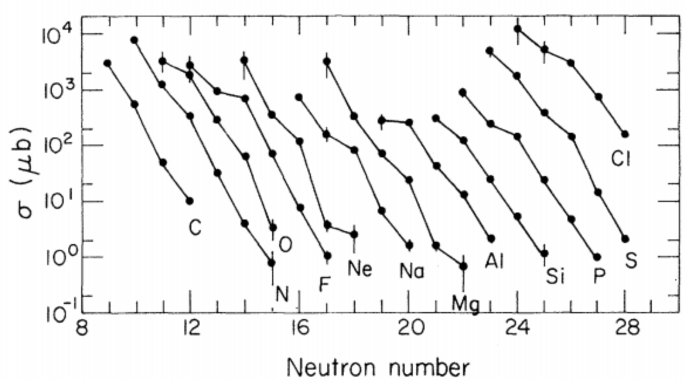

Radii of rare isotopes: history

- I. Tanihata, experiment at LBL (1984)
- ^{12}C, ^{16}O primary beams at 800 A MeV
- interaction cross section for Be, Li isotopes
- **I. Tanihata *et al.*, Phys. Rev. Lett. 55, 2676 (1985)**

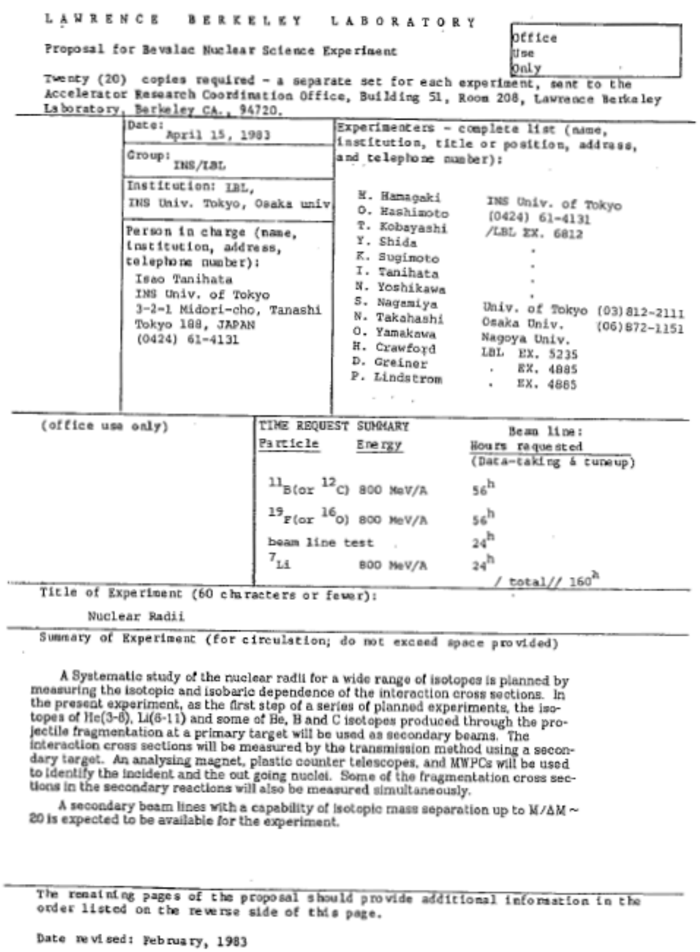

L A W R E N C E   B E R K E L E Y   L A B O R A T O R Y

Proposal for Bevalac Nuclear Science Experiment

Office Use Only

Twenty (20) copies required – a separate set for each experiment, sent to the Accelerator Research Coordination Office, Building 51, Room 208, Lawrence Berkeley Laboratory, Berkeley CA., 94720.

Date: April 15, 1983

Group: INS/LBL

Institution: LBL, INS Univ. Tokyo, Osaka univ

Person in charge (name, institution, address, telephone number):
Isao Tanihata
INS Univ. of Tokyo
3-2-1 Midori-cho, Tanashi
Tokyo 188, JAPAN
(0424) 61-4131

Experimenters – complete list (name, institution, title or position, address, and telephone number):

H. Hamagaki	INS Univ. of Tokyo (0424) 61-4131 /LBL EX. 6812
O. Hashimoto	
T. Kobayashi	
Y. Shida	
K. Sugimoto	
I. Tanihata	
N. Yoshikawa	
S. Nagamiya	Univ. of Tokyo (03) 812-2111
N. Takahashi	Osaka Univ. (06) 872-1151
O. Yamakawa	Nagoya Univ.
H. Crawford	LBL EX. 5235
D. Greiner	EX. 4885
P. Lindstrom	EX. 4885

(office use only)

TIME REQUEST SUMMARY

Particle	Energy	Beam line: Hours requested (Data-taking & tuneup)
^{11}B(or ^{12}C)	800 MeV/A	56^h
^{19}F(or ^{16}O)	800 MeV/A	56^h
beam line test		24^h
^{7}Li	800 MeV/A	24^h
		total// 160^h

Title of Experiment (60 characters or fewer):
Nuclear Radii

Summary of Experiment (for circulation; do not exceed space provided)

A Systematic study of the nuclear radii for a wide range of isotopes is planned by measuring the isotopic and isobaric dependence of the interaction cross sections. In the present experiment, as the first step of a series of planned experiments, the isotopes of He(3-8), Li(6-11) and some of Be, B and C isotopes produced through the projectile fragmentation at a primary target will be used as secondary beams. The interaction cross sections will be measured by the transmission method using a secondary target. An analysing magnet, plastic counter telescopes, and MWPCs will be used to identify the incident and the out going nuclei. Some of the fragmentation cross sections in the secondary reactions will also be measured simultaneously.

A secondary beam lines with a capability of isotopic mass separation up to M/ΔM ~ 20 is expected to be available for the experiment.

The remaining pages of the proposal should provide additional information in the order listed on the reverse side of this page.

Date revised: February, 1983

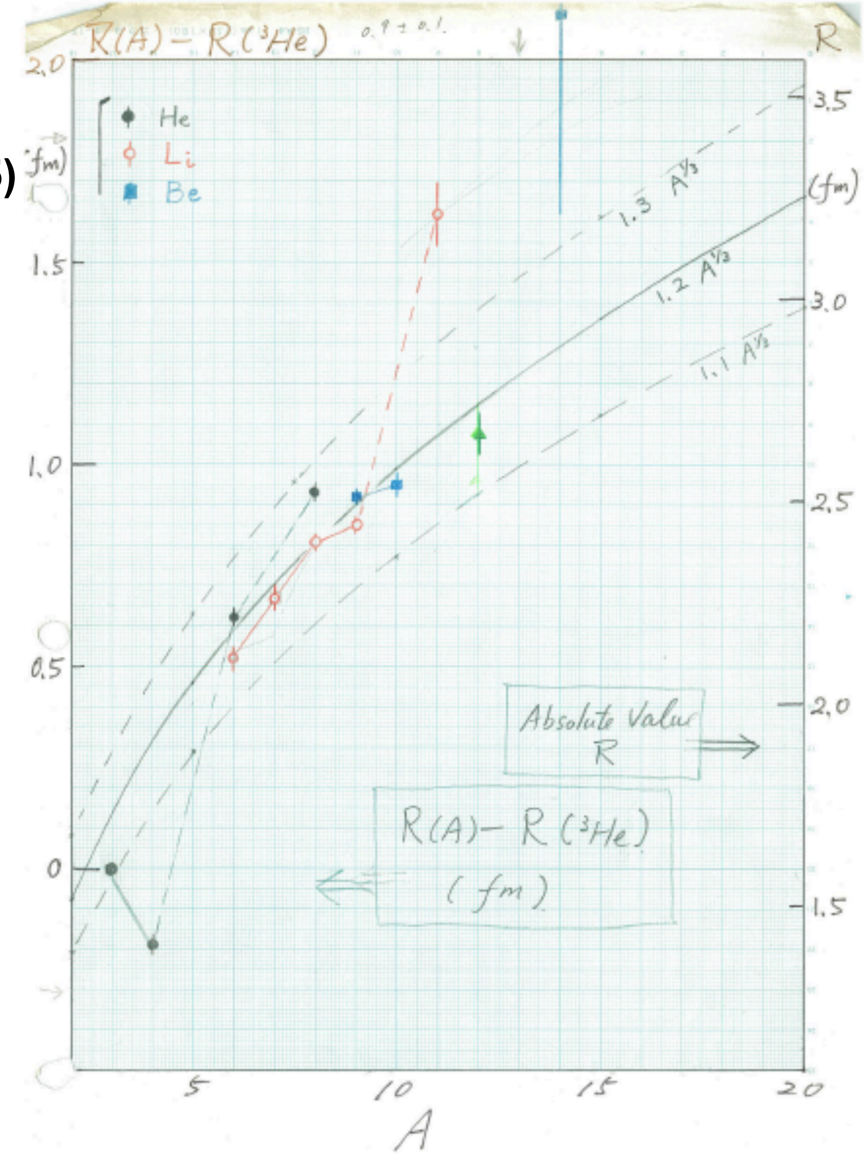

Archives (1983-1984) from I. Tanihata

Neutron Halos

- Interpretation of Halo nuclei as a diffuse neutron wave function extending « out » of the nucleus through tunneling

- Relation between radius and binding energy

  G. Hansen and B. Jonson, Eur. Phys. Letters 4, 409 (**1987**)

- A ^{9}Li-2n two body system is considered, with zero-binding energy of the 2n system

$$\psi(r) \propto \frac{e^{-r/\rho}}{r}$$ with $\rho = \hbar / \sqrt{2\mu B}$, μ reduced mass, B two-neutron binding energy

- 2n halo rms radius

$$\langle r^2 \rangle = \frac{\rho^2}{2(1+x)}(1+2x+2x^2+4x^3(1+\pi^{-2}))$$

with $x = R/\rho$, R the square-well potential radius

- Total rms matter radius

$$\langle r_m^2 \rangle^{1/2} = \left(\frac{M}{M+m}\right)^{1/2} \left[\langle r_c^2 \rangle + \frac{m}{M+m}\langle r^2 \rangle\right]^{1/2}$$

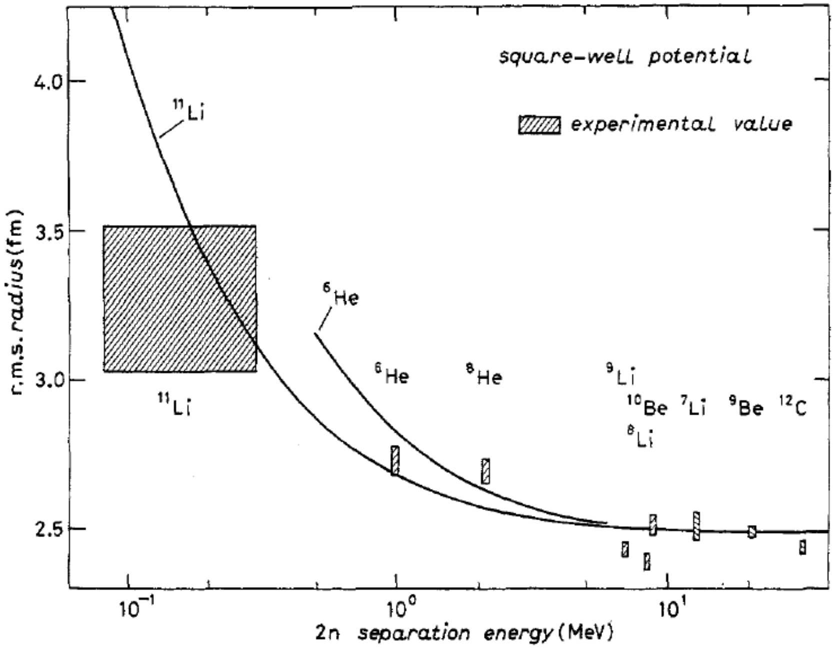

Overview of neutron Halos

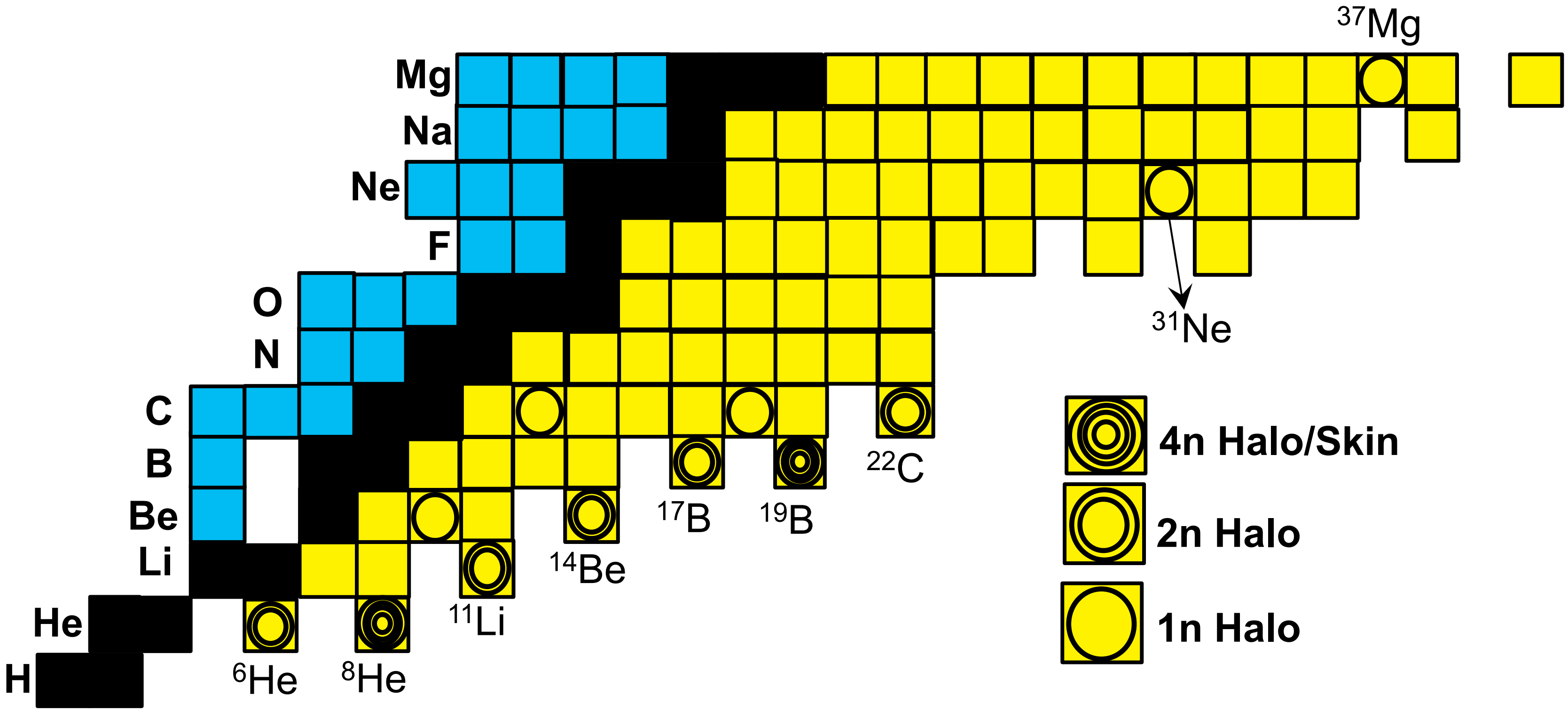

S-wave dominate: ^{11}Be, ^{15}C , ^{19}C,
P-wave dominate: ^{6}He, ^{8}He, ^{31}Ne, ^{37}Mg
^{11}Li: mix of *s* wave and *p* wave
^{14}Be: mix of *s* wave and *d* wave
…

Necessary conditions:
- ❑ Small separation energy (<1MeV)
- ❑ Low orbital angular momenta (*l*=0 or 1)

T. Aumann and T. Nakamura, Phys. Scr. T152, 014012 (2013).

Neutron Halos: other observables / characteristics

- Narrow momentum distribution (s-wave and p-wave halos)
  Heisenberg principle: $\Delta x \Delta p_x \cong$ hbar, ex. For ^{11}Li: Δp_x = 100 MeV/c

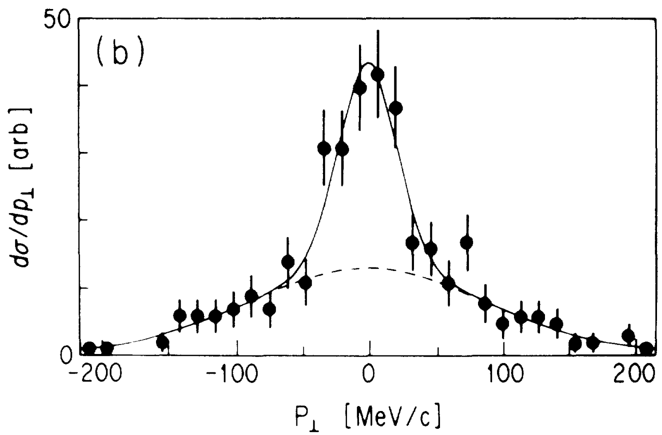

Kobayashi *et al.*, Phys.Rev.Lett. **60** (1988)

- Low-lying soft dipole mode
  Recently observed in ^{11}Li from (d,d')
  R. Kanungo *et al.*, PRL 114, 192502 (2015)

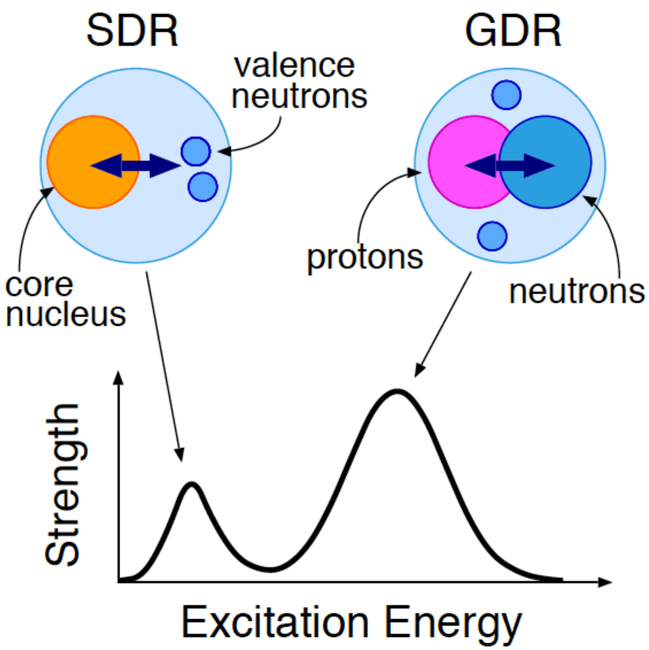

- Di-neutron correlations in momentum space for 2N halos (Borromean nuclei)
  Ex. Coulomb breakup
  Ex. Exclusive (p,p2n) measurements

- Spectroscopy, charge radius,…

Microscopic description of neutron halos (^{11}Li case)

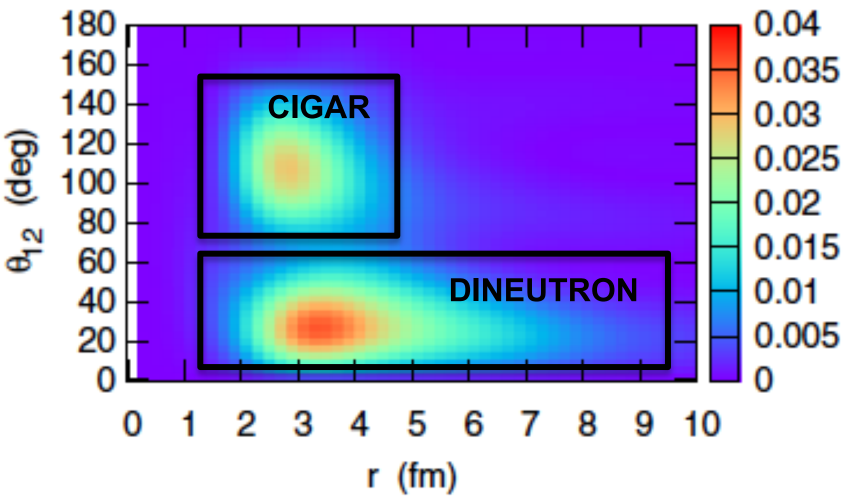

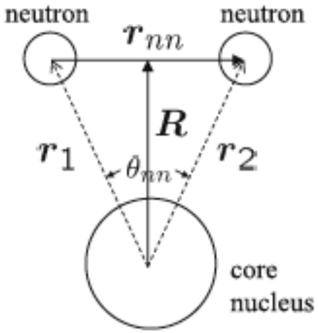

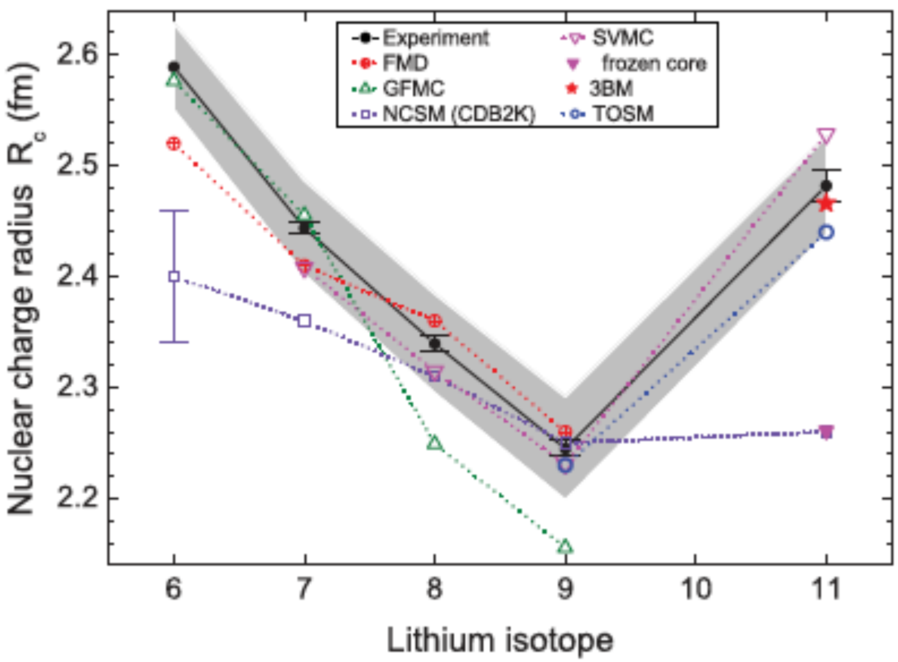

- 3-body model often used to describe 2N halos
  Hagino and Sagawa, PRC 72 044321 (2005)

- Ab-initio calculations possible but challenging (ex. No Core Shell Model)

Nortershauser, Neff *et al.*, PRC 84 (2011)
Data from Nortershauser *et al.*, PRA 83 (2011)

Halos in heavier systems

- Systematic search for halo nuclei in spherical nuclei
- Only in s,p orbitals with very low binding energy
- very few candidates in regions not accessible with current nor next-generation facilities

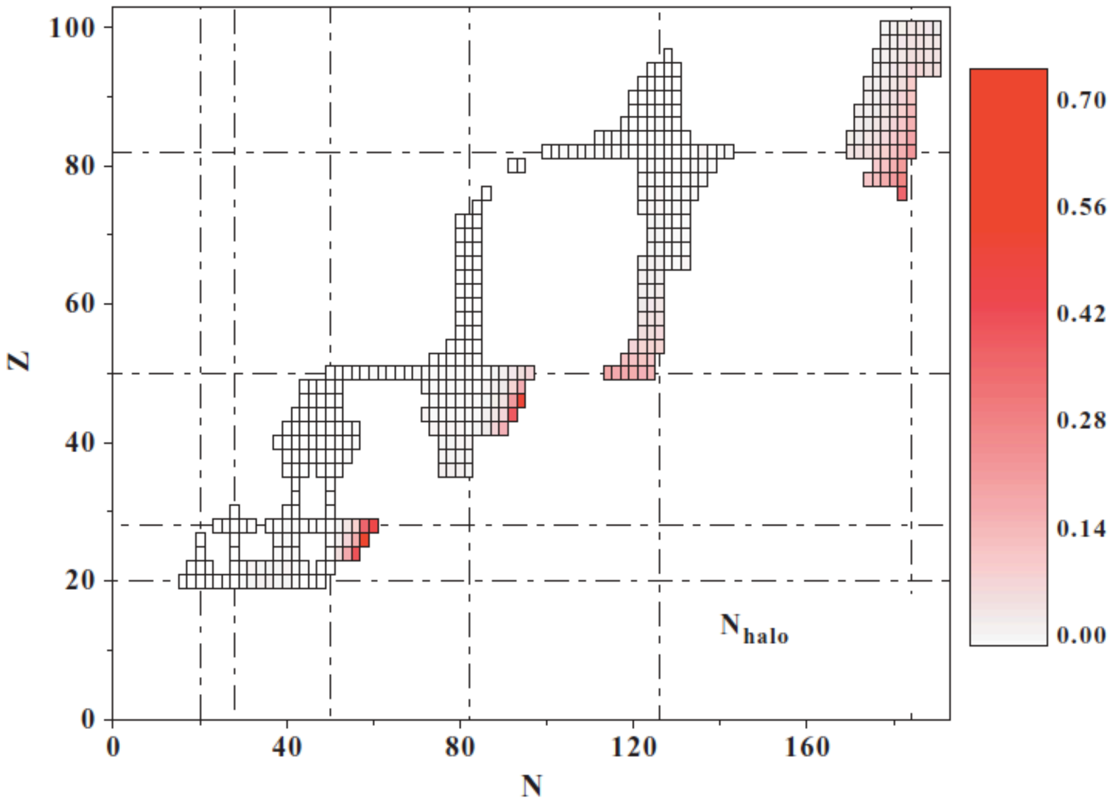

$$N_{halo} = \int_{r_0}^{+\infty} \rho(r) r^2 \, dr$$

Beyond the radius r0 : core density is one order of magnitude smaller than the halo one.

EDF with **Sly4 Skyrme** force

V. Rotival, K. Bennaceur and T. Duguet, Phys. Rev. C 79, 054309 (2009)

Matter radii for heavier nuclei

- Extension of interaction cross sections up to Ne, Mg isotopes
- Extraction of radius model dependent (density profile)
- Consistent with the development of a **neutron skin** – deformation to be taken into account

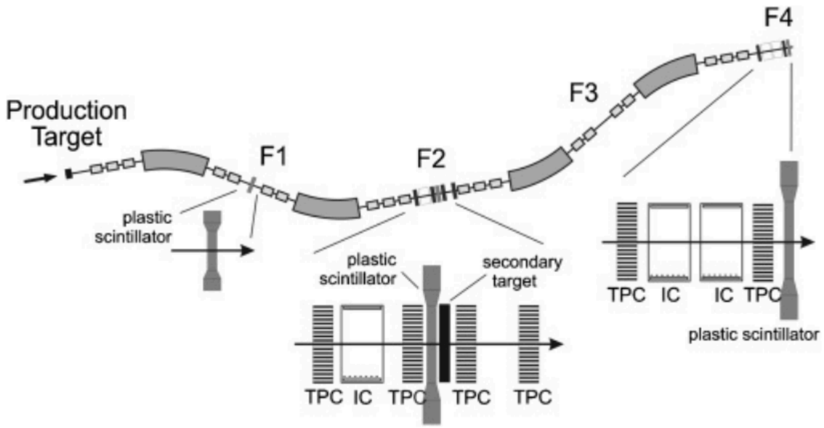

TABLE I. Measured interaction cross sections and the rms [R^m_{rms}(ex)] matter radii for $^{32-35}$Mg extracted from them are compared with the HF and RMF predictions.

Isotope	σ_I^{C} (mb)	σ_I^{H} (mb)	R^m_{rms} (ex) (fm)	HF [6][a] (fm)	RMF [20] (fm)
^{32}Mg	1331(24)	523(47)	3.17 ± 0.11	3.20	3.21
^{33}Mg	1320(23)	552(45)	3.19 ± 0.03	3.23	3.26
^{34}Mg	1372(46)	568(90)	3.23 ± 0.13	3.26	3.33
^{35}Mg	1472(70)	657(160)	3.40 ± 0.24	3.30	3.38

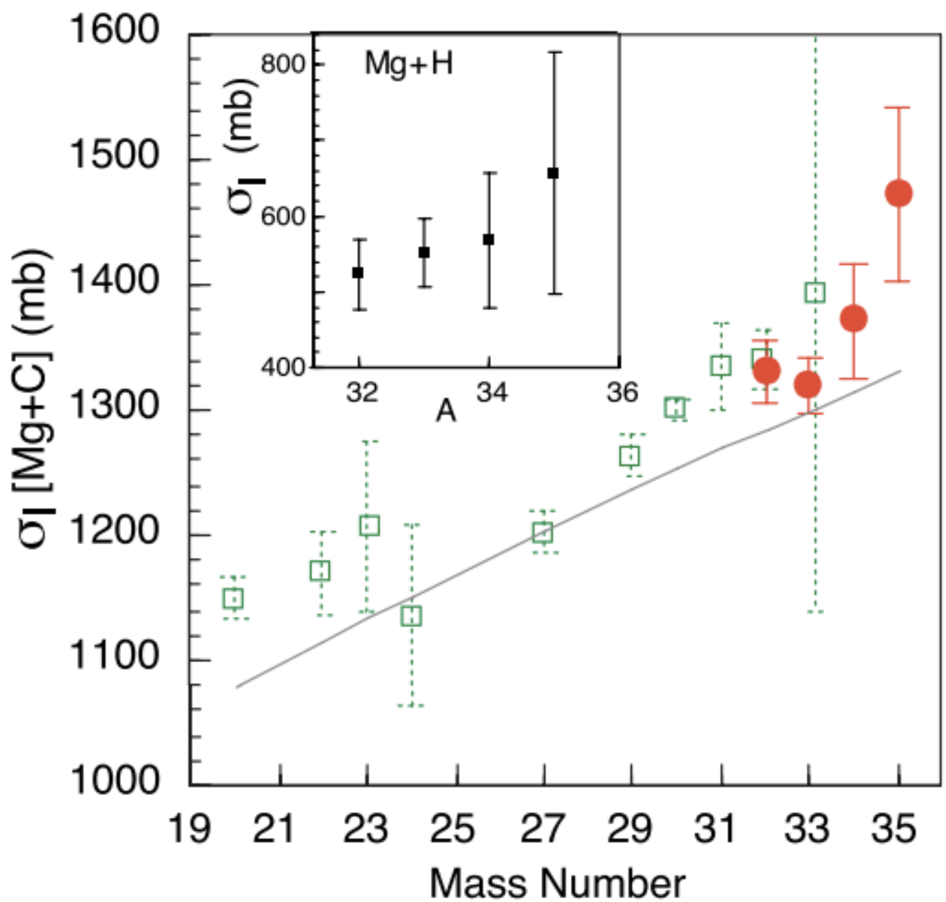

R. Kanungo *et al.*, Phys. Rev. C 83, 021302(R) (2011)

Neutron skins, EoS and neutron stars

$$\Delta r_{np} = \langle r_n^2 \rangle^{1/2} - \langle r_p^2 \rangle^{1/2}$$

$\Delta r_{np} \propto L$ Slope of the symmetry energy

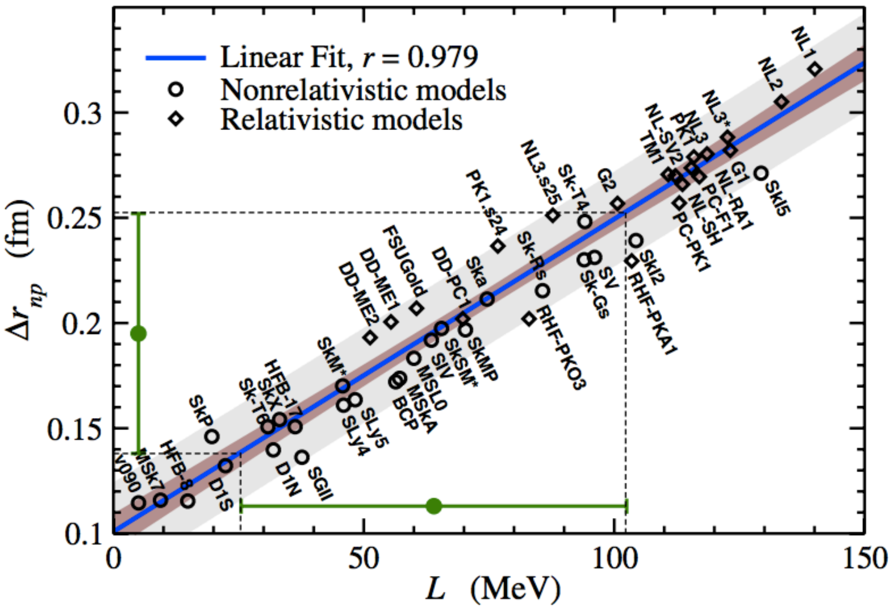

X. Roca-Maza *et al.*, PRL 106, 252501 (2011)

2N+3N forces
Relation bewtween M and R, varying E_{sym}

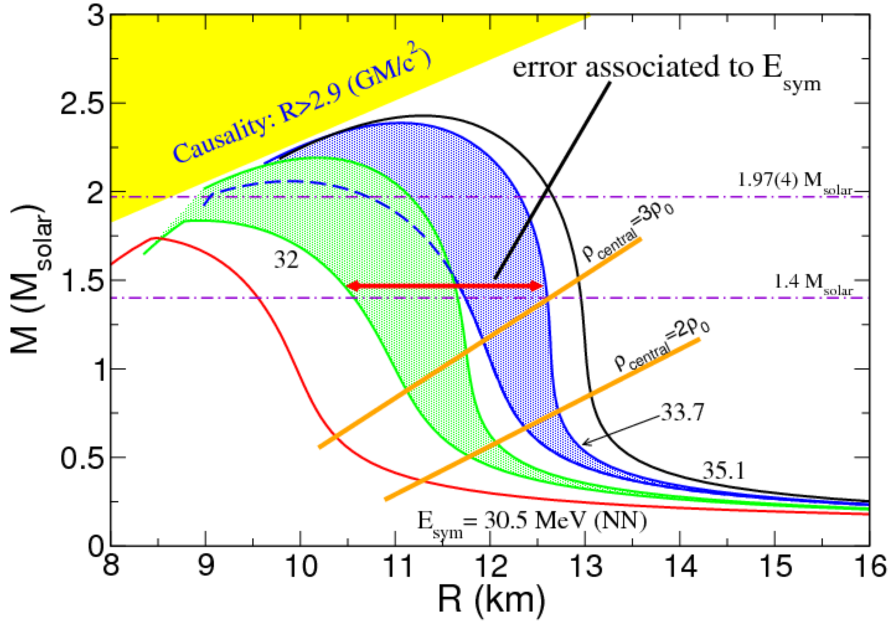

S. Gandolfi *et al.*, PRC 85, 032801(R) (2012)

The faster the symmetry energy increases with density (L), the largest the size of the neutron skin in heavy nuclei

See lecture by Christian Drischler

Lecture 1: Radii, neutron skins and halos

- Matter radii, skins and halos: history and definitions

- Hyperfine structure and isotopic shifts

- Electron elastic scattering
  - The charge form factor
  - Physics case: the historical ^{208}Pb example
  - RIB: The SCRIT facility and the LISE project at FAIR

Electric probe: Charge radius & density

- Weak interaction experiments
  - The weak charge form factor
  - Physics case: the PREX experiment and neutron skin of ^{208}Pb

Weak probe: Neutron radius

- Strong interaction experiments
  - Proton elastic scattering
  - Coherent $\pi 0$ photoproduction
  - Antiprotonic atoms

- Indirect methods (examples)
  - Inelastic scattering
  - Dipole polarizability
  - Giant Resonances

Hadronic probes: Matter radius

Fine and hyperfine atomic structure

- **Fine** structure: Schrodinger equation + relativistic corrections + electron spin effects
- **Hyperfine** structure: splitting of fine structure due to coupling of electron and nuclear spins

fine structure
$\lambda \cong$ 300 nm
$f = c/\lambda = 10^{15}$ Hz

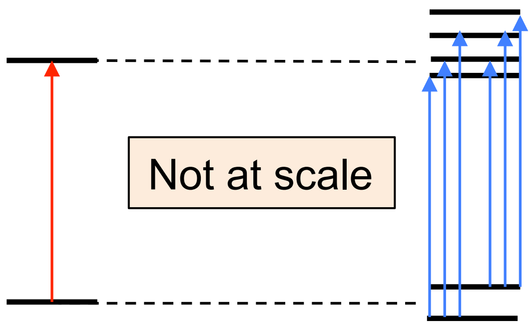

Few GHz (ppm)

Hyperfine structure = hyperfine multiplets
Nuclear spin, magnetic and quadrupole moment

- Excitation via **laser scanning**

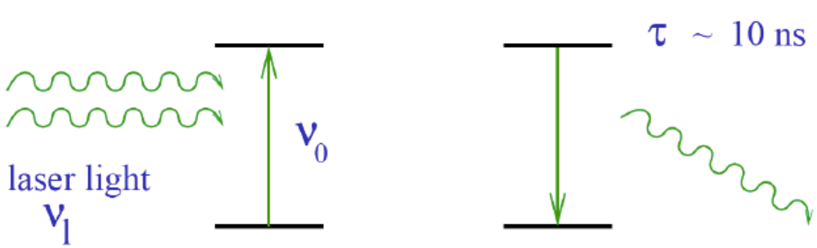

Resonant absorption ($\nu_1 = \nu_0$) Spontaneous emission

Natural width: $\Delta\nu = 1/2\pi\tau$ (Heinsenberg)
$\cong$ 16 MHz

Typical laser bandwidth $\cong$ < 1 MHz

i.e. resolution of natural width reached

$\sigma = 3\lambda^2 / 2\pi$ (larger than size of atom)

Isotopic shift from the hyperfine structure

- **Inner electronic wavefunctions (orbitals) significantly overlap with the atomic nucleus**
- Finite size of the nucleus leads to a **shift in energy of electronic transitions** compared to expectation from a point like nucleus
- **Isotopic shift** is the difference of the transition energy from one isotope to another

$$\delta\nu^{AA'} = \nu^{A'} - \nu^{A}$$

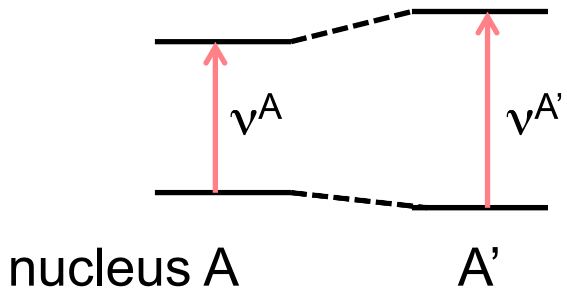

- The Isotopic shift can be decomposed into two parts:

$$\delta\nu_{IS}^{AA'} = \boxed{\delta\nu_{MS}^{AA'}} + \boxed{\delta\nu_{FS}^{AA'}}$$

  - **Nuclear volume (or field) shift** (FS): change of size (**charge radius**) of the nucleus
  - **Finite nuclear mass shift** (MS): change of mass of the nucleus from A to A'

Field shift $\delta\nu_{FS}^{AA'}$

$$\delta\nu_{IS}^{AA'} = \delta\nu_{MS}^{AA'} + \delta\nu_{FS}^{AA'}$$

- Electronic levels with finite probability $|\psi(0)|^2$ inside the nucleus are less bound
- At first order this finite nuclear size (FNS) contribution is given by

$$E_{FNS} = \frac{Ze^2}{6\varepsilon_0}\langle r_c^2\rangle|\psi(0)|^2 \quad \text{with} \quad \langle r_c^2\rangle = \frac{1}{Ze}\int \rho_c(r) r^2 d^3r$$

- E_{FNS} accessible experimentally only for hydrogen-like atoms
- Comparing two isotopes A and A', one gets the FS contribution to the isotopic shift

$$\delta\nu_{FS}^{AA'} = \frac{Ze^2}{6h\varepsilon_0}\Delta|\psi(0)|^2\left(\langle r_c^2\rangle^{A'} - \langle r_c^2\rangle^{A}\right)$$

$$= \frac{Ze^2}{6h\varepsilon_0}\Delta|\psi(0)|^2\,\delta\langle r^2\rangle^{AA'} = \boxed{F\,\delta\langle r_c^2\rangle^{AA'}}$$

F called the Field Shift constant

Mass shift $\delta\nu_{MS}^{AA'}$

$$\delta\nu_{IS}^{AA'} = \delta\nu_{MS}^{AA'} + \delta\nu_{FS}^{AA'}$$

- Motion of the nucleus in the atom center of mass frame

$$\vec{P}_{nucl} = -\sum_{electrons\, i} \vec{p}_i$$

- kinetic energy of the nucleus

$$E_{kin} = \frac{P_{nucl}^2}{2M_{nucl}} = \frac{1}{2M_{nucl}}\left(\sum_i p_i^2 + \sum_{ij, i\neq j} \vec{p}_i \cdot \vec{p}_j\right)$$

- change of nuclear motion in the mass frame when nucleons are added IMPLIES an effect on electronic levels and transition energy

$$\delta\nu_{MS}^{AA'} = \frac{M_A - M_{A'}}{M_A M_{A'}}(K_{NMS} + K_{SMS}) \propto A^{-2}$$

- Two origin of this Mass Shift:
  - effect on single orbitals (p_i^2) -- called **Normal Mass Shift** (NMS): **$K_{NMS} = m_e\nu$ (first order)**
  - effect from the change of correlation term ($p_i.p_j$) – called **Specific Mass Shift** (SMS)

- **Specific Mass Shift** cannot be calculated for systems with more than 2 electrons

Isotopic shift and charge radius

$$\delta\nu^{A,A'} = (K_{NMS} + K_{SMS}) \times \frac{m_{A'} - m_A}{m_{A'} m_A} + F \times \boxed{\delta\left\langle r_c^2 \right\rangle^{A,A'}}$$

- Need measurements on **THREE isotopes** of the same fine structure transition to extract emipirically F and (K_{NMS}+K_{SMS})

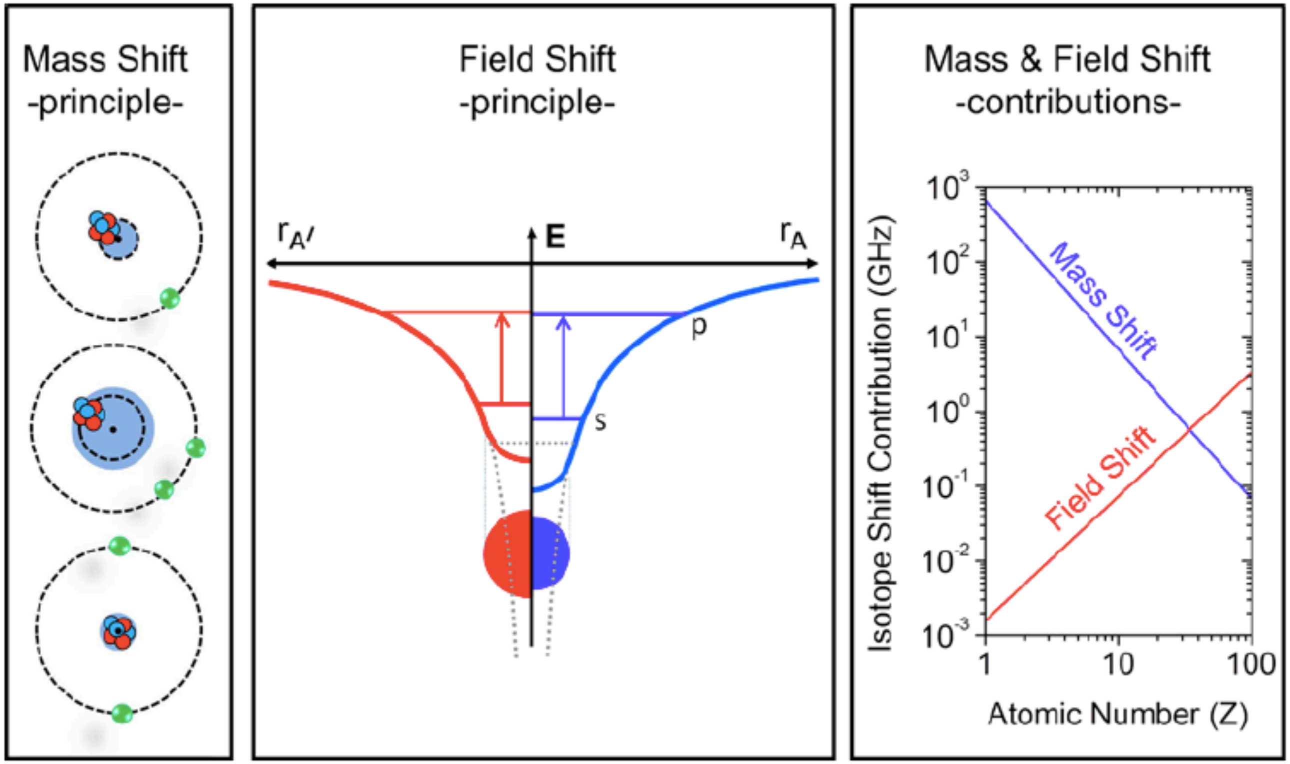

From W. Nörtershäuser and C. Geppert, the Euroschool on Exotic Beams, vol. IV, chapter 6, 2014

Isotopic shifts in Polonium isotopes

$$\delta\nu^{A,A'} = (K_{NMS} + K_{SMS}) \times \frac{m_{A'} - m_A}{m_{A'} m_A} + F \times \delta\langle r_c^2 \rangle^{A,A'}$$

Po (Z=84)

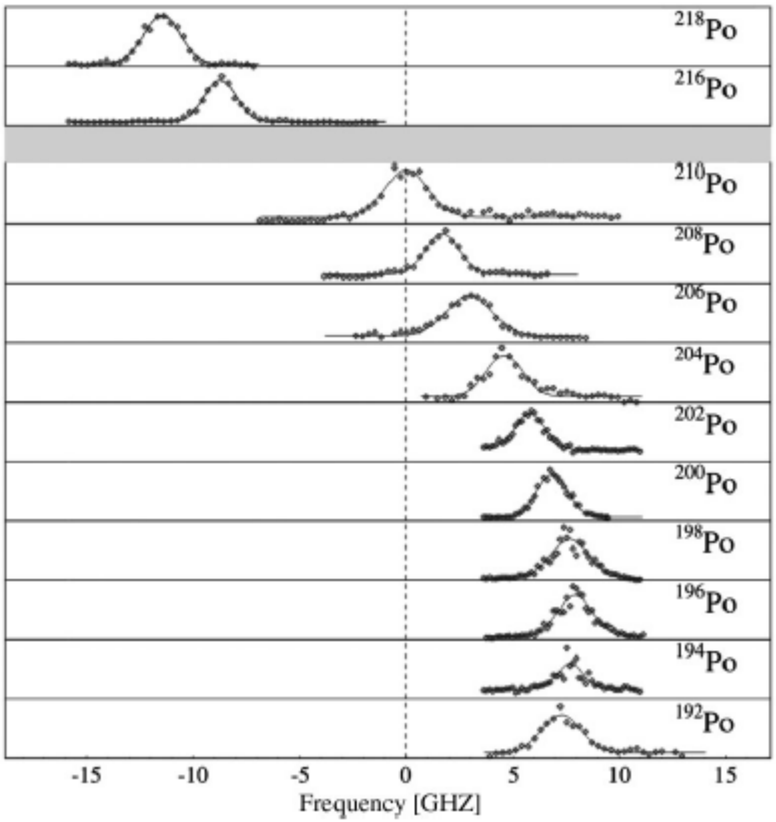

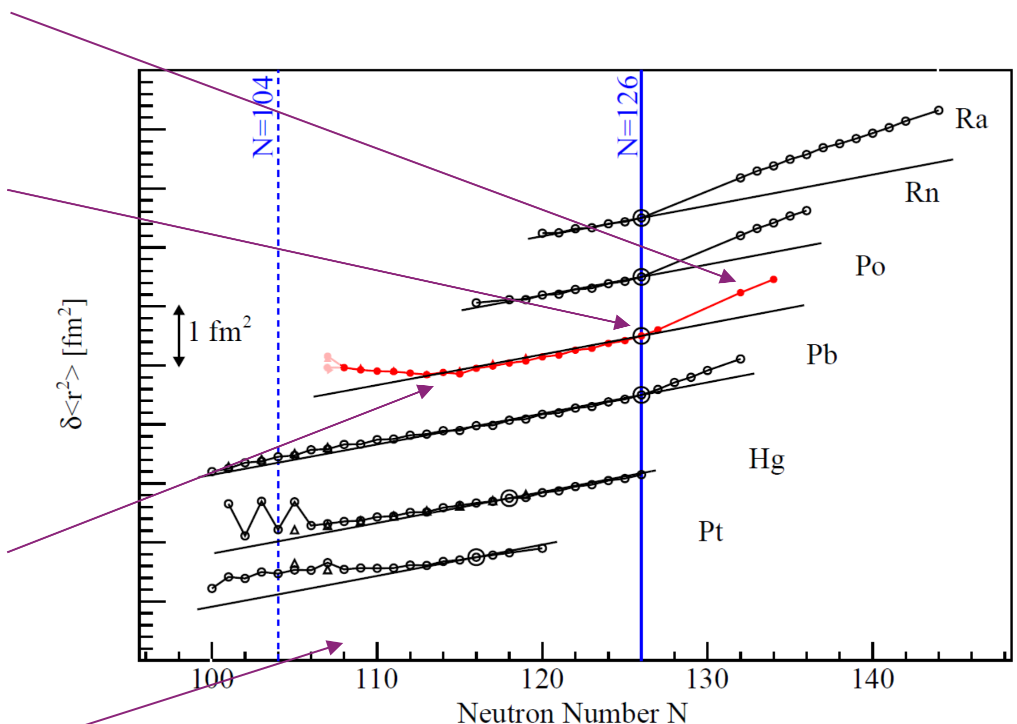

T. E. Cocolios *et al.,* Phys. Rev. Lett, 106, 052503 (2011)

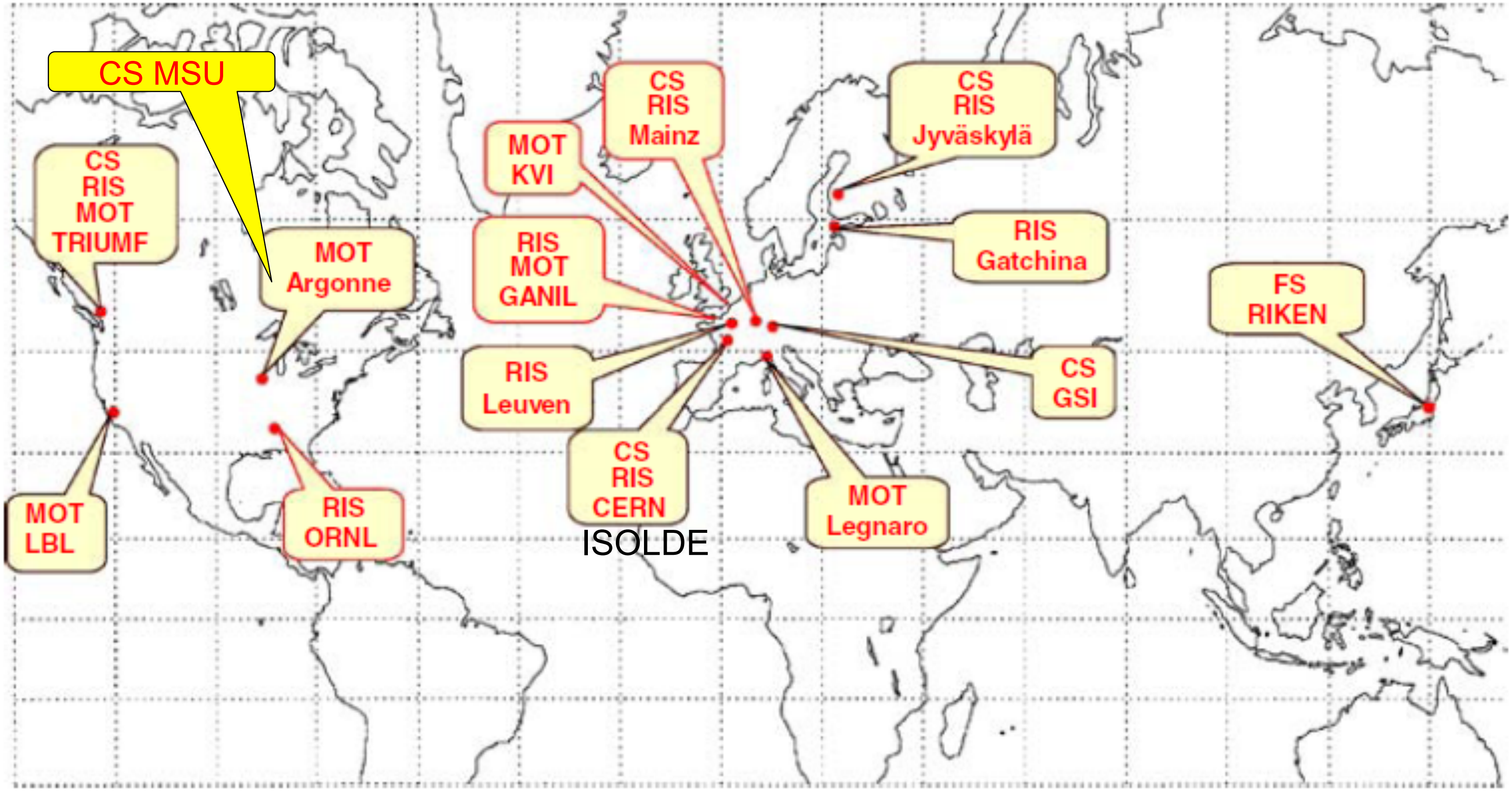

On-going laser spectroscopic activities at accelerators and nuclear reactors worldwide for determination of nuclear ground state properties. The following techniques are presently applied: *CS* collinear spectroscopy, *RIS* resonance ionization spectroscopy, and *MOT* spectroscopy in a magneto-optical trap, and *FS* fluorescence spectroscopy

H.-J. Kluge, Hyperfine Interact 196, 295 (2010)
and updated; slide from M. Kowalska (PISA school, 2015)

Laser spectroscopy with RIBs

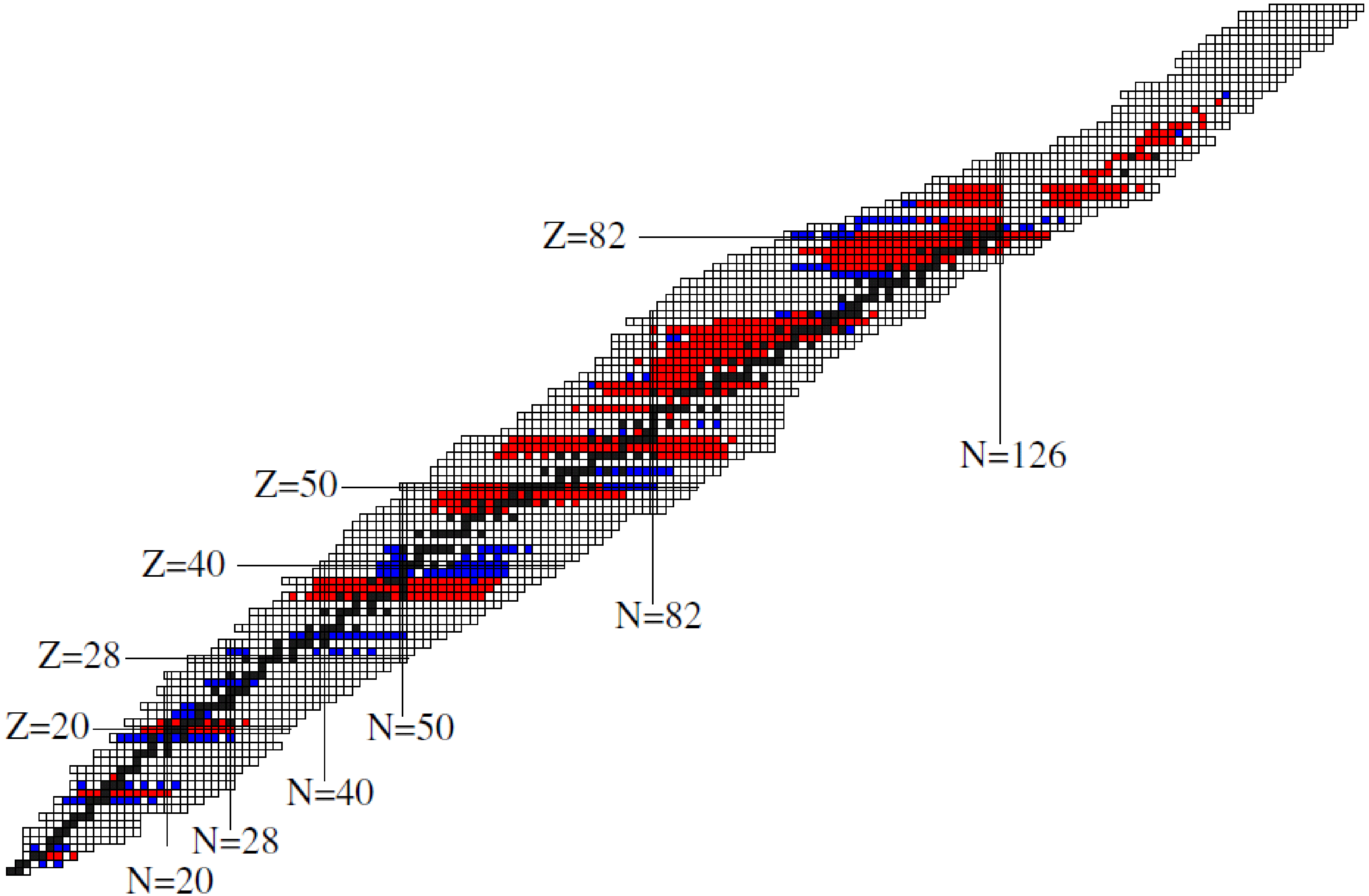

Laser spectroscopy with RIBs at Isolde

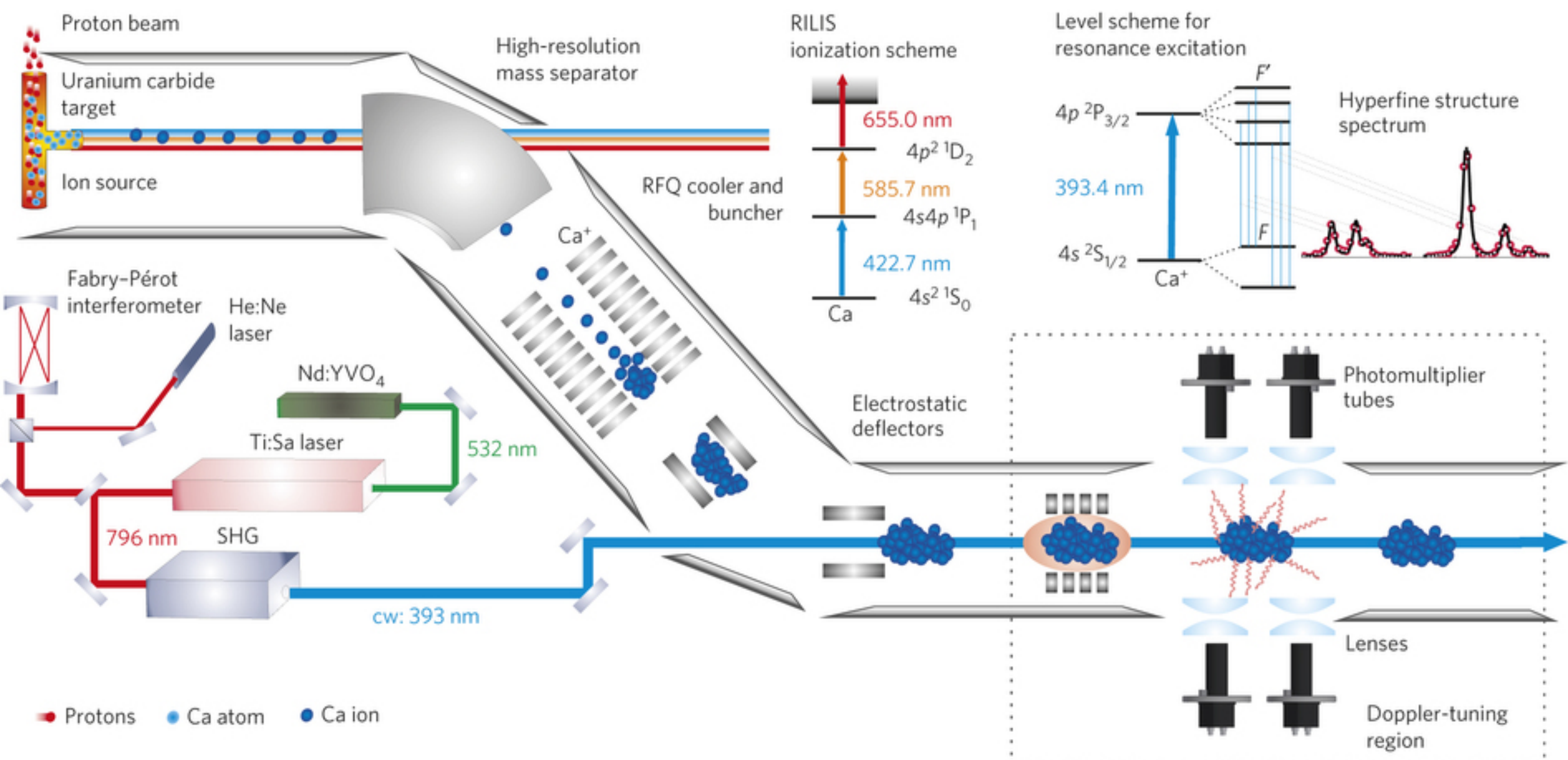

R.F. Garcia Riuz *et al.*, Nature Physics **12**, DOI: 10.1038/NPHYS3645 (2016)

Physics case 1: charge radii of Ca isotopes

- Hyperfine structure spectra measured for Ca isotopes in the 393-nm 4s $^2S_{1/2}$ ➔ 4p $^2P_{3/2}$ transition
- Weak but gradual erosion of the proton core as neutrons are added is predicted by ab initio theories (polarization effect)
- Predicted polarization is not enough to explain the data

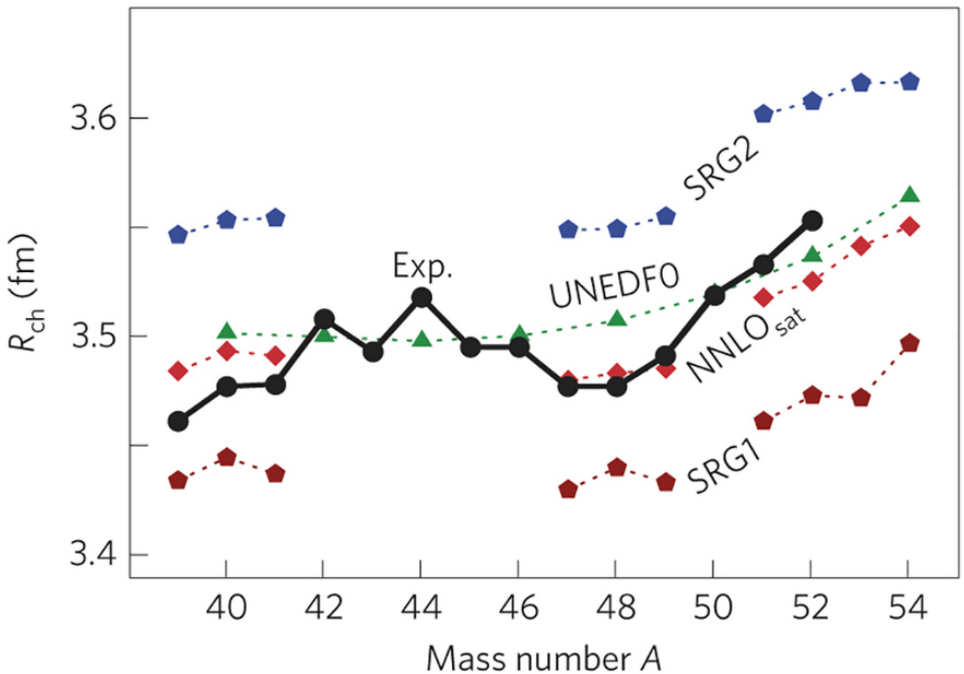

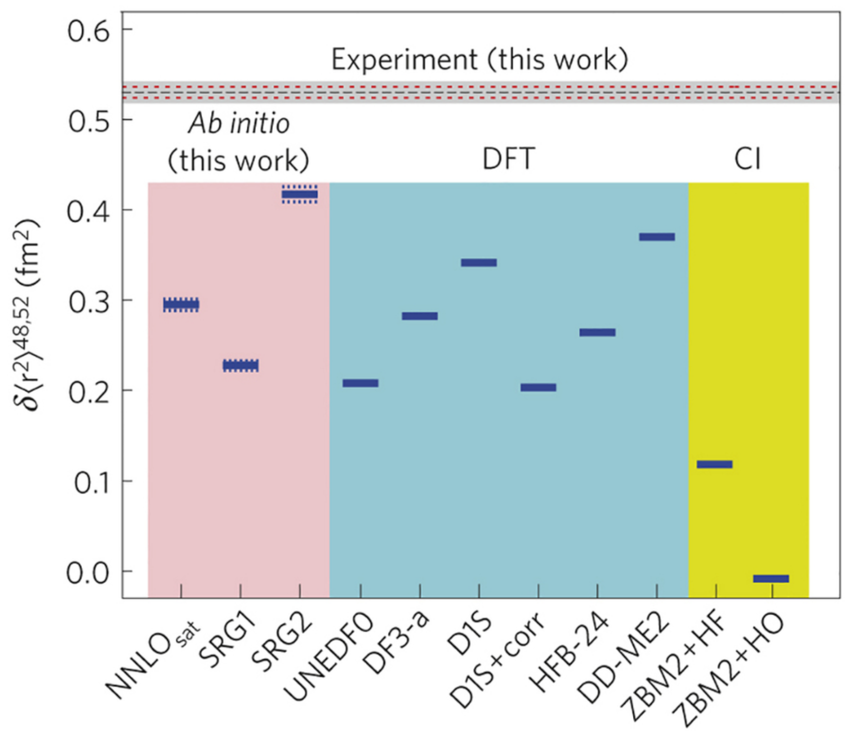

R.F. Garcia Riuz *et al.*, Nature Physics **12**, DOI: 10.1038/NPHYS3645 (2016)

Muonic atoms

- Muon's mass = 200 e^- mass

i.e. Bohr (atomic) radius 200 smaller

In ^{208}Pb: muon's mean radius is inside the nucleus

- Isotope shifts: factor 10^{-2}

  (versus 10^{-4} – 10^{-6} for electrons)

- **Technique:**
- Muons produced at accelerators (in decay of pi mesons), e.g at PSI-Zurich
- Bombard target made of isotope(s) of interest
- Muons are captured in high-n orbits and cascade down to 1s orbits
- Emitted photons are detected
- Obtain directly charge-distribution parameters

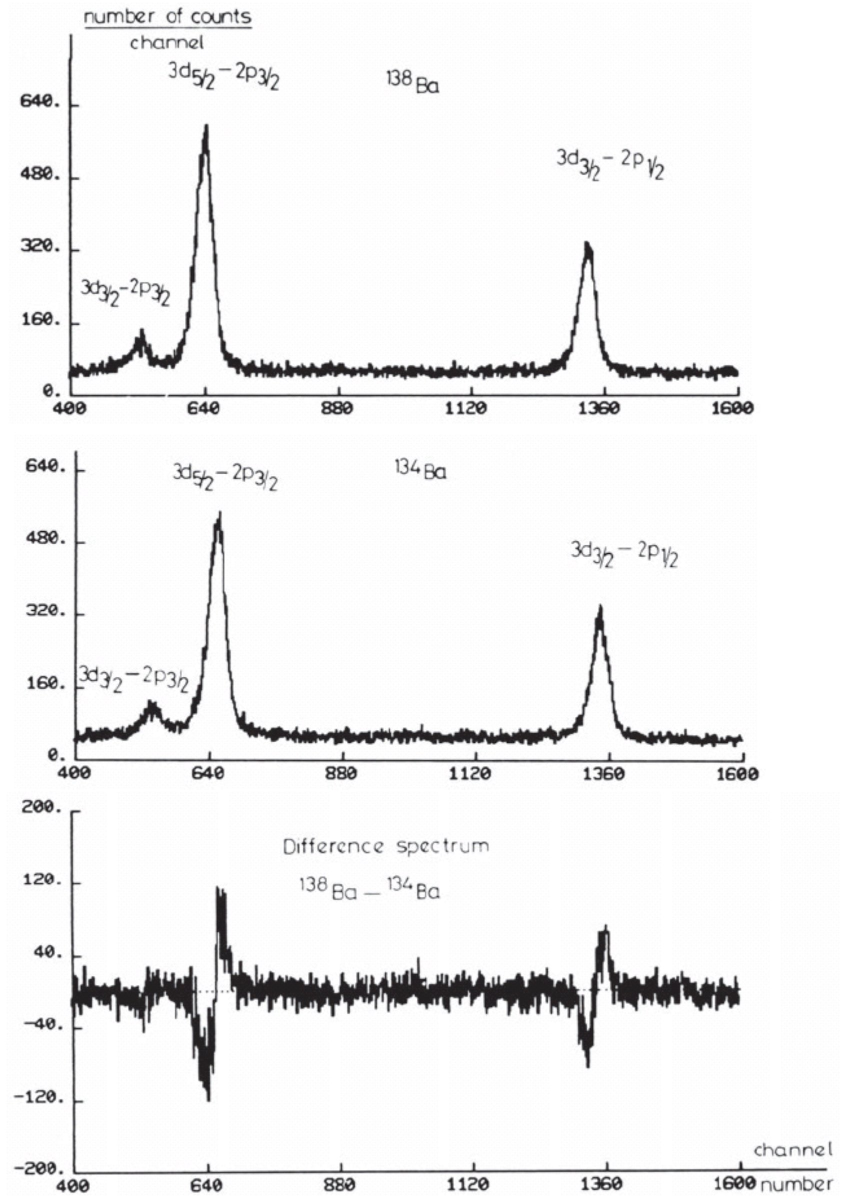

Lecture 1: Radii, neutron skins and halos

- Matter radii, skins and halos: history and definitions
- Hyperfine structure and isotopic shifts
- Electron elastic scattering
  - The charge form factor
  - Physics case: the historical ^{208}Pb example
  - RIB: The SCRIT facility and the LISE project at FAIR
- Weak interaction experiments
  - The weak charge form factor
  - Physics case: the PREX experiment and neutron skin of ^{208}Pb
- Strong interaction experiments
  - Proton elastic scattering
  - Coherent π0 photoproduction
  - Antiprotonic atoms
- Indirect methods (examples)
  - Inelastic scattering
  - Dipole polarizability
  - Giant Resonances

Charge radius & density

Matter radius

Electron elastic scattering

- **Light diffraction** off an aperture:
- Far source
- Far detection

} Fraunhofer diffraction

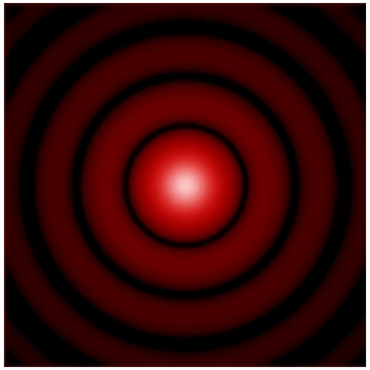

- Pattern oscillations (Airy) : $\Delta\theta = \lambda / (2R)$

➔ Depends on the **size of the aperture**

- **Electron scattering** off a nucleus:

$$\lambda = \frac{\hbar}{p}$$

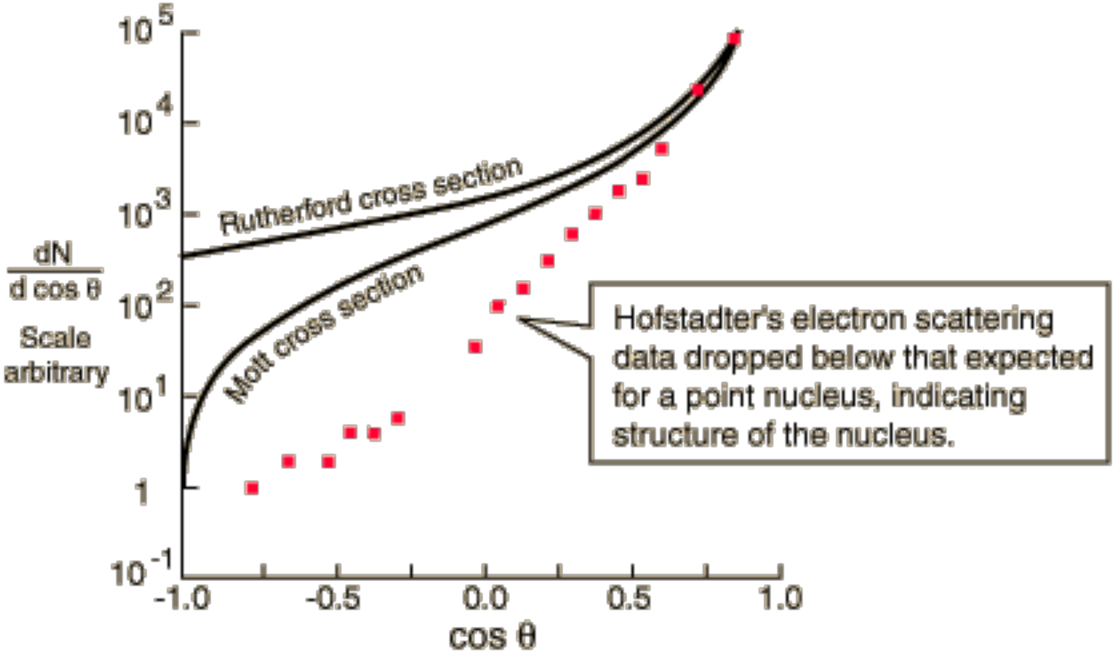

Mott cross section and charge form factor

B. Frois and C.N. Papanicolas,
Ann. Rev. Nucl. Part. Sci. **37**, 133 (1987)

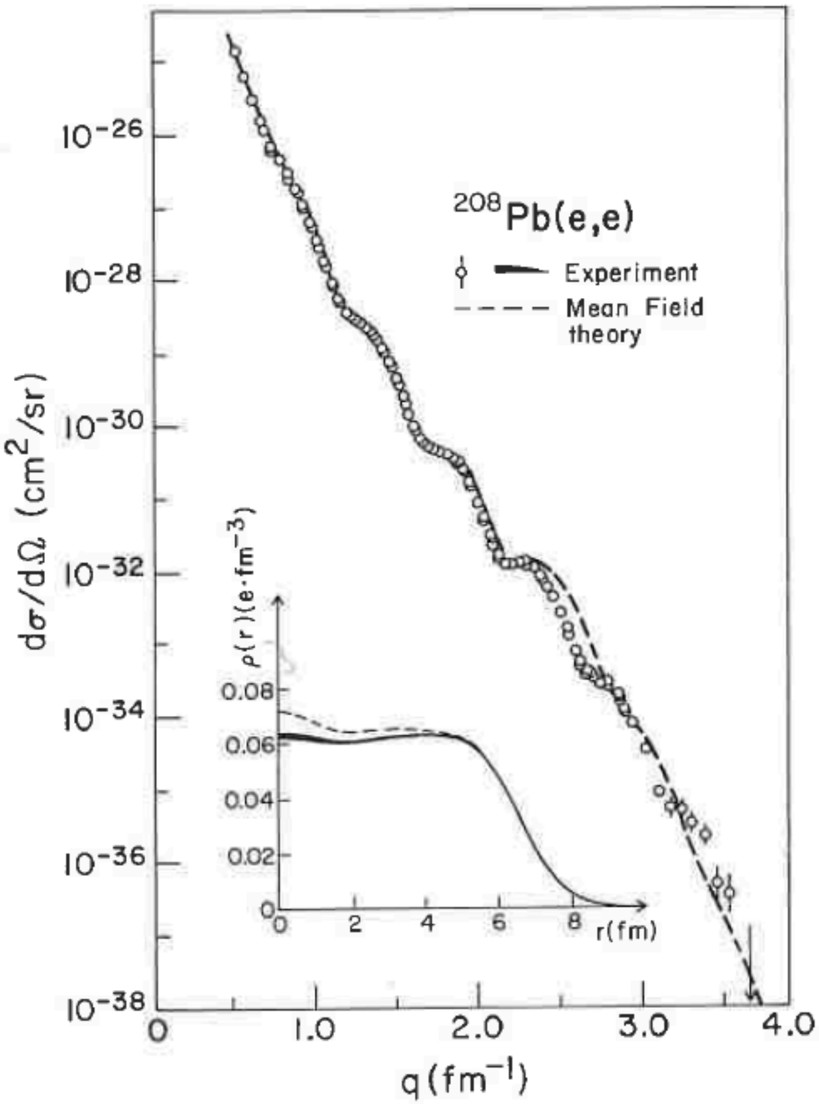

- **Elastic scattering cross section:**
  (assuming ONE exchanged direct photon)

$$\frac{d^2\sigma}{dE d\Omega} = \sigma_{Mott} \left| F(q) \right|^2$$

q: transfered momentum

$$q^2 = 4EE' \sin^2(\frac{\theta}{2})$$

- **Charge form factor:**

$$F(q) = \left\langle \phi_{k_f} \middle| V \middle| \phi_{k_i} \right\rangle$$

$$= \int e^{\frac{i\vec{q}.\vec{r}}{\hbar}} \rho(\vec{r}\,') d^3\vec{r}\,'$$

Historical example: the ALS facility

- **ALS** electron facility (Linear Accelerator of Saclay) from 1970 (decommissioned in 1990)
- Electron energy from **150 to 700 MeV**
- High performances (at the time): duty cycle of 2%, intensity up to 100 μA
- **High resolution** spectrometers dedicated to (e,e') and (e,e'p)

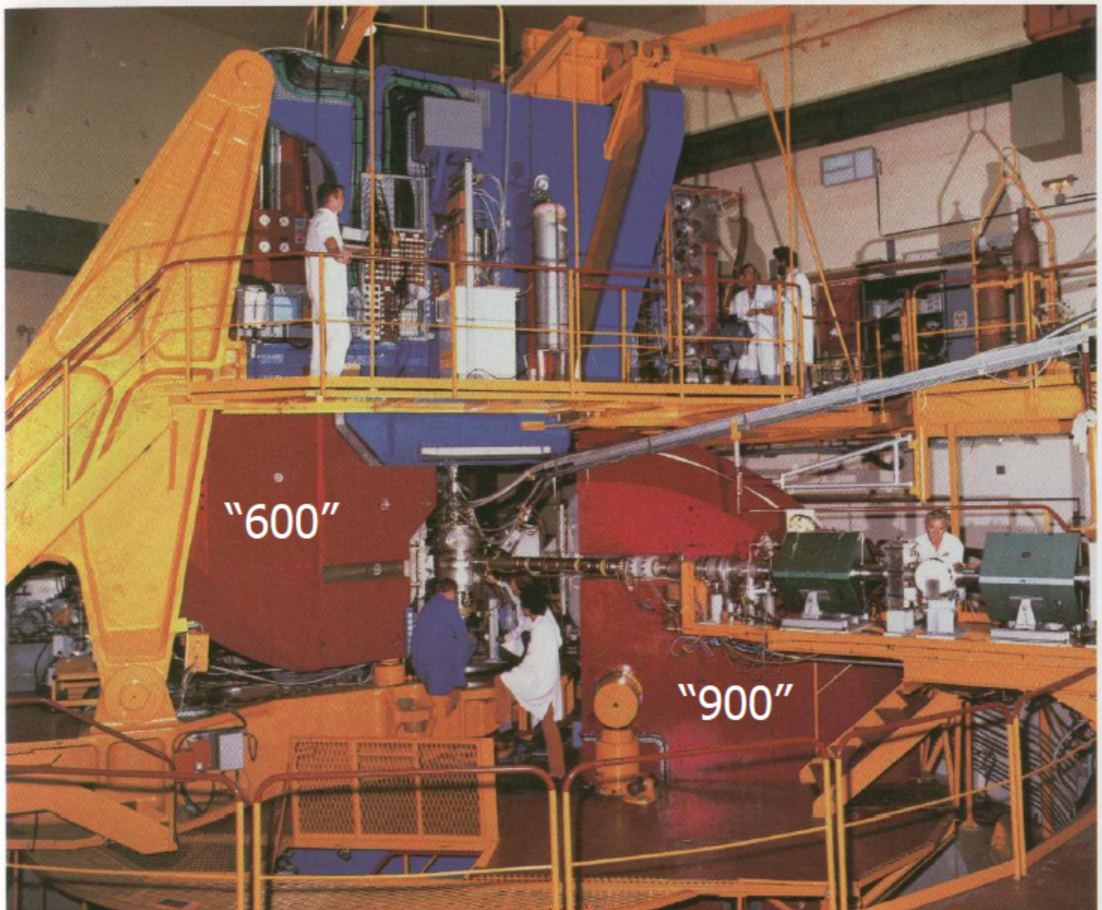

Ensemble des deux spectromètres utilisés pour la diffusion d'électrons.

Certaines expériences exigent que l'on soit capable de distinguer des processus qui donnent lieu à émission de particules dont la quantité de mouvement est très voisine. Seul un instrument capable de séparer des valeurs très proches permet une observation fine. Les spectromètres conçus à l'ALS ont des performances qui en font l'un des meilleurs appareillages sur le plan mondial.

La salle HE1, en particulier, possède un ensemble de deux gigantesques aimants, le tout pesant environ 1 000 tonnes, capables de distinguer l'énergie des particules au dix millième près.

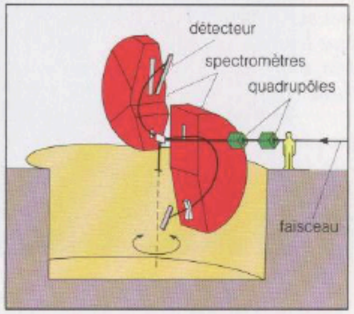

Éclaté schématique de l'ensemble des deux spectromètres.

Charge density distributions

B. Frois, C. N. Papanicolas, Ann. Rev. Nucl. Part. Sci. 37, 133 (1987)

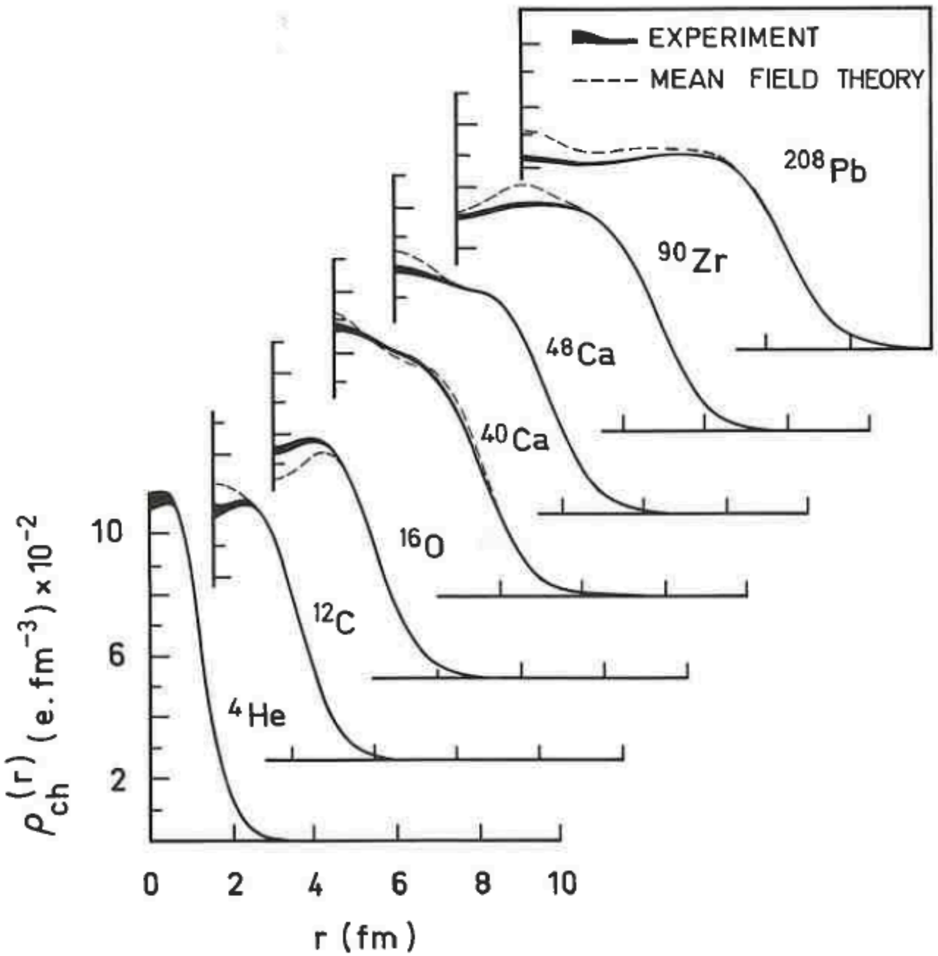

Charge density difference between ^{206}Pb and ^{205}Tl

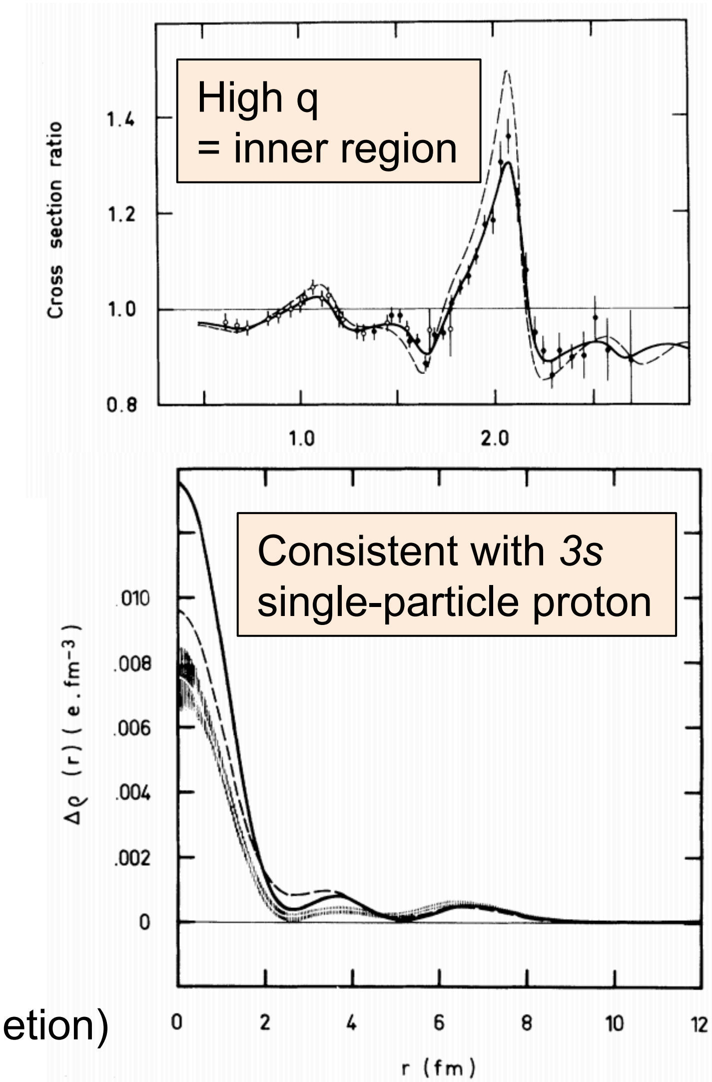

- Strong support for the mean-field approximation
- Quantification of SRC in the inner nuclear region (depletion)

RIBs: Electron scattering from unstable nuclei

- **"Tour de force!"** **e-RI scattering** at **SCRIT** in RIKEN
- **New concept**: ions trapped by electron beam
- SCRIT: facility dedicated to fission fragments
- Limited to 10^{27} cm^{-2} s^{-1} luminosity: access to charge radius and **diffusiveness** for RI.
- Proof of concept with stable nuclei

  T. Suda *et al.*, Phys. Rev. Lett. **102** (2009).
- first RI measurement of 132Sn in 2016

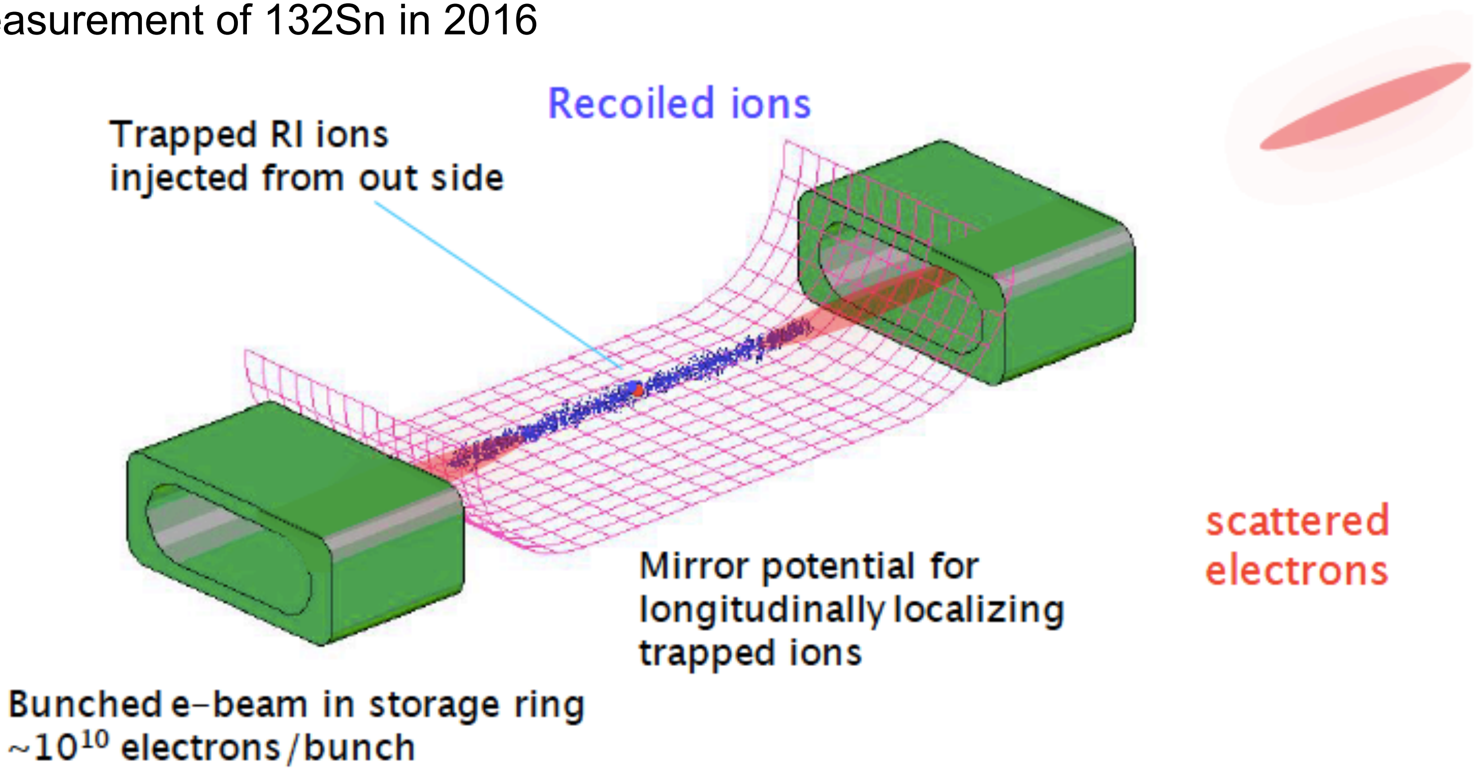

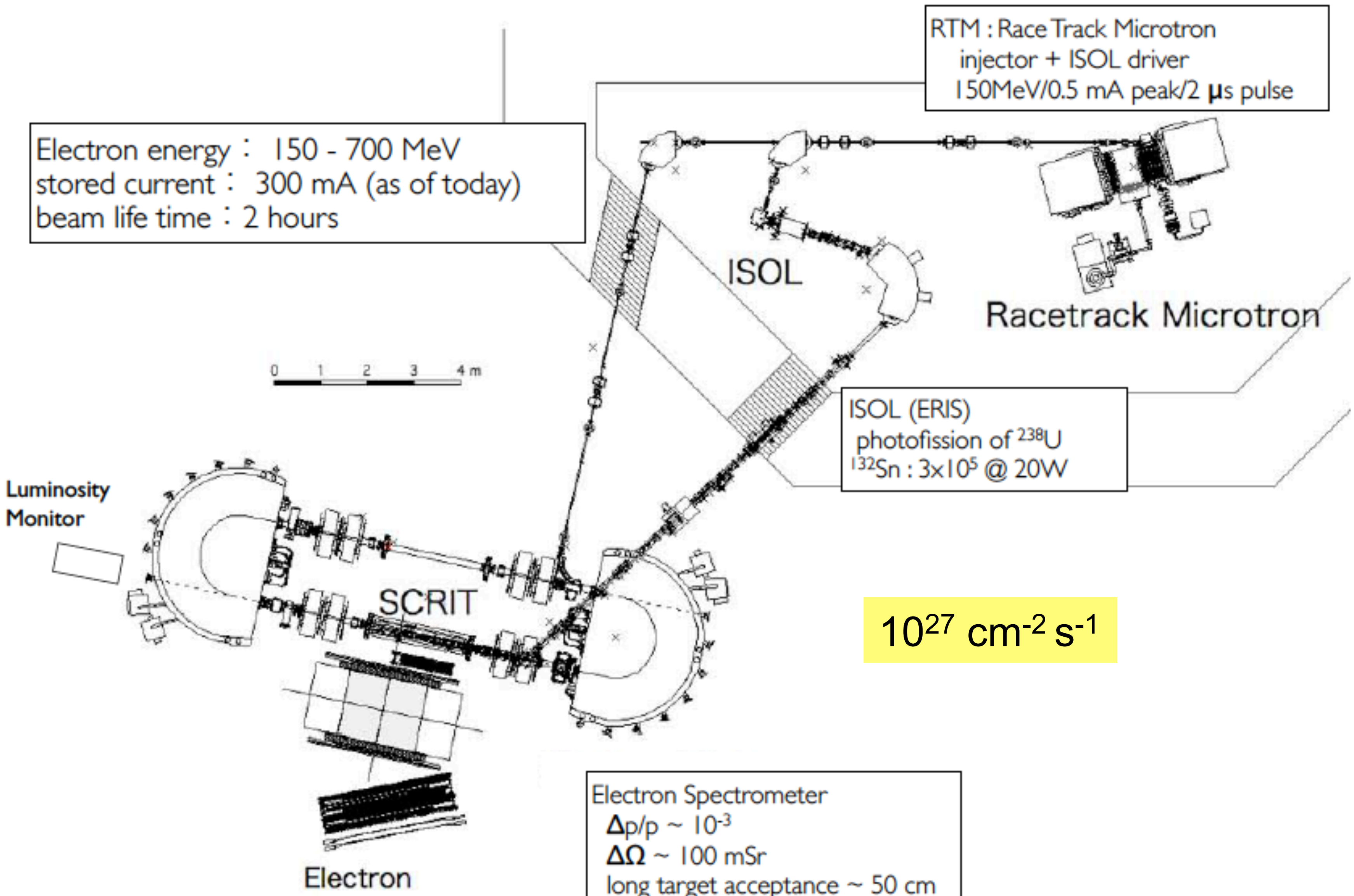

10^{27} cm^{-2} s^{-1}

Figure from M. Wakasugi, RIKEN

SCRIT

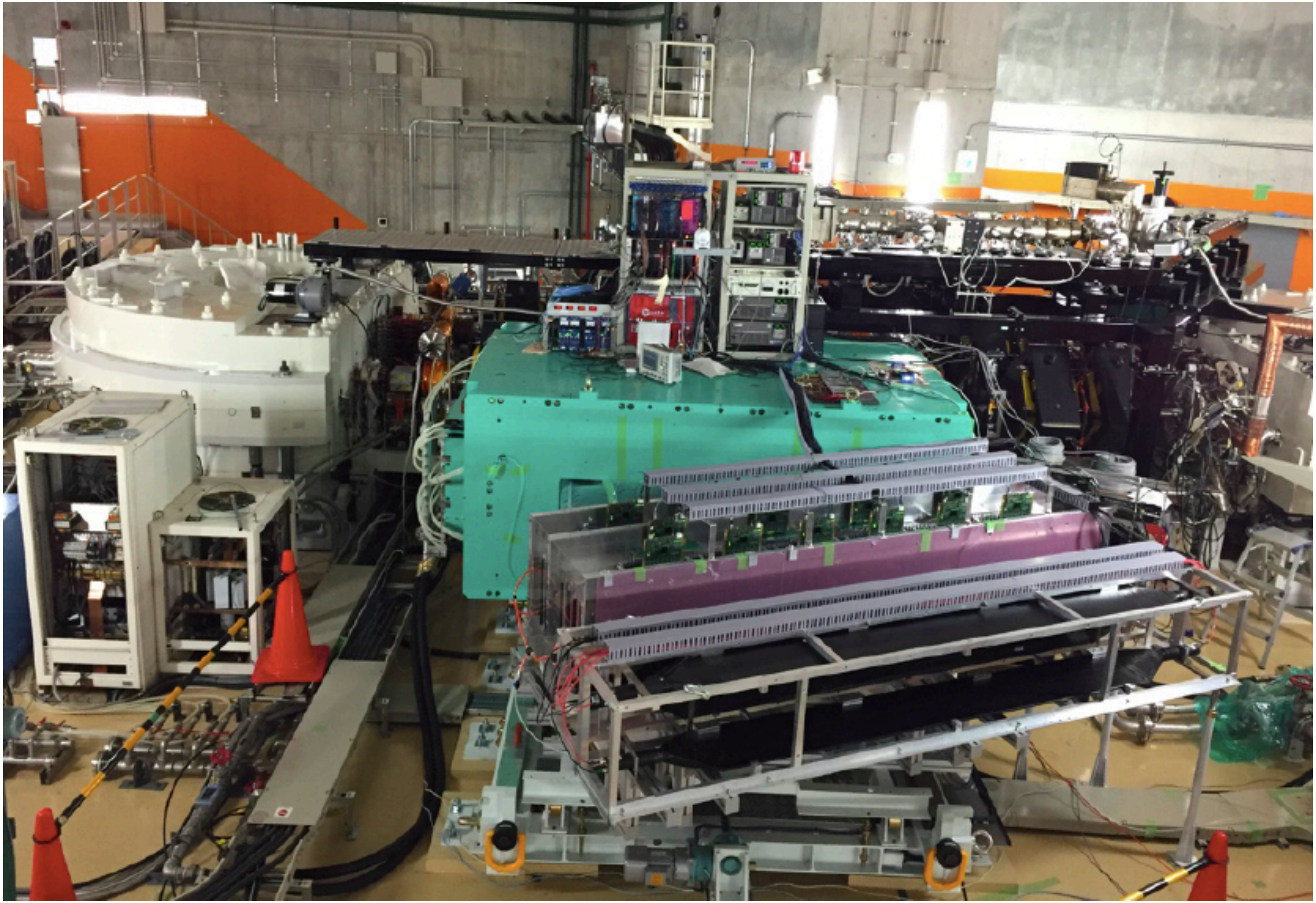

Picture from T. Suda, Tohoku University

ELISe at FAIR: electron – Radioactive Ion collider

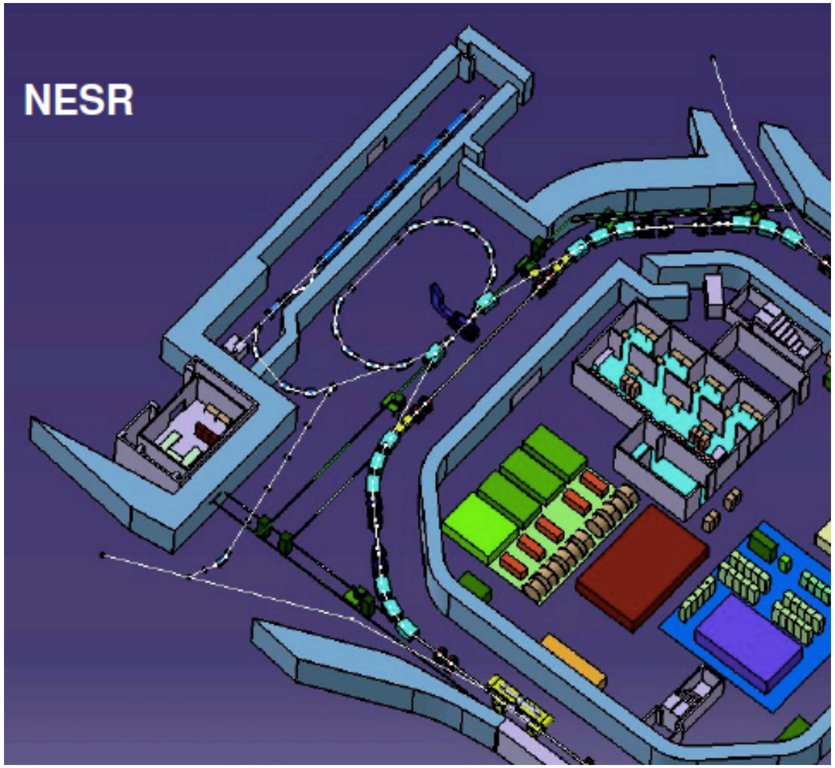

- **Electron – RIB collider**
  - 125-500 MeV electrons
  - 200-700 MeV/u RIBs

Part of the FAIR facility (expected >2030)

- Luminosity <10^{28} cm^2s^{-1}
- Lorentz focusing
- High resolution spectrometer
- Access to all species of ions
- in-flight fission induced by electrons fELISE program

Lecture 1: Radii, neutron skins and halos

- **Matter radii, skins and halos: history and definitions**
- **Hyperfine structure and isotopic shifts**
- **Electron elastic scattering**
  - The charge form factor
  - Physics case: the historical ^{208}Pb example
  - RIB: The SCRIT facility and the LISE project at FAIR
- **Weak interaction experiments**
  - The weak charge form factor
  - Physics case: the PREX experiment and neutron skin of ^{208}Pb
- **Strong interaction experiments**
  - Proton elastic scattering
  - Coherent $\pi 0$ photoproduction
  - Antiprotonic atoms
- **Indirect methods (examples)**
  - Inelastic scattering
  - Dipole polarizability
  - Giant Resonances

Charge radius & density

Matter radius

Z^0 of the weak interaction: a probe for neutrons

	proton	neutron
Electric charge	1	0
Weak charge	0.08	1

T.W. Donnelly, J. Dubach, I. Sick
Nucl. Phys. A 503, 589, 1989

C. J. Horowitz, S. J. Pollock, P. A. Souder, R. Michaels
Phys. Rev. C 63, 025501, 2001

^{208}Pb

Neutron form factor

$$F_N(Q^2) = \frac{1}{4\pi}\int d^3r\; j_0(qr)\;\rho_N(r)$$

Parity Violating Asymmetry

$$A = \frac{G_F Q^2}{2\pi\alpha\sqrt{2}}\left[\underbrace{1 - 4\sin^2\theta_W}_{\approx 0} - \frac{F_N(Q^2)}{F_P(Q^2)}\right]$$

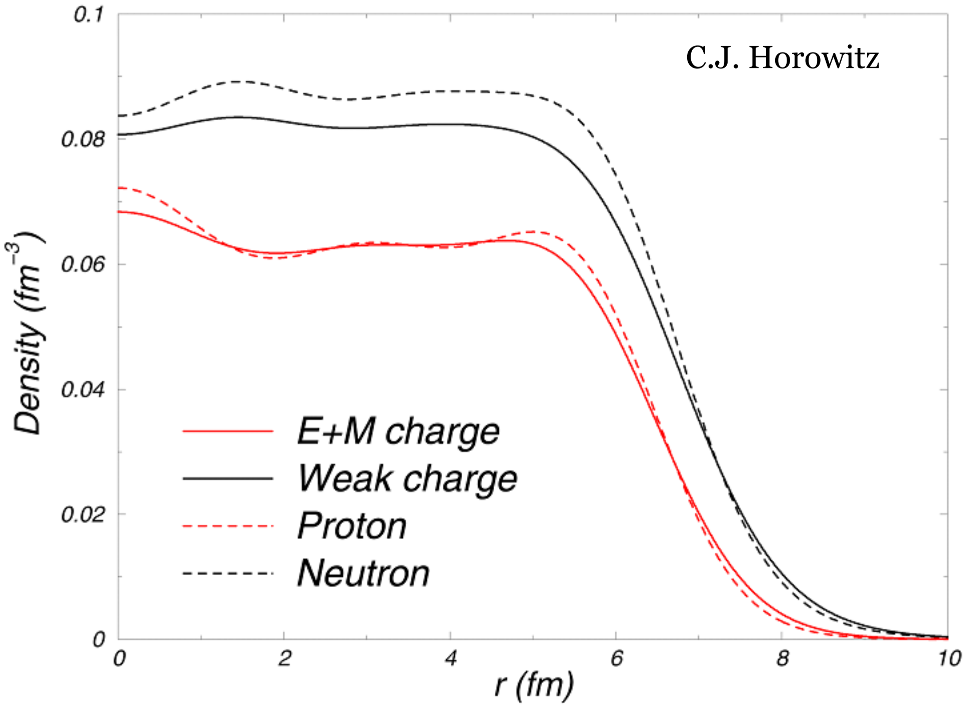

The weak interaction & parity violation

Observed NOT to be invariant under parity transformations

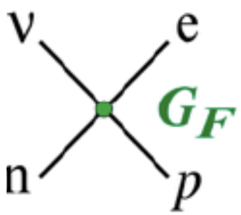

- Fermi theory for weak interactions: coupling constant G_F
- Effective theory that explains many properties of radioactive decays
- **Parity transformation** is defined as follows (spin is a pseudo-vector)

$$x, y, z \rightarrow -x, -y, -z$$

$$\vec{p} \rightarrow -\vec{p}$$

$$\vec{L} \rightarrow \vec{L}$$

$$\vec{s} \rightarrow \vec{s}$$

- Signature of parity violation in **1957**:
  observed **anisotropy in beta-emission** when nuclei are aligned to a magnetic field

Wu's experiment (1957)

- Principle proposed by T.D.Lee and C.N. Yang in 1956
- Polarized 60Co source
- Count the electrons along the magnetic field direction
- Electron preferentially emitted in the opposite direction of B

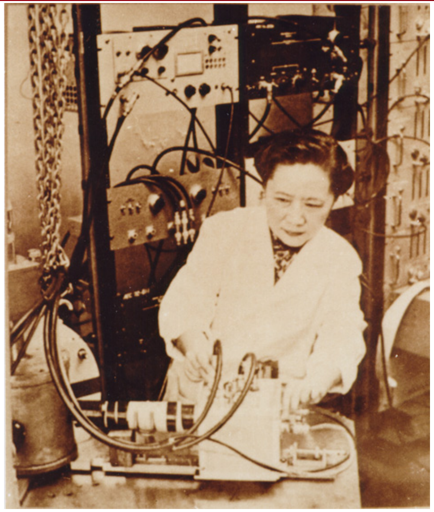

De-excitation of a polarized ^{60}Co :

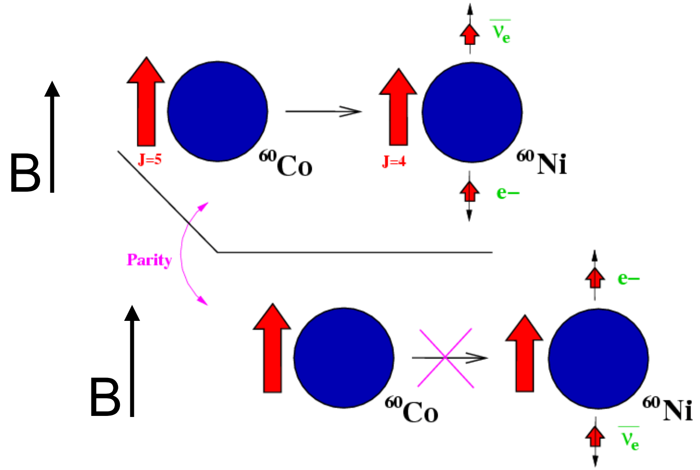

$N_e^+ - N_e^-$

Pseudo-scalar: $s_e.p_e<0$ $s_e.p_e>0$ (or $B.p_e$)

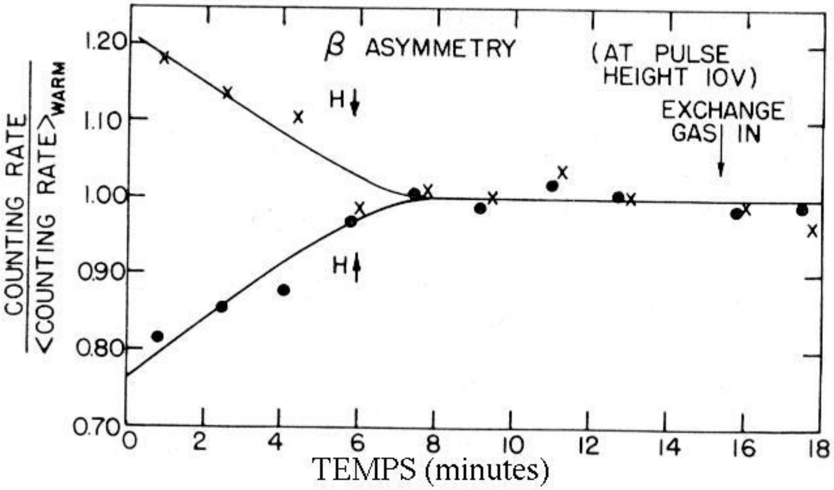

Electron scattering, parity violation & asymmetry

β decay   electron scattering

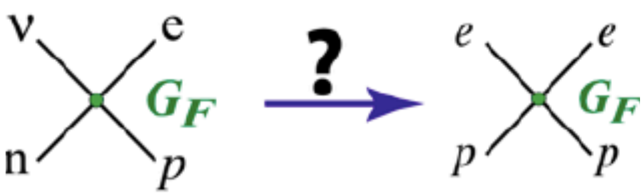

> Is electron scattering parity violating? **YES** (1959)
> Zel'dovich, JETP 36, 964 (1959)

- Cross section has an **interference term** between EM and weak amplitudes
- Can be extracted from **asymmetry measurements** from spin-polarized experiments
- **10^{-6} relative effect**
- Uncertainties dominated by statistics

$$\sigma \propto |A_{EM} + A_{weak}|^2$$

$$\sim |A_{EM}|^2 + 2A_{EM}A^*_{weak} + \ldots$$

Parity-violating

$$A_{PV} = \frac{\sigma_{\uparrow} - \sigma_{\downarrow}}{\sigma_{\uparrow} + \sigma_{\downarrow}}$$

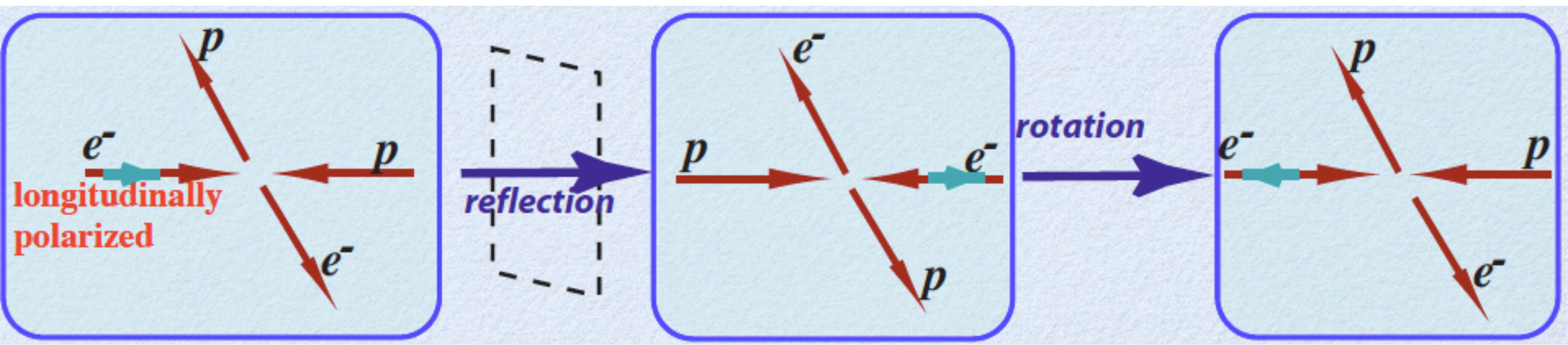

Image from K. Kumar, Stony Brook University and ACFI

The PREX experiment at JLab

1 GeV electron beam, 50-70 μA

high polarization, ~89%

helicity reversal at 120 Hz

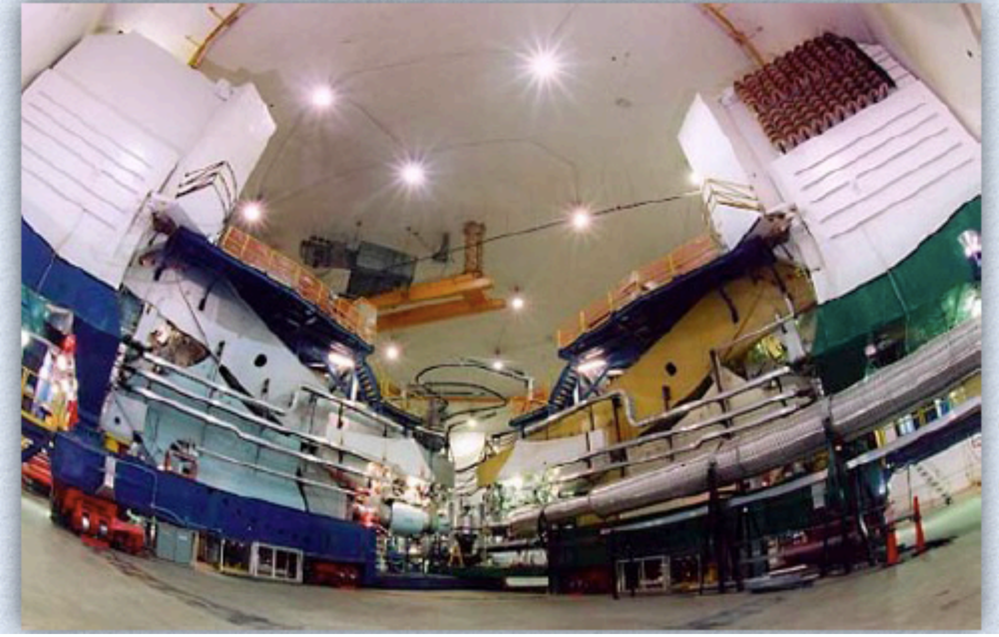

0.5 mm isotopically pure ^{208}Pb target

5° scattered electrons

$Q^2 = 0.0088\ GeV^2/c^2$

new thin quartz detectors

Slide from K. Kumar, Stony Brook University and ACFI

Result of PREX

- Main source of uncertainty: statistics

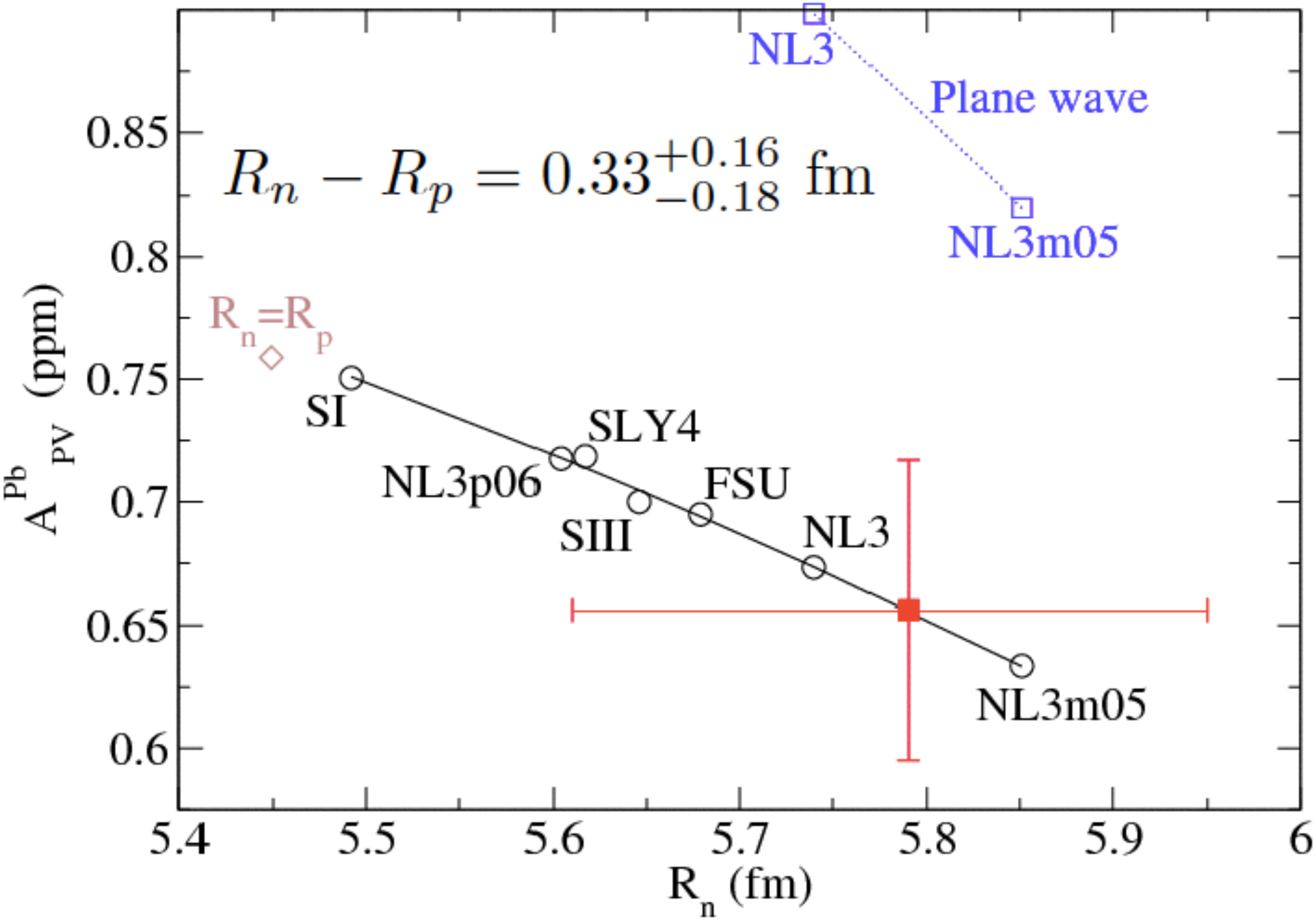

Lecture 1: Radii, neutron skins and halos

- Matter radii, skins and halos: history and definitions
- Hyperfine structure and isotopic shifts
- Electron elastic scattering
  - The charge form factor
  - Physics case: the historical ^{208}Pb example
  - RIB: The SCRIT facility and the LISE project at FAIR
- Weak interaction experiments
  - The weak charge form factor
  - Physics case: the PREX experiment and neutron skin of ^{208}Pb
- **Strong interaction experiments**
  - Proton elastic scattering
  - Coherent $\pi 0$ photoproduction
  - Antiprotonic atoms
- Indirect methods (examples)
  - Inelastic scattering
  - Dipole polarizability
  - Giant Resonances

Charge radius & density

Matter radius

Proton elastic scattering

- Heavy-ion elastic scattering exhibits the same characteristics than electron scattering:
  - ➢ Nuclear absorption
  - ➢ Fraunhofer-type interferences (far side and near side): **Δθ ≅ 1/R**
- Proton scattering sensitive to the **nuclear radius**

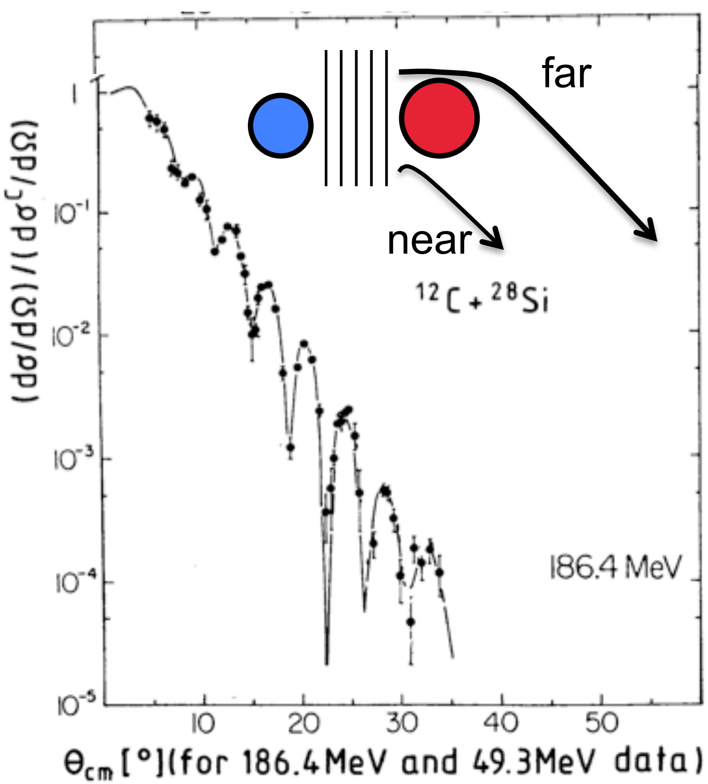

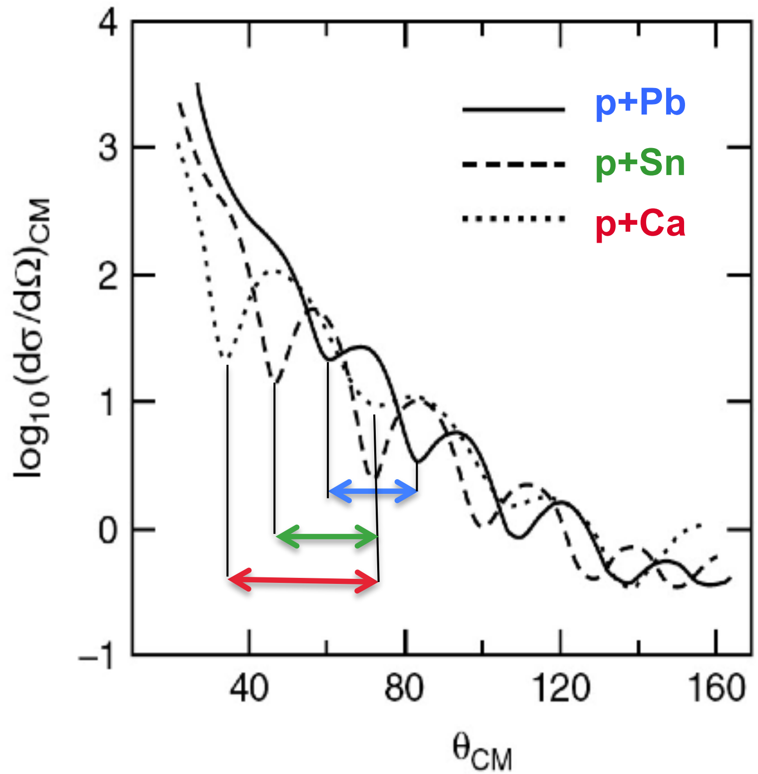

C. Bertulani, Wiley Encyclopedia of Physics

Solving the Schrodinger equation for elastic scattering

$$(H - E)\psi = 0$$

$V_\alpha = V_\alpha(\vec{r}_\alpha)$ optical potential approximation

$H = h_\alpha + T_\alpha + V_\alpha$ with h_α is the intrinsic hamitonian

$\psi = \Phi_A \chi$ intrinsic wave **X** relative motion

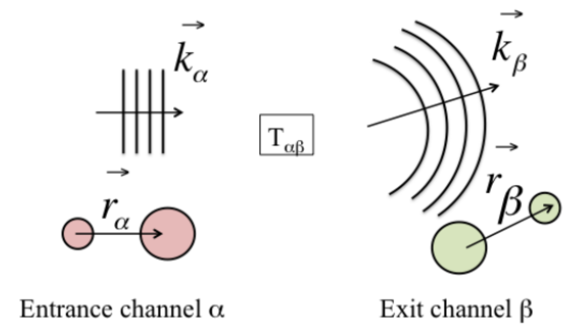

Homogenous equation (no interaction potential)

$$(h_\alpha + T_\alpha - E)\phi_\alpha = 0 \Rightarrow \phi_\alpha = e^{i\vec{k}_\alpha . \vec{r}_\alpha}\Phi_\alpha$$

Inhomogenous equation: $(T_\alpha - E)\chi = -V_\alpha \chi$

$$\Rightarrow \chi = \phi_\alpha - \frac{V_\alpha}{T_\alpha - E}\chi$$ distorted wave

$T_{\alpha\beta} = \langle \phi_\beta | V_\alpha | \chi_\alpha \rangle$ transition matrix element (prior form)

Remark if one assumes $\psi_\alpha = \phi_\alpha$ (**First Born approximation**)

$T_{\alpha\beta} = \langle \phi_\beta | V | \phi_\alpha \rangle = \int e^{i(\vec{k}_\alpha - \vec{k}_\beta).\vec{r}} V(\vec{r})\, d^3\vec{r}$ for elastic scattering

Optical potentials

1) **Empirical** Optical Potentials (Parameterized on data)

$V(R) = V_0(R) + i\,W(R) + \ldots$ (surface, spin-orbite, Coulomb)

2) **Microscopic** Optical Potential

Simple folding

$$V(\vec{R}) = \int \rho_A v(\vec{r_{12}})$$

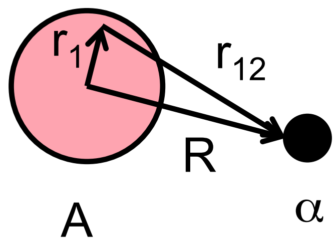

Double folding

$$V(\vec{R}) = \int\int \rho_\alpha \rho_A v(\vec{r_{12}})$$

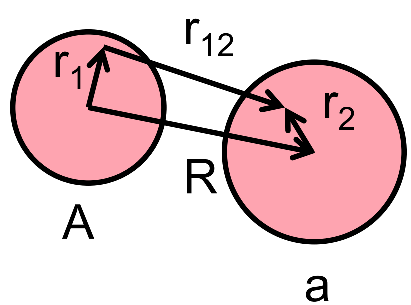

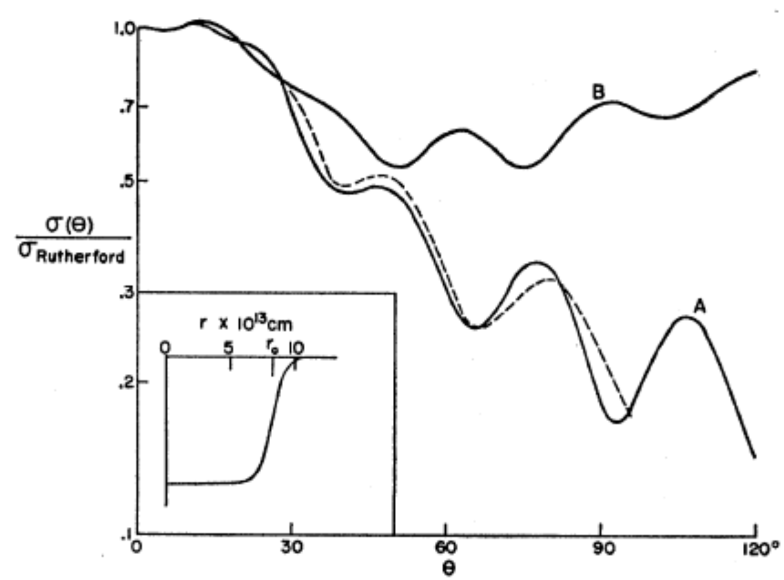

FIG. 1. Elastic scattering of 22-Mev protons by Pt relative to Rutherford scattering. The dashed curve is the experimental result of Cohen and Neidigh (see reference 3), the normalization of which is somewhat uncertain. Curve A is calculated for a diffuse surface model with $V=38$ Mev, $W=9$ Mev, $r_0=8.24\times10^{-13}$ cm, and $a=0.49\times10^{-13}$ cm. The shape of the well is shown in the small drawing at the lower left. Curve B is calculated for a square well of comparable size and depth.

Example: proton elastic scattering from ^8He

^8He+p at 16 MeV/nucleon, with MUST2 @ GANIL

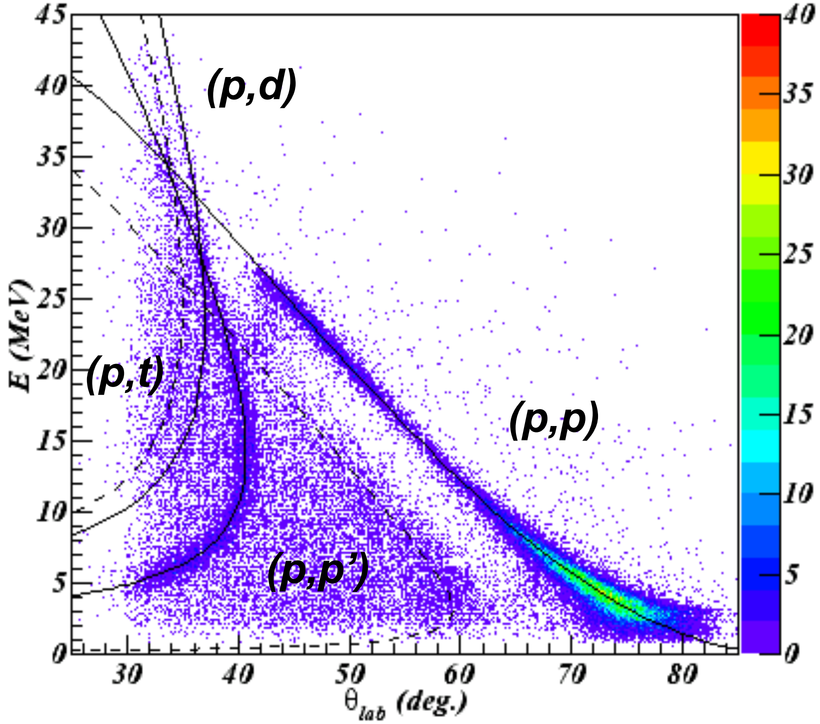

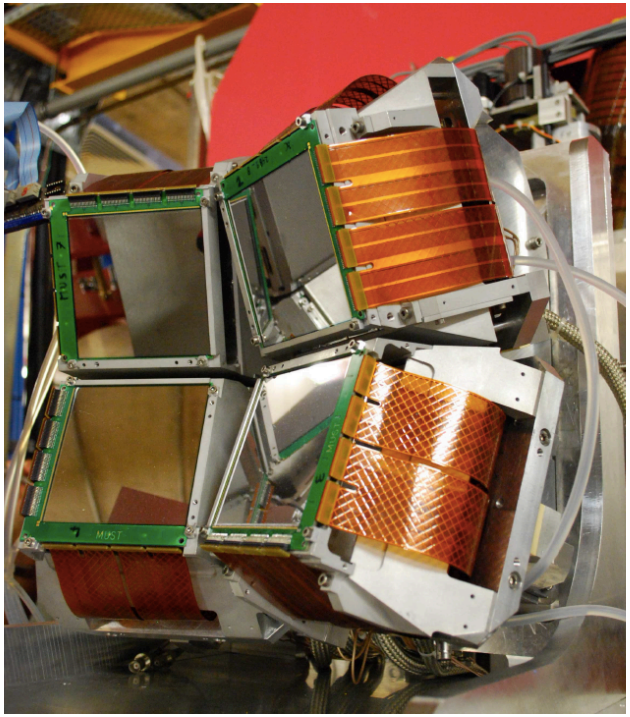

- recoil light particles **identified** by ΔE-E or ToF-E
- Excitation energy spectra via **missing-mass** method

$$m_{A*}^2 c^4 = m_A^2 c^4 + 2 p_A p_p c^2 \cos(\theta_p) - 2T_p (E_A + m_p c^2)$$

$$E_x^A = (m_{A*} - m_A) c^2$$

- **Angular cross sections** to individual ground and excited states

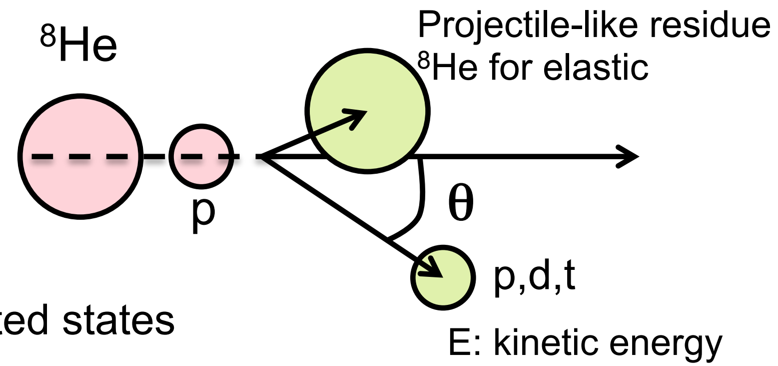

Physics case 3: matter radii of oxygen isotopes

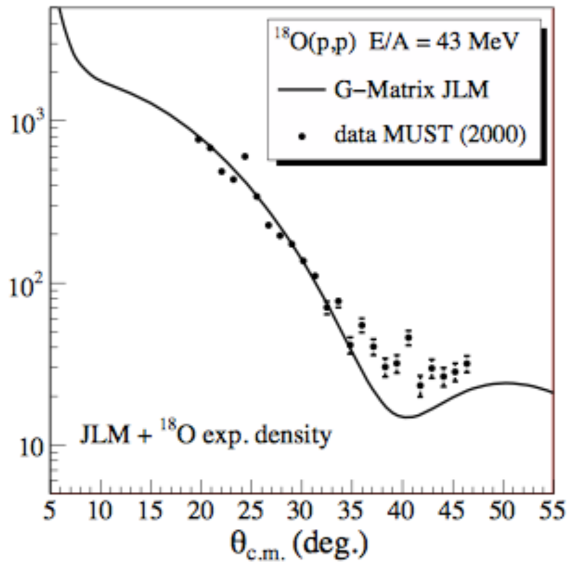

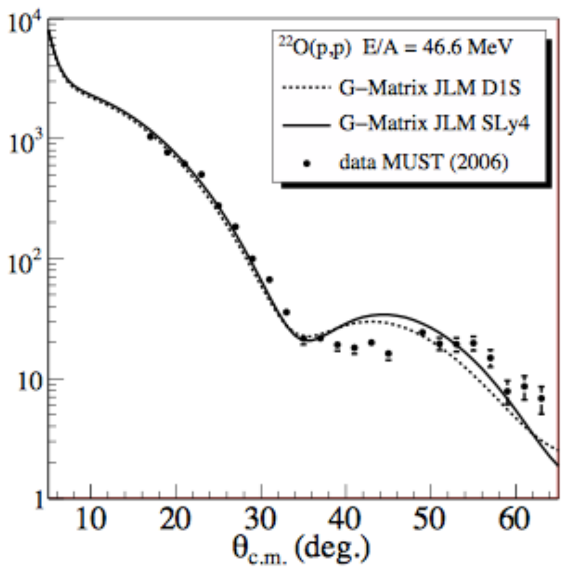

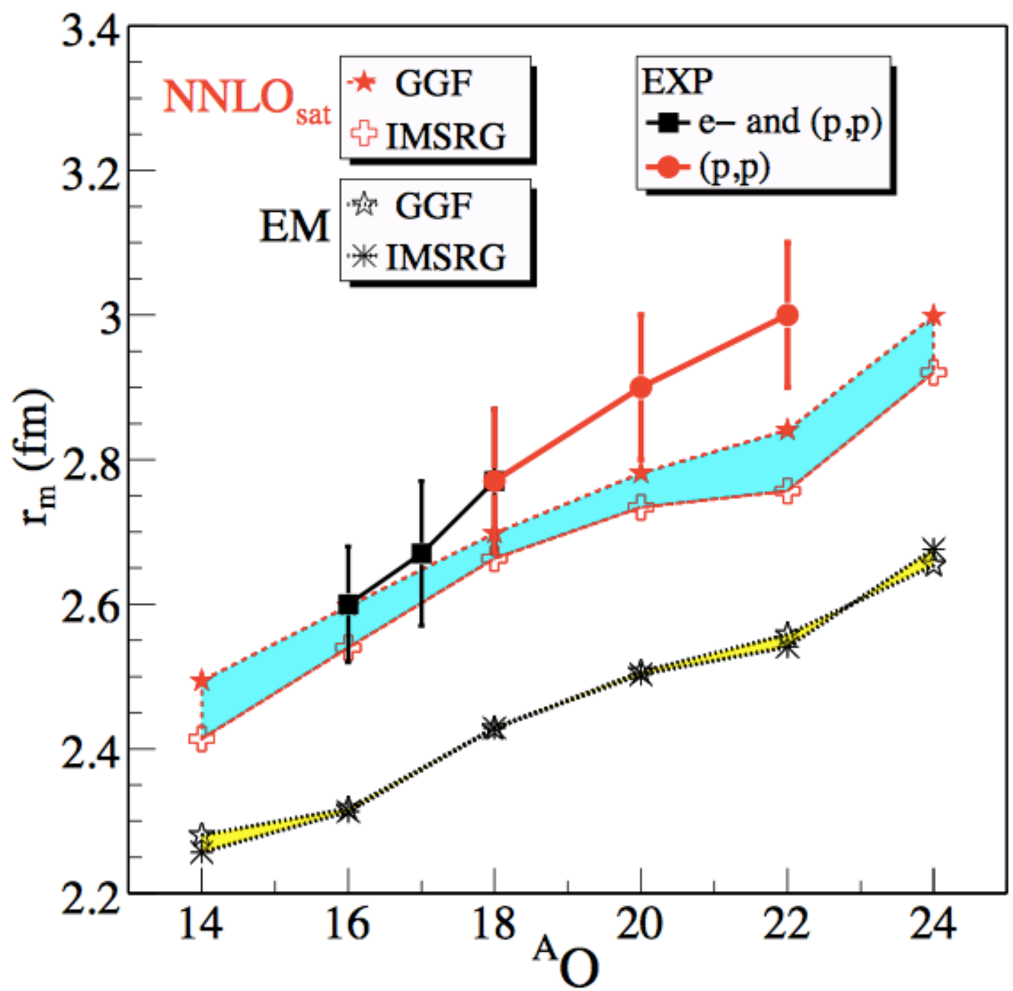

V. Lapoux *et al.,* Phys. Rev. Lett. **117**, 052501 (2016)

Future: in-ring (in)elastic scattering

- ❑ Other solution for low-energy recoil detection:
  Gas jet target and in-ring recirculation (up to 10^6 cycles)

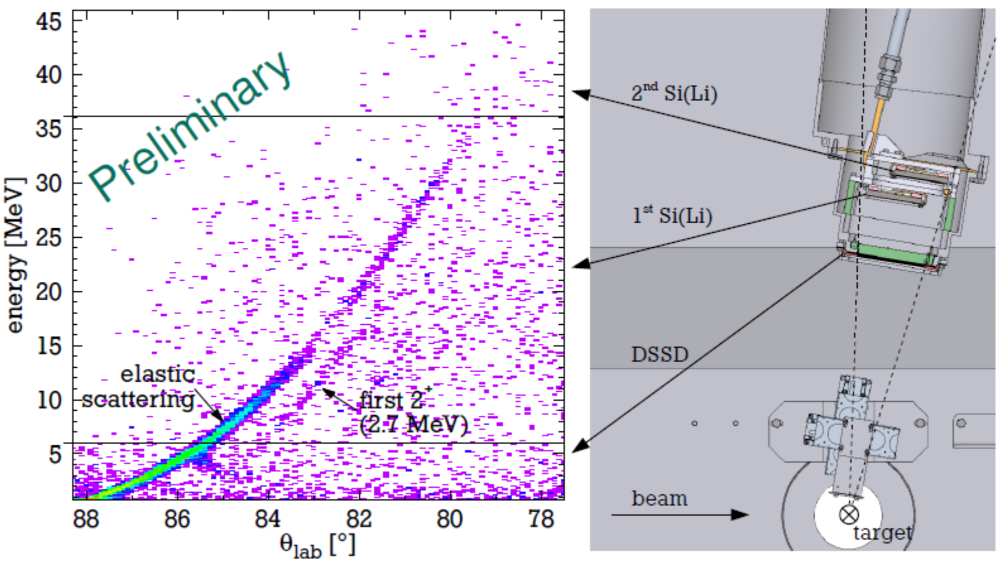

^{56}Ni(p,p') at 400 MeV/nucleon, GSI

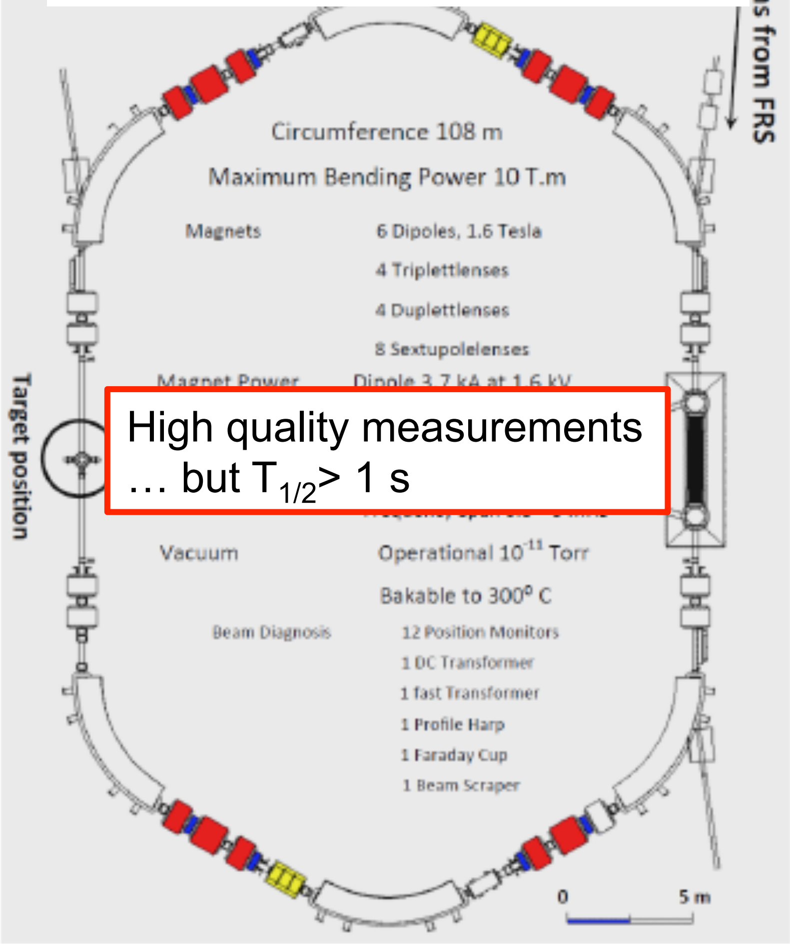

High quality measurements … but $T_{1/2}$ > 1 s

- ❑ **Ongoing projects:**
- ➢ principle experiment at GSI for future FAIR program
  M. Von Schmidt *et al.*, EPJ WoC 66, 03093 (2014)
- ➢ new ring (TSR) at ISOLDE for low energy
  M. Grieser *et al.*, EPJA 207, 1 (2012)

Towards an *Ab initio* description of reactions

- On the way to a **fully consistent treatment of reaction and structure**
  i.e. same initial Hamiltonian, parameter free and theoretical uncertainties

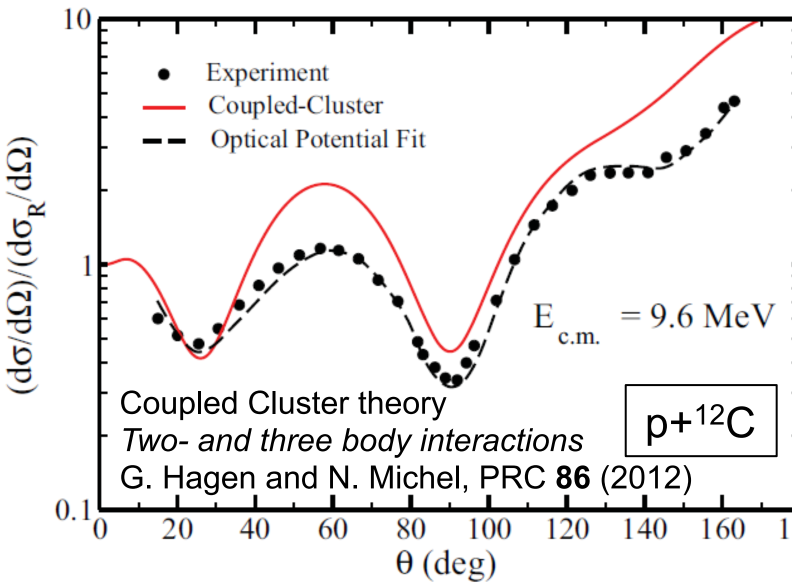

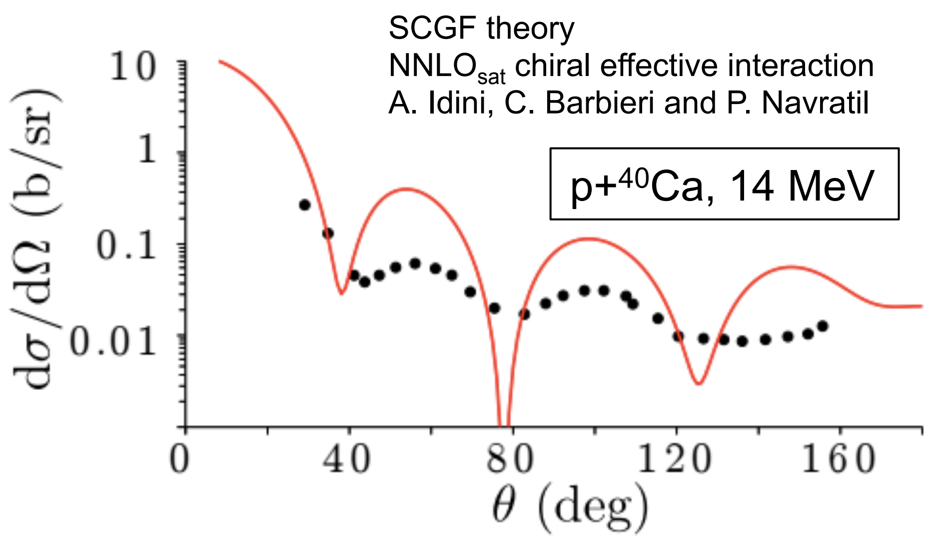

- Developments in Coupled Cluster and Self-Consistent Greens Function theories
  G. Hagen and N. Michel, PRC **86** (2012)
  A. Idini, C. Barbieri, P. Navratil, ArXiv 1612.01478 (2016)

- First ab initio description of low energy fusion reactions (No Core SM)
  P. Navratil and S. Quaglioni, PRL **108** (2012);

Coherent $\pi 0$ photoproduction

Photon probe ✓
Interaction well understood

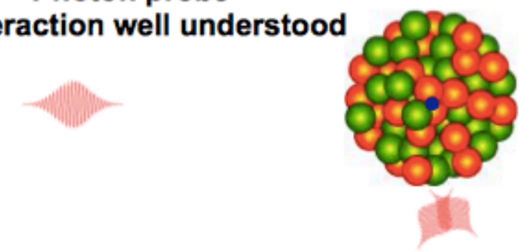

Reconstruct π^0 from $\pi^0 \rightarrow 2\gamma$ decay

π^0 meson – produced with ~equal probability on protons *AND* neutrons.

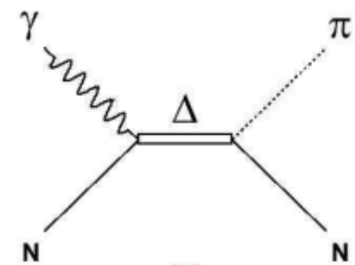

- Coherent: target nucleus (^{208}Pb) remains in it ground state
- Angular (transfered momentum) distribution of π_0: contains **matter form factor** i.e. sensitive to matter radius and diffusiveness

- Plane Wave Impulse Approximation (PWIA):

$$\frac{d\sigma}{d\Omega}(PWIA) = \frac{s}{m_N^2} A^2 \left(\frac{q_\pi^*}{2k_\gamma} \right) F_2(E_\gamma^2, \theta_\gamma^*)^2 \boxed{|F_m(q)|^2} \sin^2(\theta_\pi^*)$$

  - **s**: square of total energy of γ-nucleus pair (MeV2)
  - **q**: Momentum transfer (MeV/c)
  - **F_2**: spin-independent amplitude
  - **lFm(q)l^2**: Matter form factor
  - * denotes quantities in the γ-nucleus center-of-mass system

Coherent $\pi 0$ photoproduction

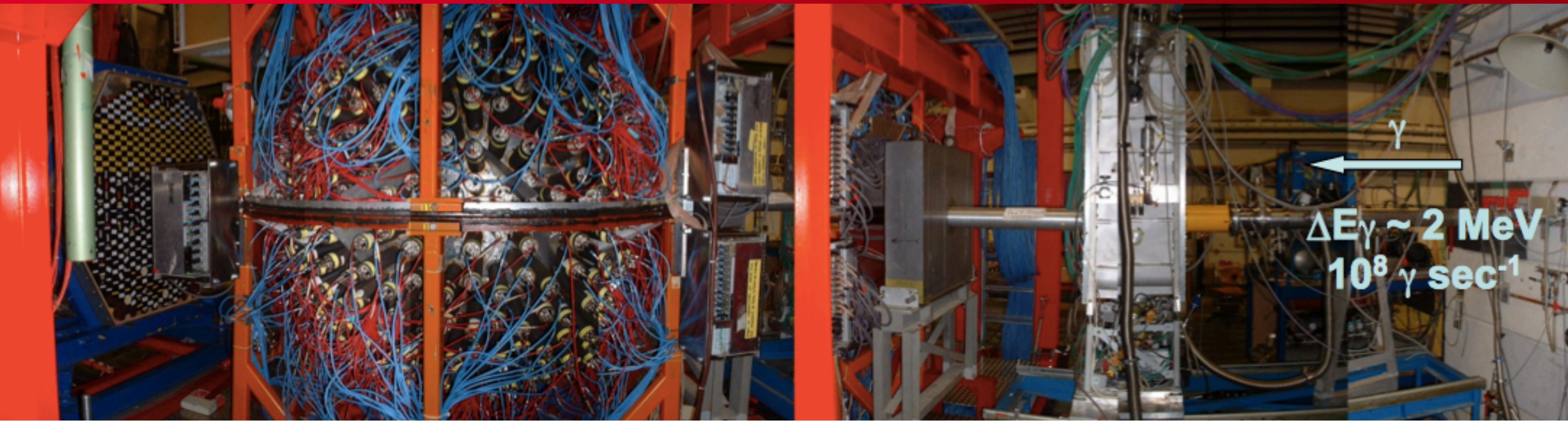

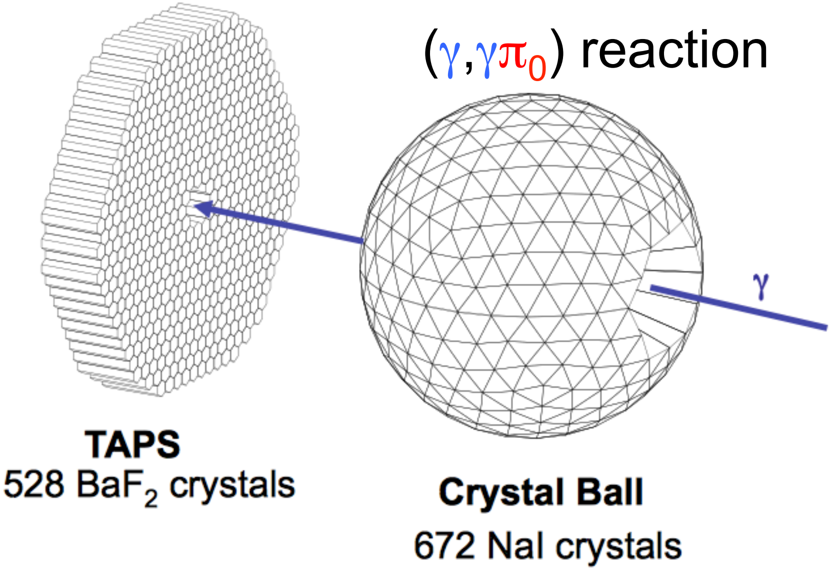

π_0 reconstruction from γ decay

- Experiment at MAMI, Mainz
- Gamma beam from microtron e^- machine
- Energies from 175 to 210 MeV

- Invariant mass of pions from γ decay
- Detection with Crystal Ball (CB)

- Angular distribution of π_0 production
- Final state interactions considered via distorted wave impulse approximation

Coherent π0 photoproduction

C. M. Tarbert *et al.*, Phys. Rev. Lett. **112**, 242502 (2014)

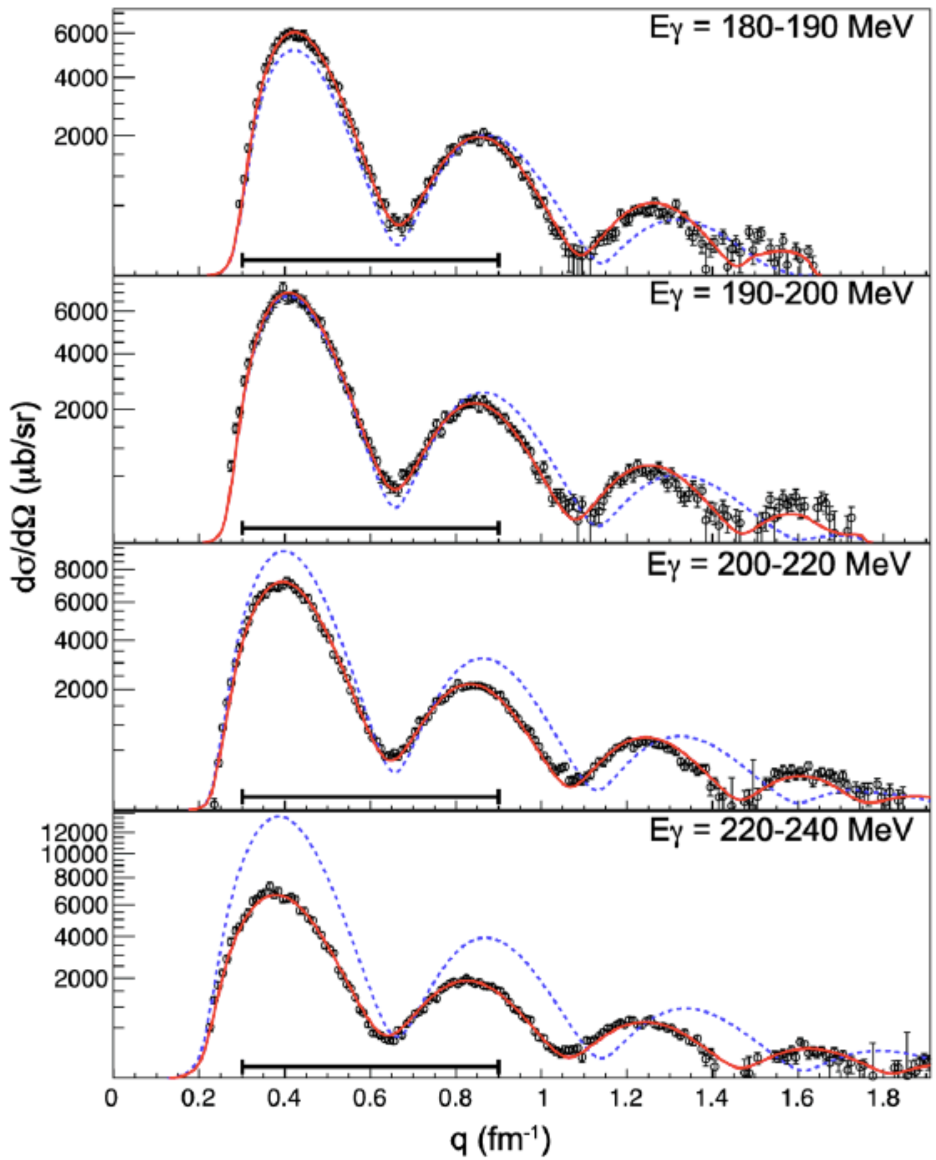

$$\rho(r) = \frac{\rho_0}{1+\exp\left(\frac{r-c}{a}\right)}$$

- ❑ Fitting procedure:

1) Calculate grid c_n=6.28-7.07 fm
a_n=0.35-0.65 fm

2) predictions smeared by q resolution

3) Interpolate fit to experimental data (q=0.3-0.9)

Free parameter: norm, cn, an
Fixed parameter: cp=6.68, ap=0.447

- ❑ Low Eγ: D dominates, model valid
- ❑ High Eγ: π FSI not too large

Coherent π0 photoproduction

- Main source of uncertainty: bakground substraction (0.01 fm)
- Model dependence (delta production) not fully quantified

$$\Delta r_{np} = 0.15 \pm 0.03(stat.)^{+0.01}_{-0.03}(sys.)$$

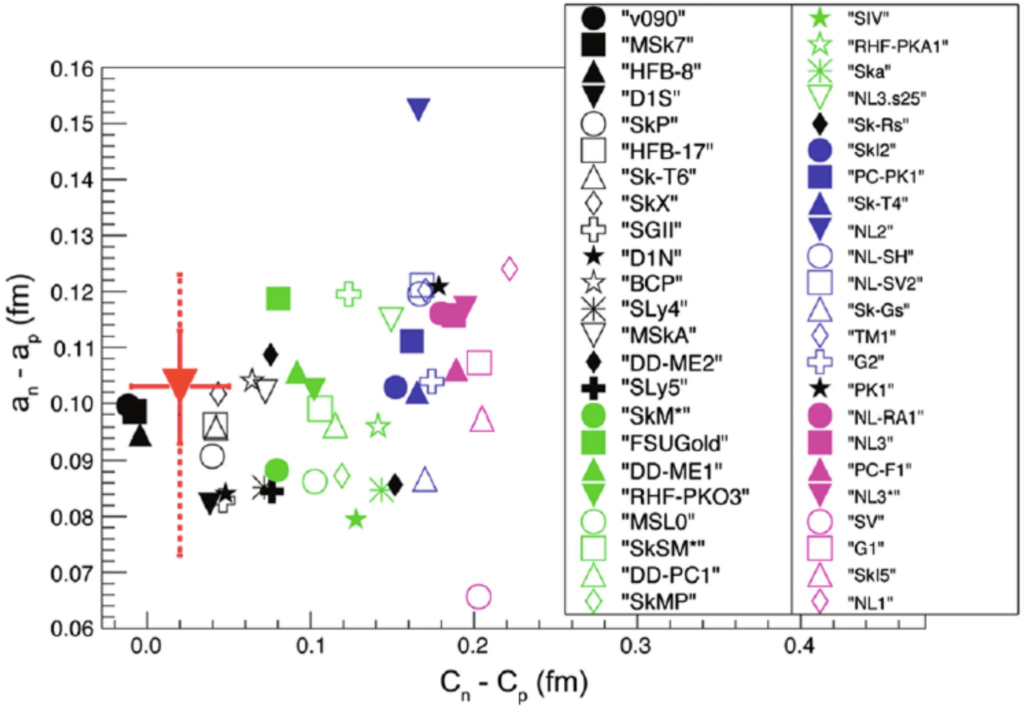

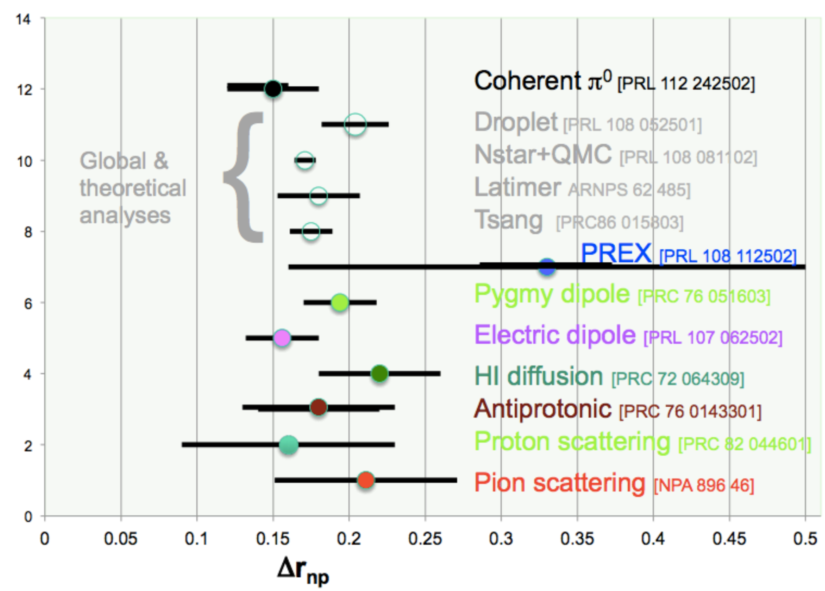

C. M. Tarbert *et al.*, Phys. Rev. Lett. **112**, 242502 (2014)

Antiproton-nucleon annihilation

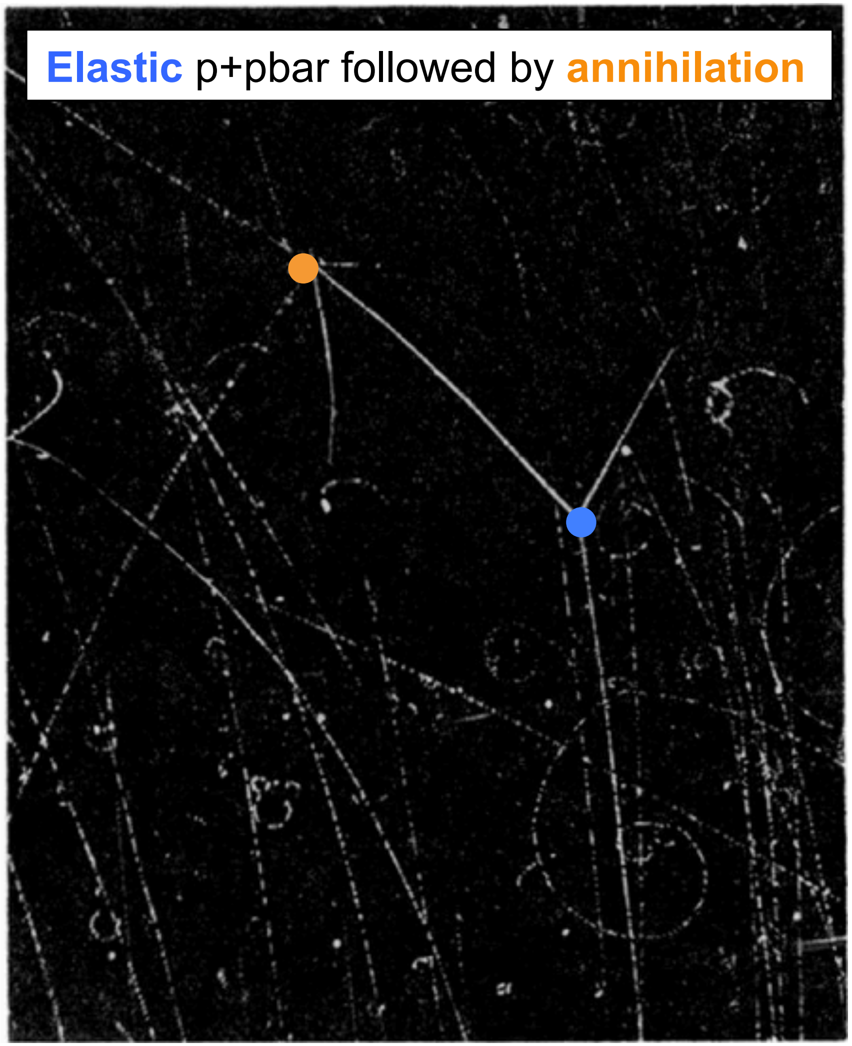

L. Agnew *et al.,* Phys. Rev. 110 (1958)

✓ **Annihilation with protons AND neutrons**
✓ **Mostly pions emitted**
✓ **Electrical charge conserved**
-1: neutron annihilation
0: proton annihilation

Proton-antiproton annihilation at rest:

- charged pion M= 3.0(2), neutral M=2.0(2)
- Fraction of neutral annihilation: 4% (*ex.* multiple π^0)

Neutron-antiproton annihilation at rest:

- $2\pi^-\pi^+n\pi^0$: 60%
- $3\pi^-2\pi^+n\pi^0$: 23%
- $3\pi^-2\pi^+n\pi^0$: 15%
- …

Antiprotonic atoms: annihilation mechanism

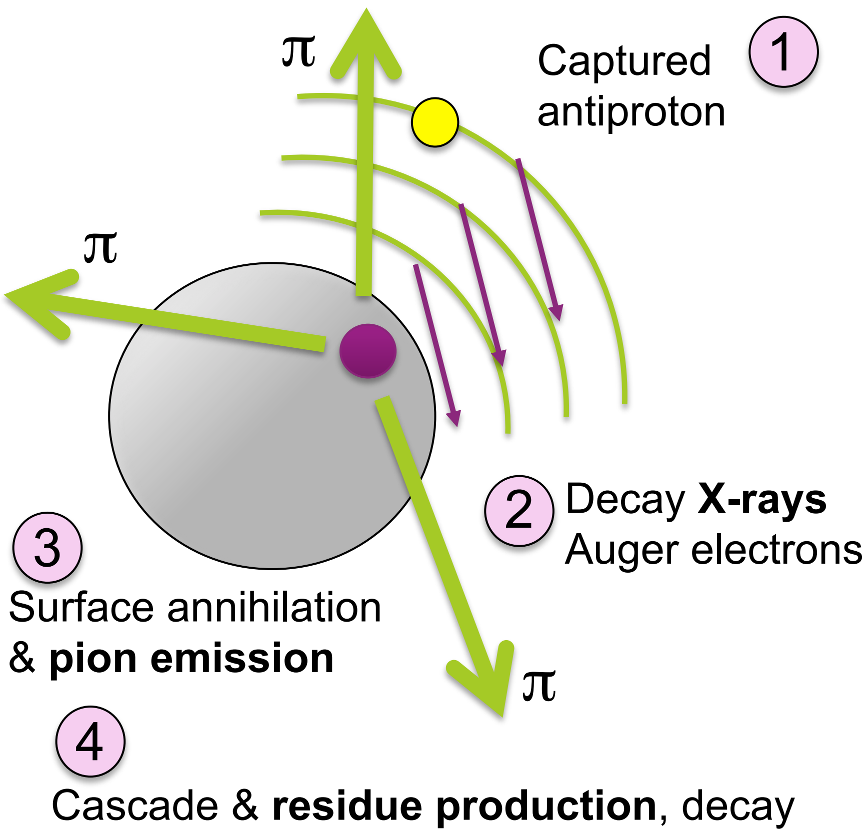

High cross section (≈100 Mbarns)
at low relative energy (≈100 eV)
J.S. Cohen, PRA 69 (2004)

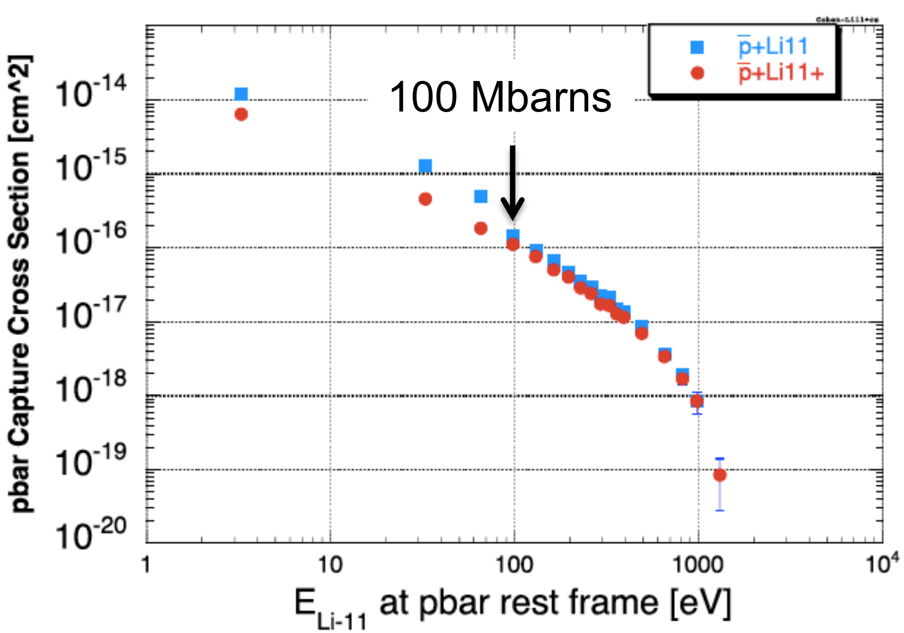

Antiprotonic atoms: sensitivity

Ex. **^{172}Y,** R. Schmidt *et al.,* PRC 58, 3195 (1998)

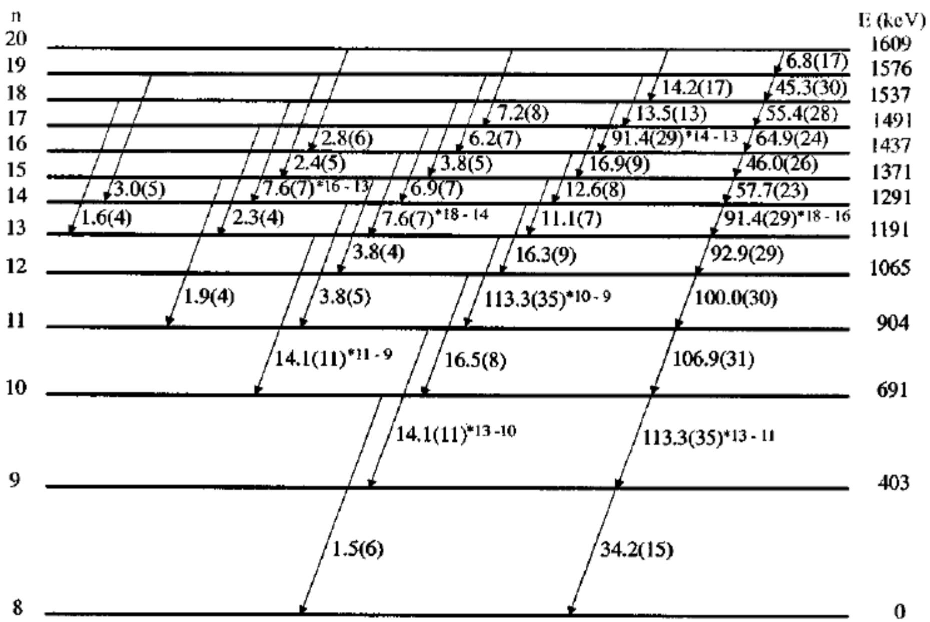

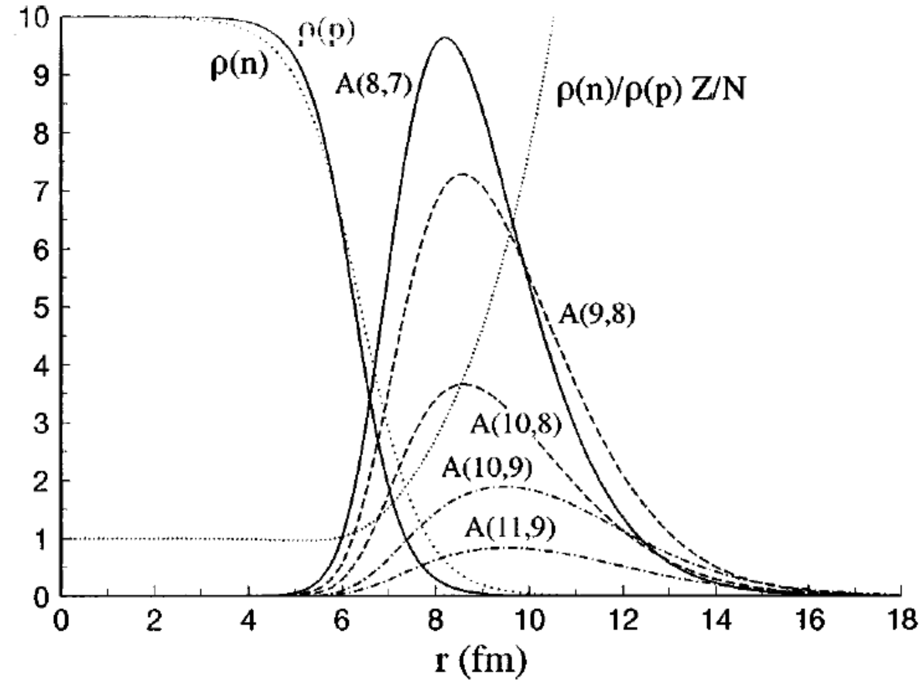

Γ reaction probability

Φ_{nl} antiproton radial wave function

V(r) antiproton-nucleus potential

a effective N-antiproton scattering length
ex. a=-1.53 – 2.5 ***i*** fm (Batty, NPA 1997)

$\rho(r)$ nuclear density convoluted with pbar-N range (0.75-1 fm if finite range)

$$\Gamma_{n\ell} = \int \operatorname{Im} V(r) \left|\Psi_{n\ell}(r)\right|^2 r^2 dr$$

$$with\; V(r) = \frac{2\pi}{\mu} a \rho(r)$$

	Γ_{low} (eV)	Γ_{up} (eV)	ϵ (eV)
Experiment	312(26)	5.9(8)	88(20)
	Batty potential		
SkP	274	5.2	14
SkX	231	4.2	16
DD-ME2	315	6.2	12
	Friedman potential		
SkP	278	5.3	6
SkX	244	4.5	7
DD-ME2	307	6.1	2

B. Klos *et al.*, Phys. Rev. C 76, 014311 (2007).

Radio-chemical analysis

Concept: selection of « cold » residues after annihilation, *i.e.* (Z-1,A-1) and (Z,A-1)

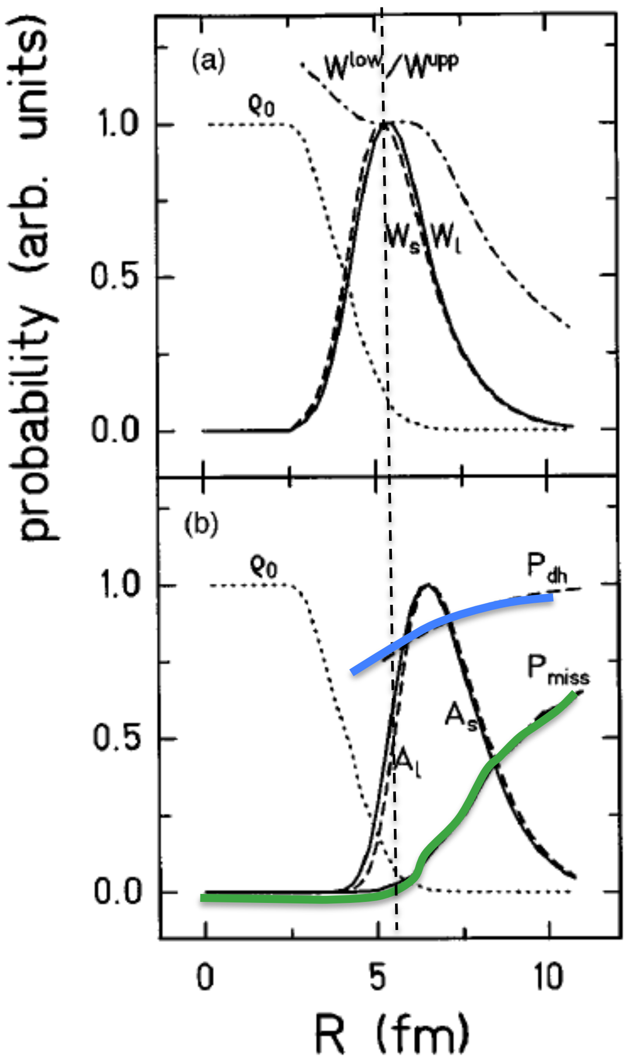

No selection

$$\mathrm{Im}\,V(r)\left|\Psi_{n\ell}(r)\right|^2$$

Selection on cold residues by counting radioactive decays

$$\mathrm{Im}\,V(r)\left|\Psi_{n\ell}(r)\right|^2 P_{miss}(r)P_{dh}(r)$$

Probability that the populated final state is bound (SF)

Probability that pions do not interact with the residue

S. Wycech *et al.*, PRC **54**, 1832 (1996).

Neutron skins from radio-chemical analysis

- Stable nuclei from ^{40}Ca to ^{238}U
- X-ray method « consistent » with radiochemical with **R=1** (R=0.63 in previous works)

$$f_{halo} = \frac{N(Z,A-1)}{N(Z-1,A-1)} \times \frac{Z_t}{N_t} \times R$$

- Neutron distributions (2pF) « deduced » from X-ray data
- **a = 2.5(3) + *i* 3.4(3) fm, zero range**
- charge distributions from published tables
- assume pure halo: $\mathbf{c_n{=}c_p}$
- Δa_{np} ajusted to best reproduce E shift, width

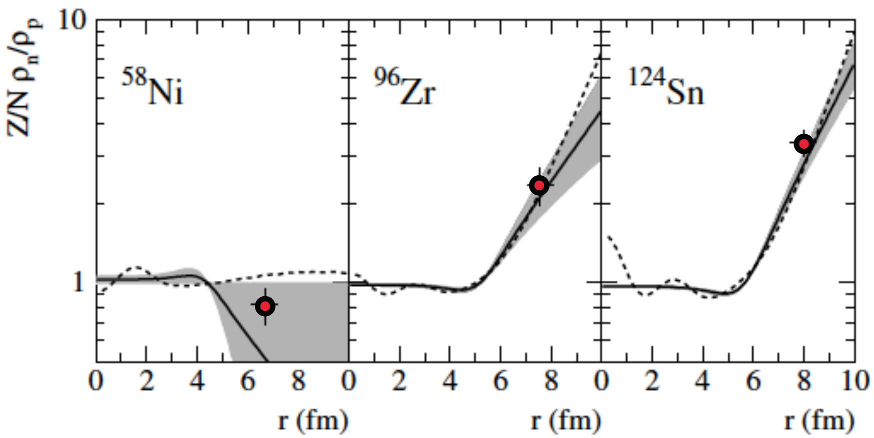

radioachemical

from X-ray measurement

HFB

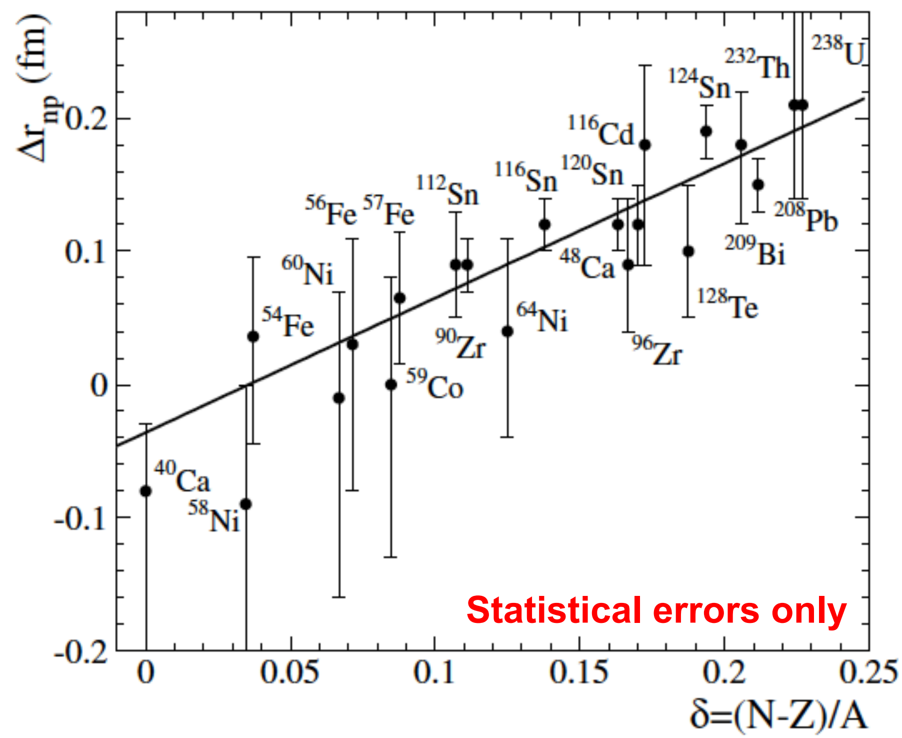

A. Trzcinska *et al.,* Phys. Rev. Lett. **87**, 082501 (2001)

Neutron-to-proton density ratio in the nuclear tail

Annihilation with both **protons AND neutrons**

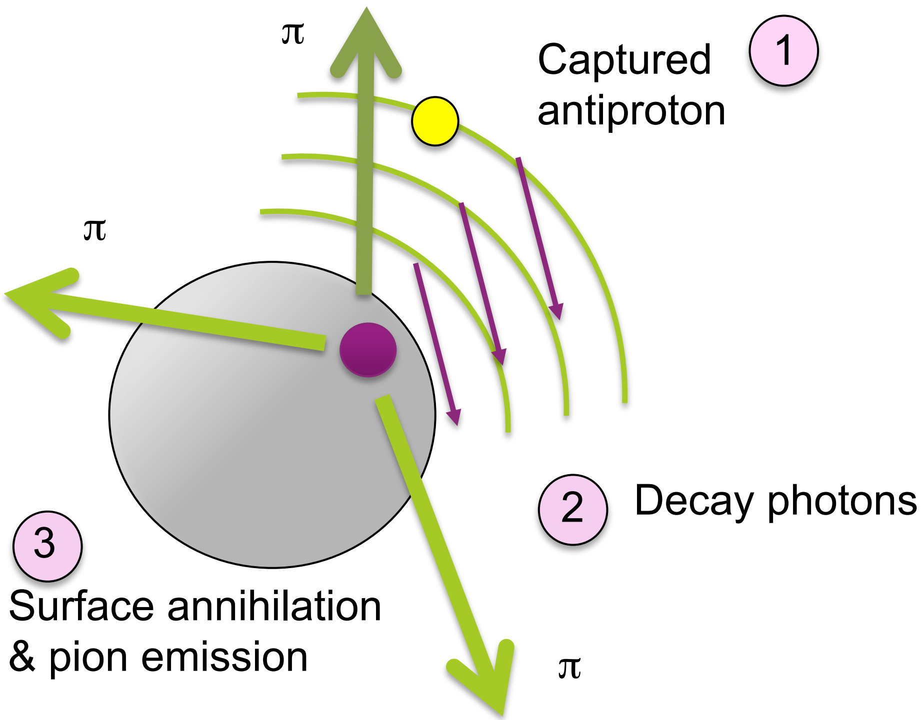

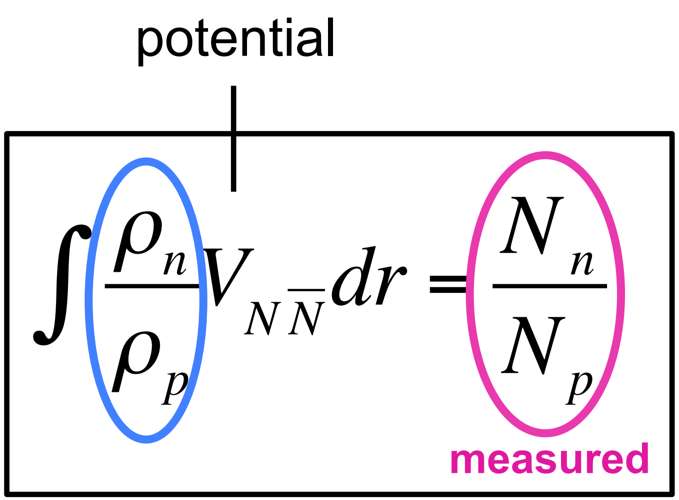

$$\int \frac{\rho_n}{\rho_p} V_{N\overline{N}} dr = \frac{N_n}{N_p}$$

Net electric charge is conserved:
Sum of charges of pions = -1: neutron annihilation
Sum of charges of pions = 0: proton annihilation

M. Wada, Y. Yamazaki, Nucl. Instr. Meth. B **214** (2004).

Antiprotonic atoms: perspectives with RIBs, PUMA

- PUMA: antiProton Unstable Matter Annihilation

- The antiproton filling at CERN/ELENA
- Transportation of antiprotons to CERN/ISOLDE
- In-trap annihilations and measurement **from 2020**

- PUMA has recently started

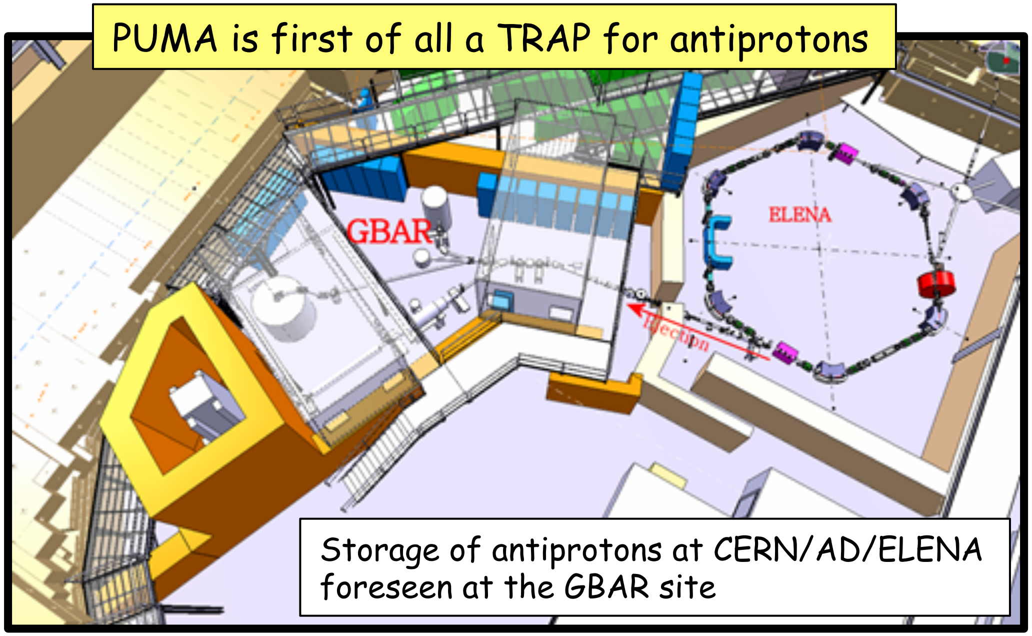

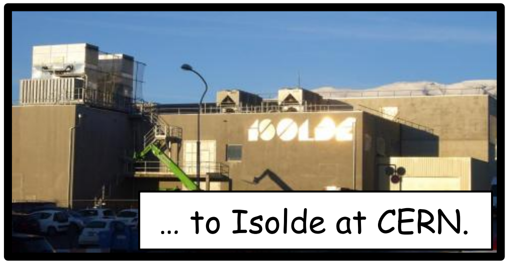

PUMA: antiproton could lifetime & extreme vacuum

- Antiprotons annihilate with residual gas in the trap. Vacuum should be extremely low.
- Capture cross section: $$\sigma(H) = 3\pi a_0^2 \sqrt{E_0 / E}$$ with E_0= 27.2 eV, a_0 Bohr radius
- Annihilation rate: $$R = n \sigma v_{rel}$$
- Lifetime of the cloud of antiprotons: $$\tau = 1/R$$

Under the perfect gas assumption, pressure, temperature and lifetime are linked by

$$P_H(mbar) = 6 \times 10^{-16}\, T(K) / \tau(jours)$$

Application:
For a 5 K crysotat and a 2 month lifetime, a **5. 10^{-17} mbar** vacuum is necessary

- Best vacuum gauges today can measure down to 10-^{12} mbar. Antimatter is the only way to measure such low vacua.

Lecture 1: Radii, neutron skins and halos

- **Matter radii, skins and halos: history and definitions**
- **Hyperfine structure and isotopic shifts**
- **Electron elastic scattering**
  - The charge form factor
  - Physics case: the historical ^{208}Pb example
  - RIB: The SCRIT facility and the LISE project at FAIR
- **Weak interaction experiments**
  - The weak charge form factor
  - Physics case: the PREX experiment and neutron skin of ^{208}Pb
- **Strong interaction experiments**
  - Proton elastic scattering
  - Coherent $\pi 0$ photoproduction
  - Antiprotonic atoms
- **Indirect methods (examples)**
  - Inelastic scattering
  - Dipole polarizability
  - Giant Resonances

Charge radius & density

Matter radius

Proton inelastic scattering

^{6}He(p,p') at 40.9 MeV/nucleon, with MUST, GANIL

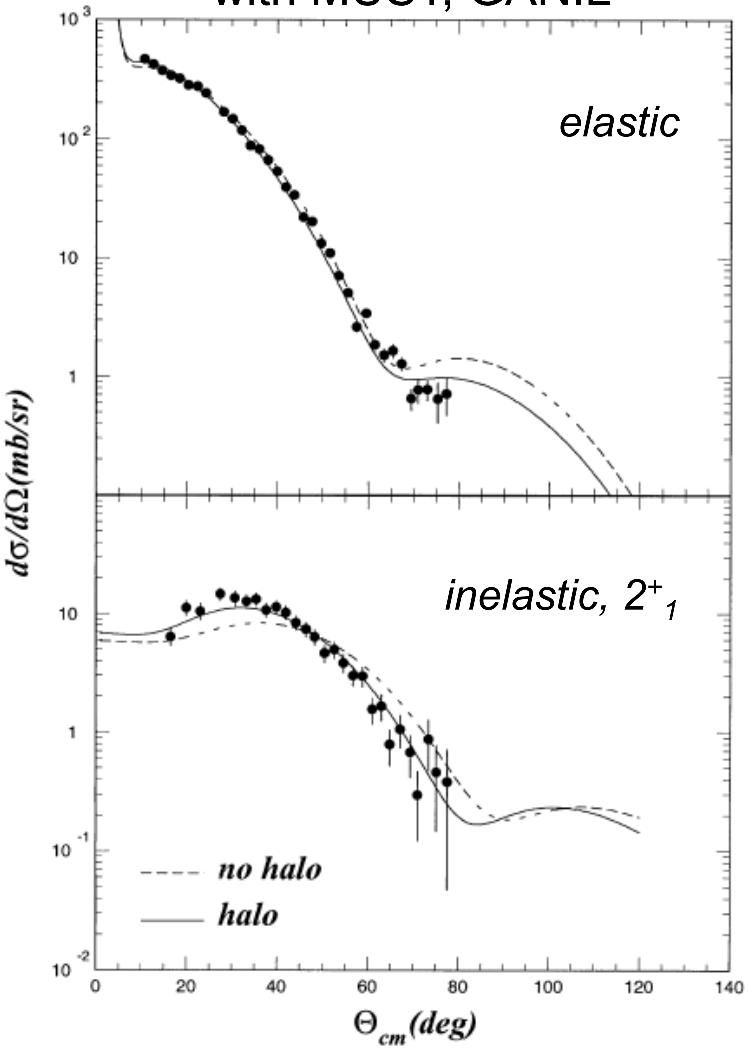

A. Lagoyannis et al., PLB **518** (2001).

The **Distorted Wave Born approximation**

Distorsion of the incoming & outgoing waves
Optical potential V_{op}

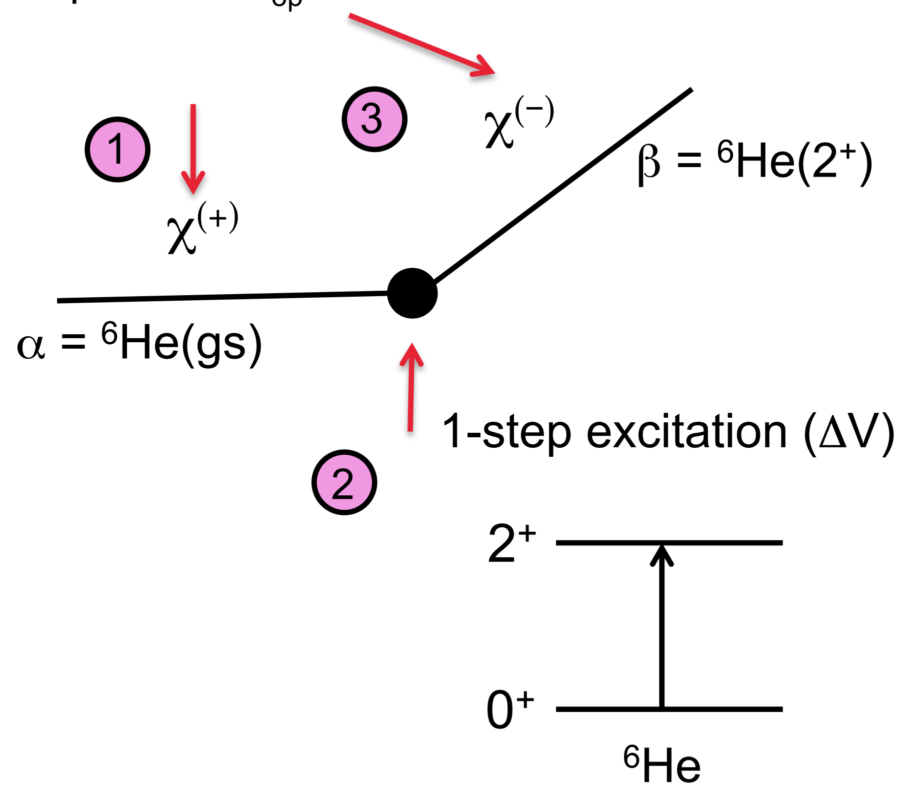

Proton inelastic scattering

^{6}He(p,p') at 40.9 MeV/nucleon, with MUST, GANIL

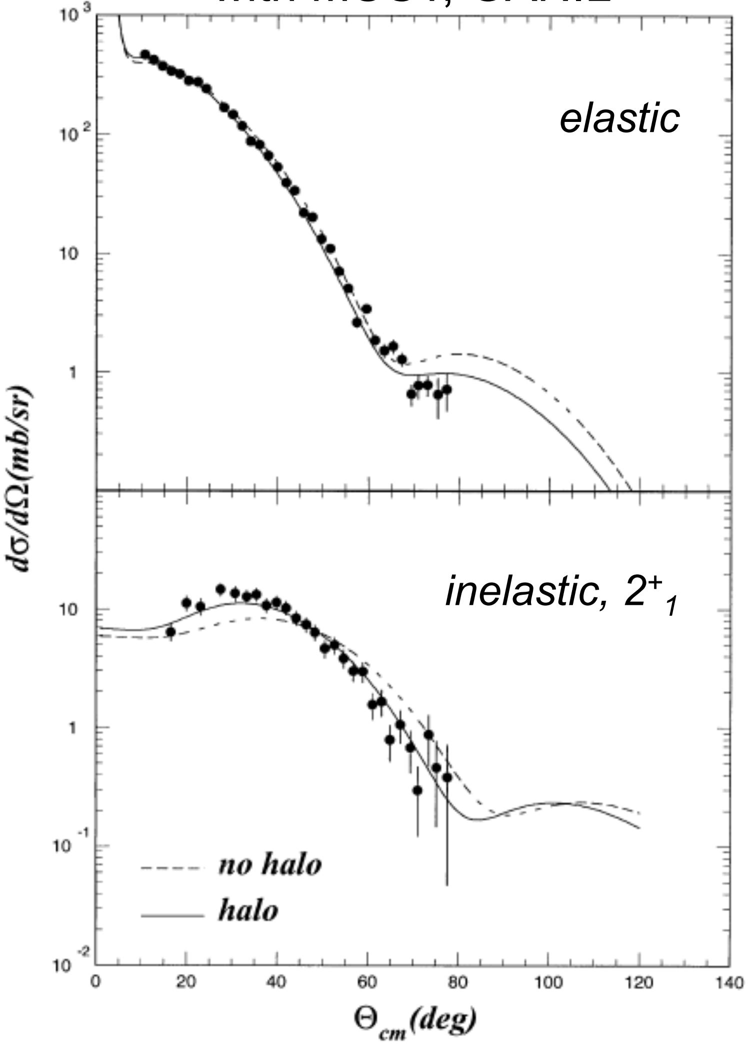

A. Lagoyannis et al., PLB **518** (2001).

Two potential equation

$$(H - E)\psi = 0$$

$$H = h_\alpha + T_\alpha + V_{OP} + \Delta V$$

Distorted wave χ:

$$(h_\alpha + T_\alpha + V_{OP} - E)\chi_\alpha^{(+)} = 0$$

Transition matrix element (**DWBA** approximation)

$$T_{\alpha\beta} = \left\langle \chi_\beta^{(-)}\Phi_\beta \middle| \Delta V \middle| \chi_\alpha^{(+)}\Phi_\alpha \right\rangle$$

$$= \int\int \chi_\beta^{(-)}(\vec{k_\beta},\vec{r_\beta}) \left\langle \Phi_\beta \middle| \Delta V \middle| \Phi_\alpha \right\rangle \chi_\alpha^{(+)}(\vec{k_\alpha},\vec{r_\alpha}) d^3r_\alpha d^3r_\beta$$

Nota Bene: ΔV depends on a structure model

1) **Microscopic** description of $<\Phi_\beta|\Delta V|\Phi_\alpha>$

2) **Collective model** (*ex.* rotational)

Amplitude of ΔV governed by a parameter

$$\delta_{LM} = deformation\ length$$

Giant resonances

1. Collective excitation mode : most of the nucleons are involved in the excitation

2. Feature :
 - Important cross section (100 mb)
 - Exhaust a large part of the energy weighted sum rule (EWSR)
 - Properties change smoothly with the number of nucleons

3. Quantum numbers:
 - Spin ***S***
 - Isospin ***T***
 - Multipolarity ***L***

Electric GR :	***T*** = 0 isoscalar	***T*** = 1 isovectorial
$L = 0$ monopole (GMR)	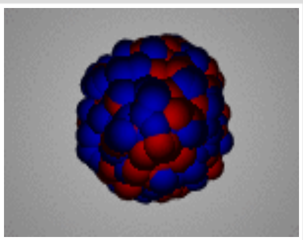	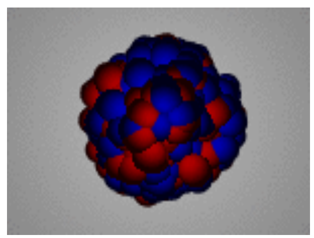
$L = 1$ dipole (GDR)	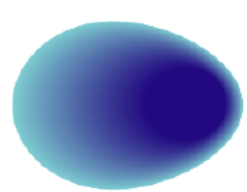	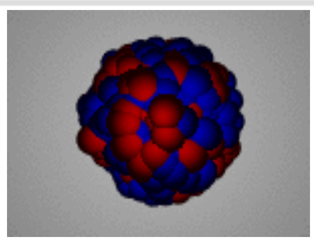
$L = 2$ quadrupole (GQR)	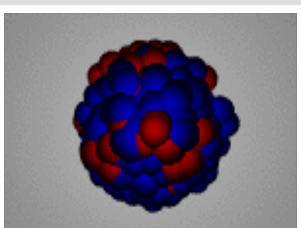	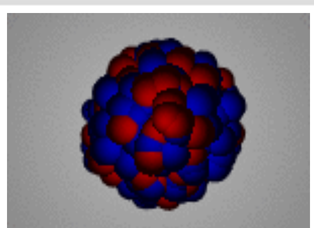

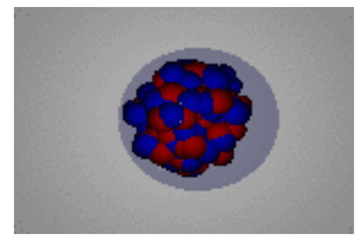

Additional mode at lower energy (<10MeV) than the IVGDR and less collective:

Pygmy Dipole Resonance (PDR)

- Neutron in excess which are less bound
- Appearance of **neutron skin** (oscillation around the symmetric p/n core)

Pygmy Dipole Resonance in ^{68}Ni (GSI)

^{86}Kr, 900 MeV/nucleon $\xrightarrow{\text{Be}}$ ^{68}Ni , 600 MeV/nucleon $\xrightarrow{\text{Au}}$ ^{68}Ni*

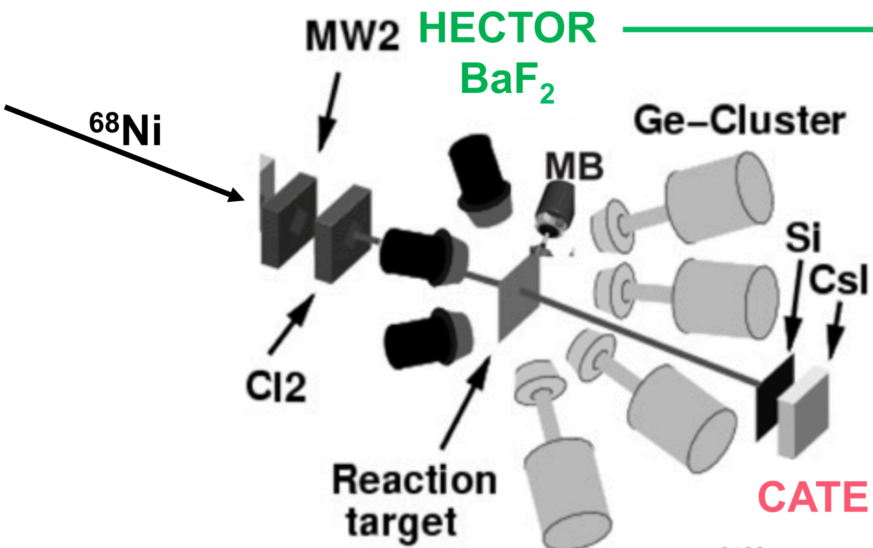

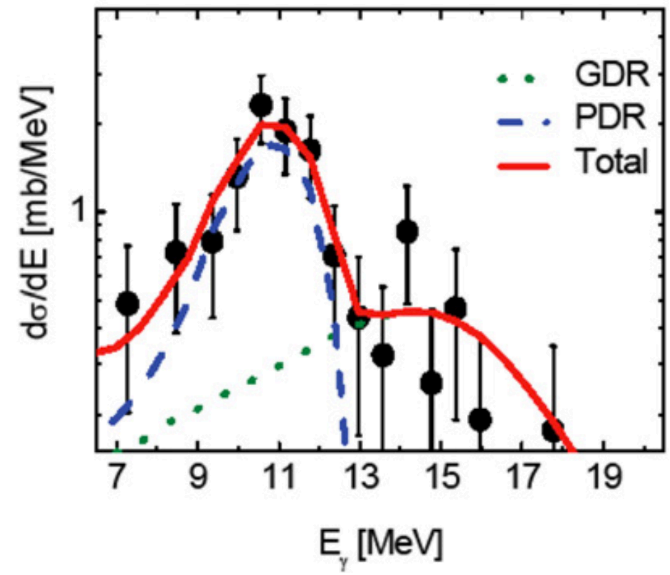

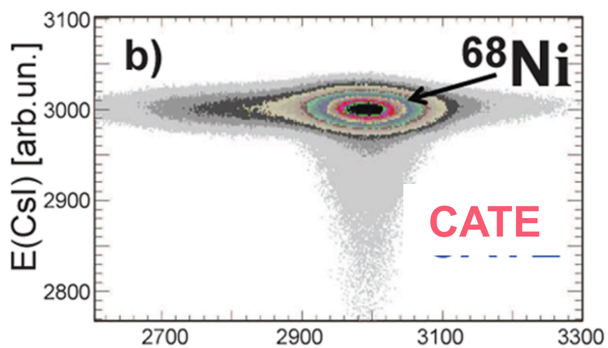

PDR at 11MeV exhausting 5% of the EWSR

O. Wieland *et al*, PRL 102, 092502 (2009)

Energy-Weighted Sum Rule (EWSR) of the PDR

Energy Weighted Sum Rule (EWSR):

$m_1 = \Sigma\,(E_n - E_0)\,|\langle 0|O_{L,T,S}|\nu\rangle|^2$

Equation of State:

$E/A\,(\rho,\delta) = E/A(\rho,\delta{=}0) + S(\rho)\delta^2$

$S(\rho)$ is the symmetry energy: $S'(\rho)|_{\rho=\rho_0} \propto L$

L is the "slope" parameter

From the slope of the symmetry energy to the neutron skin thickness

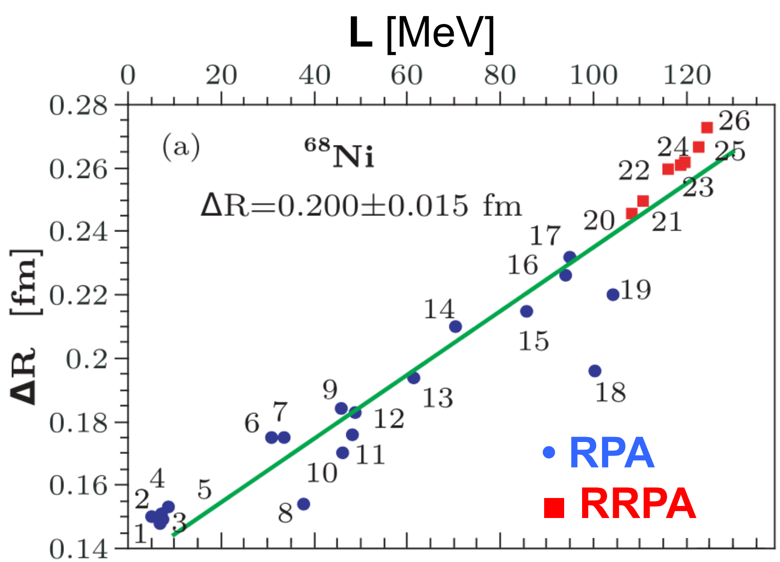

L in the interval 64.8±15.7 MeV
ΔR = 0,200±0.015 fm

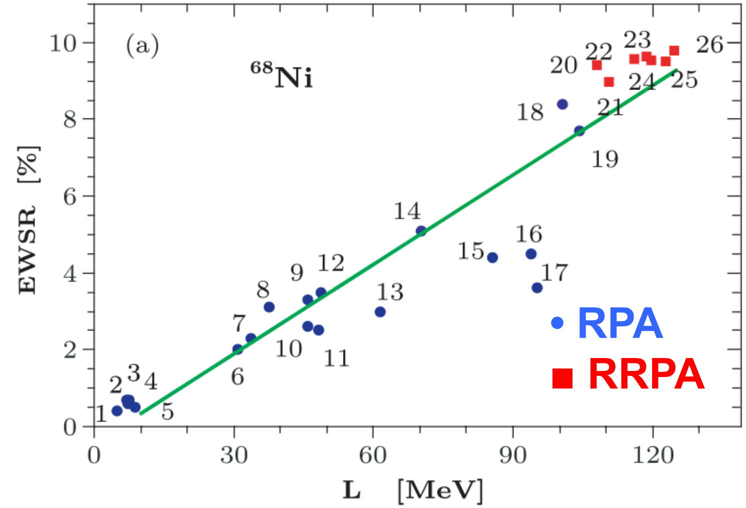

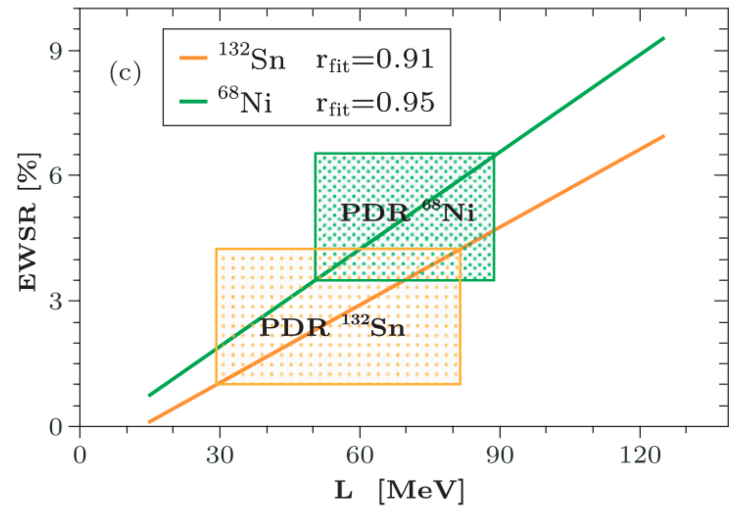

PDR (11MeV) exhausts 5%±1.5% of the EWSR
L is constrained in the interval 50.3-89.4 MeV

A. Carbone *et al.*, PRC 81, 041301 (R) (2010)

Electric dipole polarizability

- Electric dipole polarizability: nuclear dipole response under an electric field

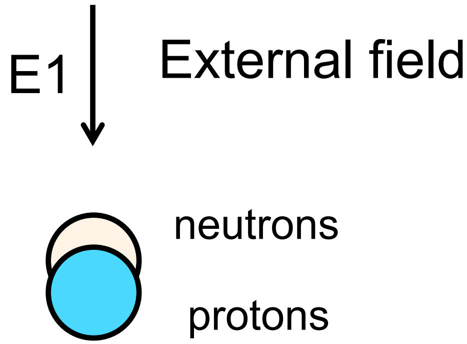

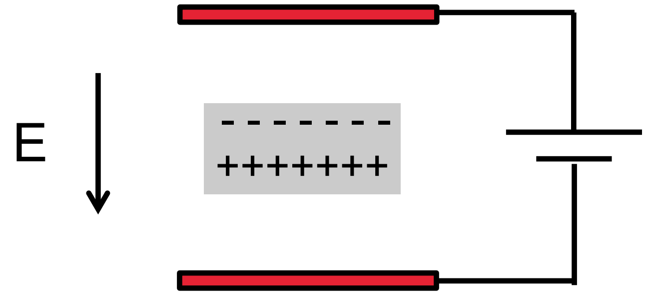

Electric dipole polarizability

Electric dipole polarization

$$p = \alpha_D E$$

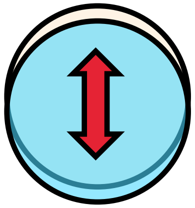

Dipole polarizability

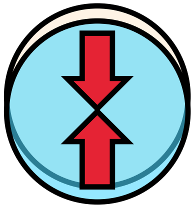

Restoring force

Symmetry energy

Smaller restoring force
↕
Larger neutron skin
↕
Larger dipole polarizability

Slide idea taken from A. Tamii, RCNP

Dipole polarizability and neutron skin thickness

- ❑ Electric dipole polarizability: nuclear dipole response under an electric field

Dipole moment $$p = \alpha_D E$$

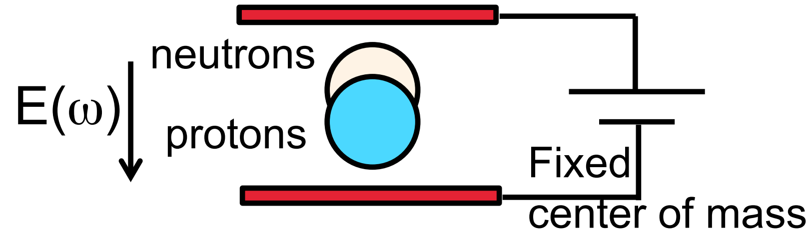

- ❑ Inversely energy weighted sum-rule of B(E1)

$$\alpha_D = \frac{\hbar c}{2\pi^2}\int \frac{\sigma_{abs}^{E1}}{\omega^2} d\omega = \frac{8\pi e^2}{9}\int \frac{dB(E1)}{\omega}$$

First order perturbation:
A.B. Migdal (1944), O. Bohigas *et al.,* Phys. Lett. B **102** (981)

- ❑ Theory predicts a strong correlation of the dipole polarizability with **neutron skin thickness** *Ex.* ^{208}*Pb*

- ❑ Dipole polarizability also correlated to the slope of the symmetry energy

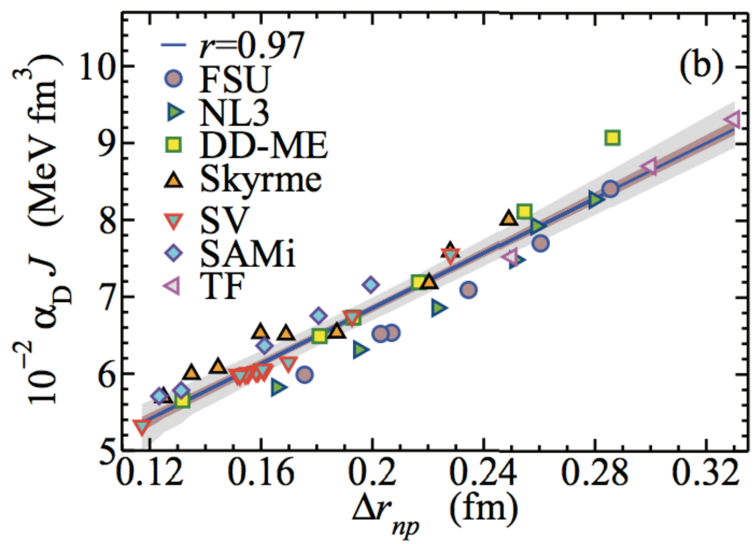

X. Roca-Maza *et al.,* Phys. Rev. C **88**, 024306 (2013)

α_D from polarized proton inelastic scattering

- Differerent probes can excite the electric dipole response:
  - Real photons (g,g')
  - Virtual photons (inelastic scattering: heavy ions, protons,…)

- Measurement of the full B(E1) strength for ^{208}Pb from proton inelastic scattering at RCNP, Japan

- polarized proton beam at 295 MeV
- high resolution spectrometer for missing mass measurement (recoil proton) at zero degree
- polarization: separation of E1/M1 response (in addition to multipole decomposition)

- Result for ^{208}Pb: $\alpha_D = 20.1 \pm 0.6\ fm^3/e^2$

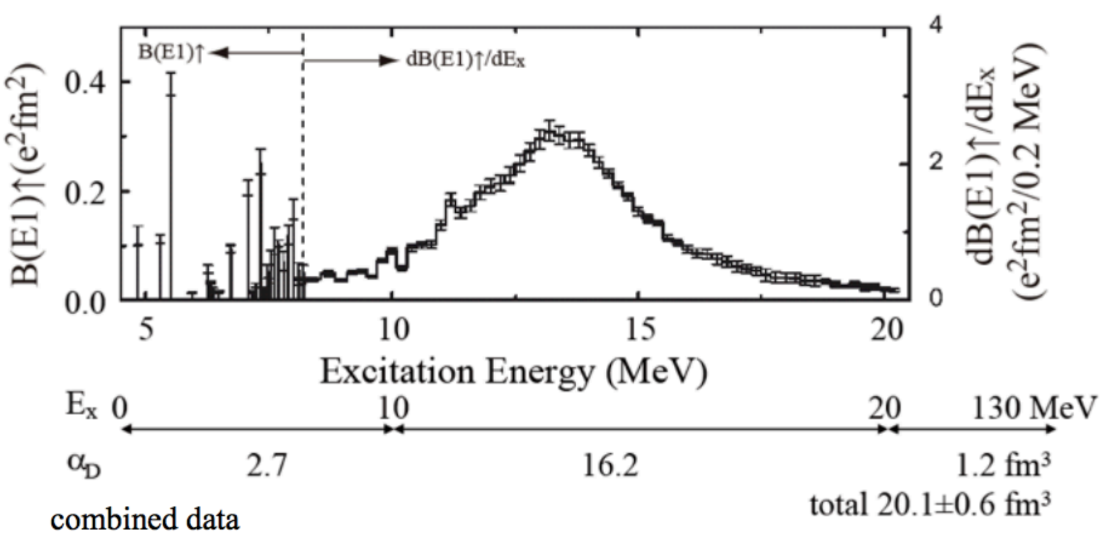

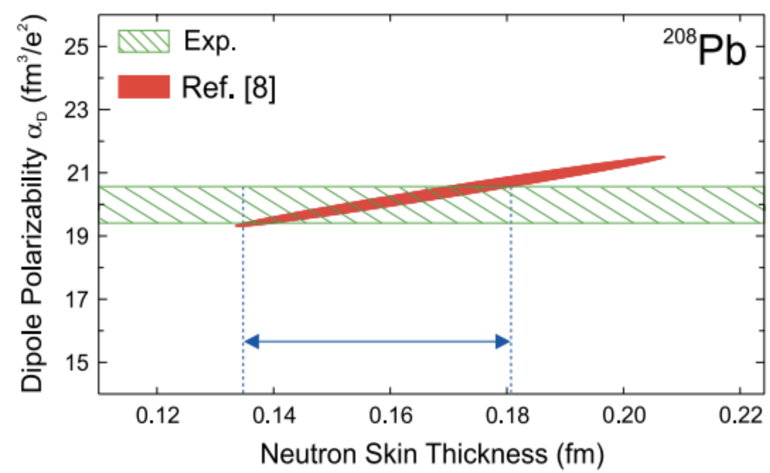

Summary

Method		Observable	Extracted quantity	precision	limitation
Fine structure	Laser	Isotopic shifts	Relative charge radii	High	Higher order terms
e^- scattering	300-800 MeV	Differential cross section	Charge density	High	Restricted to stable nuclei
SCRIT/ELISE	HI-e^- collider	Differential cross section	Charge radius, diffusiveness		Luminosity <10^{-27} cm^{-2} s^{-1}
PV scattering	e^-, few GeVs	Asymmetry	Point in the weak FF (neutrons)		statistics
π_0 photoprod.	P0 beam, several 100 MeV	Differential cross section	Matter radius	0.1 fm	Optical model
Interaction cross section	HI beam, > 100 A MeV	Interaction cross section	Interaction radius	Several 0.1 fm	Not precise
Proton elastic scattering	From 10 to several 100 MeV	Differential cross section	Matter radius	0.1-0.2 fm	Optical model
Antiprotonic atoms	Low-E antiproton capture	Annihilation ratios	ρ_n/ρ_p at tail	Down to few % (to be proven)	Statistics / FSI

- + many indirect methods sensitive to matter, charge radii, neutron skin thickness